

INVESTIGATION OF CRITICAL SUBMERGENCE AT SINGLE AND
MULTIPLE- HORIZONTAL INTAKE STRUCTURES HAVING AIR-
ENTRAINING VORTICES

A THESIS SUBMITTED TO
THE GRADUATE SCHOOL OF NATURAL AND APPLIED SCIENCES
OF
MIDDLE EAST TECHNICAL UNIVERSITY

BY

SERKAN GÖKMENER

IN PARTIAL FULFILLMENT OF THE REQUIREMENTS
FOR
THE DEGREE OF MASTER OF SCIENCE
IN
CIVIL ENGINEERING

JANUARY 2016

Approval of the thesis:

**INVESTIGATION OF CRITICAL SUBMERGENCE AT SINGLE AND
MULTIPLE- HORIZONTAL INTAKE STRUCTURES HAVING AIR-
ENTRAINING VORTICES**

submitted by **SERKAN GÖKMENER** in partial fulfillment of the
requirements for the degree of **Master of Science in Civil Engineering**
Department, Middle East Technical University by,

Prof. Dr. Gülbin Dural Ünver
Dean, Graduate School of **Natural and Applied Sciences**

Prof. Dr. İsmail Özgür Yaman
Head of Department, **Civil Engineering**

Prof.Dr. Mustafa Göğüş
Supervisor, **Civil Engineering Dept., METU**

Examining Committee Members:

Prof. Dr. A. Burcu Altan Sakarya
Civil Engineering Dept., METU

Prof. Dr. Mustafa Göğüş
Civil Engineering Dept., METU

Assoc. Prof. Dr. Mete Köken
Civil Engineering Dept., METU

Asst. Prof. Dr. Talia Ekin Tokyay Sinha
Civil Engineering Dept., METU

Asst. Prof. Dr. Aslı Numanoğlu Genç
Civil Engineering Dept., Atılım University

Date: 29.01.2016

I hereby declare that all information in this document has been obtained and presented in accordance with academic rules and ethical conduct. I also declare that, as required by these rules and conduct, I have fully cited and referenced all material and results that are not original to this work.

Name, Last name: Serkan GÖKMENER

Signature: _____

ABSTRACT

INVESTIGATION OF CRITICAL SUBMERGENCE AT SINGLE AND MULTIPLE- HORIZONTAL INTAKE STRUCTURES HAVING AIR- ENTRAINING VORTICES

Gökmener, Serkan

M.S., Department of Civil Engineering

Supervisor: Prof. Dr. Mustafa Gögüş

January 2016, 127 pages

In this experimental study the variation of the critical submergence of air-entraining vortices with important flow and geometrical parameters were investigated at single and multiple- horizontal intake structures. In the scope of this study, three identical pipes of diameter $D_i=0.265$ m were tested at a wide range of discharge with varying side wall clearances under symmetrical and asymmetrical approach flow conditions. Using dimensional analysis dimensionless equation was developed for critical submergence as a function of relevant flow and geometrical parameters. Regression analysis was used to derive empirical equations for the critical submergence. Moreover, these empirical equations were compared with the similar studies in the literature. Results of the experiments show that, for a given Froude number, the critical

submergence values are higher for multiple water intake structures than those of single water intake structures. By using these equations it is possible to determine the required critical submergence depths above which there will be no air- entraining vortices, at single and multiple- horizontal intakes within the ranges of dimensionless parameters tested in this study. Moreover, floating rafts at different sizes were tested as anti- vortex devices to prevent the formation of air- entraining vortices and very successful results were achieved.

Keywords: Horizontal intakes, Multiple intakes, Air-entraining vortices, Critical submergence, Anti- vortex devices.

ÖZ

TEKLİ VE ÇOKLU YATAY SU ALMA YAPILARINDA HAVA SÜRÜKLEYEN GİRDAPLARIN OLUŞMASI İÇİN GEREKLİ OLAN KRİTİK BATIKLIK DERİNLİKLERİNİN ARAŞTIRILMASI

Gökmener, Serkan

Yüksek Lisans, İnşaat Mühendisliği Bölümü

Tez Yöneticisi: Prof. Dr. Mustafa Göğüş

Ocak 2016, 127 sayfa

Bu deneysel çalışmada, tekli ve çoklu yatay su alma yapılarında hava sürükleyen girdapların oluşması için gerekli olan kritik batıklık derinliklerinin önemli akım ve geometrik parametreleri ile değişimi araştırılmıştır. Bu çalışma kapsamında çapları $D_i=0.265$ m olan aynı özelliklerde üç adet boru, geniş bir debi aralığında değişen yan duvar açıklıklarında, simetrik ve asimetrik akım şartlarında test edilmiştir. Boyut analizi kullanılarak, kritik batıklık ilgili akım ve geometrik parametrelerin fonksiyonu olarak ifade edilmiştir. Regrasyon analizi kullanılarak, kritik batıklık için ampirik denklemler elde edilmiş ve bu denklemler literatürdeki benzer çalışmalar ile karşılaştırılmıştır. Yapılan deneylerin sonuçları, verilen bir Froude sayısı için çoklu su alma yapılarında

kritik batıklığın, tekli su alma yapılarına kıyasla daha yüksek deęerlerde olduđunu göstermiřtir. alıřma sonucunda bulunan denklemler kullanılarak, tekli ve oklu yatay su alma yapılarında hava srkleyen girdapların oluřmaması iin gerekli olan kritik batıklık derinliklerinin hesaplanması mmkndr. Ek olarak, farklı boyutlardaki yzer levhalar hava srkleyen girdapların oluřmasını nleyici dzenekler olarak kullanılmıř ve bunlardan olduka bařarılı sonular elde edilmiřtir.

Anahtar Kelimeler: Yatay su alma yapıları, oklu su alma yapıları, Hava srkleyici girdaplar, Kritik batıklık derinliđi, Girdap nleyici dzenekler.

To my family

ACKNOWLEDGEMENTS

I would like to thank my supervisor Prof. Dr. Mustafa GÖĞÜŞ for his assistance and support during my study. He has always understood and encouraged me during experiments when I was tired.

I would like to express my gratitude to my mother Tuna GÖKMENER and my father Emin Bülent GÖKMENER for their endless love, patience and confidence during my life.

I would like to thank Mehmet Vahit AŞIK, Erkan KOYUNCUOĞLU, Orçin AKGÖNÜL, Melih AKSOY, Berkay BEYAZOK and Cemre ÇAĞLAR for their support and friendship.

I would like to express my appreciation to Emre HASPOLAT, Kutay YILMAZ, Ali Ersin DİNÇER, Berhan MELEK, Ahmet Nazım ŞAHİN, Ezgi KÖKER and Cüneyt YAVUZ for their advices, helpfulness and friendship during my study period.

I would like to thank also Semih KONDAKÇI, Melih Uğur KONDAKÇI, Ceyhun KILIÇ and Ali MART from Hidroyapı Engineering for their patience and support during my study period.

During my study, I spent a lot of my time at Hydromechanics Laboratory to conduct my experiments. I would also thank to the technicians of the laboratory, who arranged required changes in the setup during experiments, for their help.

This study was supported by TUBITAK (The Scientific and Technological Research Council of Turkey) under Project No: 113M326

TABLE OF CONTENTS

ABSTRACT	v
ÖZ.....	vii
ACKNOWLEDGEMENTS	x
TABLE OF CONTENTS	xi
LIST OF TABLES	xvi
LIST OF FIGURES.....	xxi
LIST OF SYMBOLS.....	xxviii
CHAPTERS	
1.INTRODUCTION.....	1
1.1 Introductory Remarks on the Intake Vortex and Critical Submergence... 1	1
1.2 Sources of Vortex Formation on Free Surface	2
1.3 Types of Intakes.....	2
1.4 Types of Vortices.....	3
1.5 Prevention of Vortices	6
1.6 Scope of the Study	6
2.LITERATURE REVIEW	7
3.MODELLING OF AIR ENTRAINING VORTICES	21
3.1 Introduction.....	21
3.2 Application of Dimensional Analysis to the Related Parameters.....	22
3.3 Effect of Froude Number.....	25

3.4 Effect of Reynolds Number	25
3.5 Effect of Weber Number.....	26
3.6 Effect of Kolf Number	26
4.EXPERIMENTAL SETUP AND METHODOLOGY	27
4.1 Experimental Setup.....	27
4.2 Methodology of the Experiments.....	32
5.ANALYSIS AND EVALUATION OF THE EXPERIMENTAL RESULTS	43
5.1 Introduction.....	43
5.2 Single Water Intake Structure.....	44
5.2.1 Symmetrical Approach Flow Conditions.....	44
5.2.1.1 Variation of S_c/D_i with Dimensionless Flow Parameters under Symmetrical Approach Flow Conditions	44
5.2.1.2 Comparison of Results of Present Study and Göğüş et al.'s (2015) Study	46
5.2.1.3 Derivation of Empirical Equations for Dimensionless Critical Submergence	48
5.2.1.3.1 The General Case.....	48
5.2.1.3.2 Simplified Empirical Equations for S_c/D_i	49
5.2.1.4 Comparison of the Results of Present Study with the Empirical Equations Proposed by Göğüş et al. (2015)	52
5.2.2 Asymmetrical Approach Flow Conditions.....	55
5.2.2.1 Variation of S_c/D_i with Dimensionless Flow Parameters under Asymmetrical Approach Flow Conditions.....	55

5.2.2.2 Comparison of the Results of Present and Göğüş et al.'s (2015) Studies	57
5.2.2.3 Derivation of Empirical Equations for Dimensionless Critical Submergence	62
5.2.2.3.1 The General Case.....	62
5.2.2.3.2 Simplified Empirical Equations for S_c/D_i	63
5.2.2.4 Comparison of the Results of Present Study with the Empirical Equations Proposed by Göğüş et al. (2015)	65
5.3 Double Water Intake Structure	68
5.3.1 Symmetrical Approach Flow Conditions.....	68
5.3.1.1 Variation of S_c/D_i with Dimensionless Flow Parameters under Symmetrical Approach Flow Conditions	68
5.3.1.2 Derivation of Empirical Equations for Dimensionless Critical Submergence	70
5.3.1.2.1 The General Case.....	70
5.3.1.2.2 Simplified Empirical Equations for S_c/D_i	71
5.3.2 Asymmetrical Approach Flow Conditions	74
5.3.2.1 Variation of S_c/D_i with Dimensionless Flow Parameters under Asymmetrical Approach Flow Conditions.....	74
5.3.2.2 Derivation of Empirical Equations for Dimensionless Critical Submergence	76
5.3.2.2.1 The General Case.....	76
5.3.2.2.2 Simplified Empirical Equations for S_c/D_i	77
5.4 Triple Water Intake Structure	80
5.4.1 Symmetrical Approach Flow Conditions.....	80

5.4.1.1 Variation of S_c/D_i with Dimensionless Flow Parameters under Symmetrical Approach Flow Conditions	80
5.4.1.2 Derivation of Empirical Equations for Dimensionless Critical Submergence	82
5.4.1.2.1 The General Case.....	82
5.4.1.2.2 Simplified Empirical Equations for S_c/D_i	83
5.4.2 Asymmetrical Approach Flow Conditions.....	86
5.4.2.1 Variation of S_c/D_i with Dimensionless Flow Parameters under Asymmetrical Approach Flow Conditions	86
5.4.2.2 Derivation of Empirical Equations for Dimensionless Critical Submergence	88
5.4.2.2.1 The General Case.....	88
5.4.2.2.2 Simplified Empirical Equations for S_c/D_i	89
5.5 Comparison of Simplified Empirical S_c/D_i Equations for Single, Double and Triple Water Intake Structures at Symmetrical and Asymmetrical Approach Flow Conditions	92
5.5.1 Comparison of S_c/D_i Equations Derived for Symmetrical Approach Flow Conditions	92
5.5.2 Comparison of S_c/D_i Equations Derived for Asymmetrical Approach Flow Conditions	94
5.5.3 Comparison of S_c/D_i versus Fr Curves of Symmetrical and Asymmetrical Approach Flows.....	96
5.6 Prevention of Air- Entraining Vortices for Symmetrical and Asymmetrical Approach Flow Conditions	99
5.6.1 Prevention of Air- Entraining Vortices for Symmetrical Approach Flow Conditions	99

5.6.2 Prevention of Air- Entraining Vortices for Asymmetrical Approach Flow Conditions	102
6.CONCLUSIONS AND RECOMMENDATIONS.....	105
REFERENCES	109
APPENDIX A	113
EXPERIMENTAL RESULTS OF SYMMETRICAL APPROACH FLOW	113
APPENDIX B.....	119
EXPERIMENTAL RESULTS OF ASYMMETRICAL APPROACH FLOW	119

LIST OF TABLES

TABLES

Table 5.1 The ranges of important hydraulic and geometrical parameters used and calculated in the experiments of symmetrical approach flow conditions..	44
Table 5.2 The ranges of important hydraulic and geometrical parameters used and calculated in the experiments of asymmetrical approach flow conditions	55
Table 5.3 The ranges of important hydraulic and geometrical parameters used and calculated in the experiments of symmetrical approach flow conditions..	68
Table 5.4 The ranges of important hydraulic and geometrical parameters used and calculated in the experiments of asymmetrical approach flow conditions	74
Table 5.5 The ranges of important hydraulic and geometrical parameters used and calculated in the experiments of symmetrical approach flow conditions..	80
Table 5.6 The ranges of important hydraulic and geometrical parameters used and calculated in the experiments of asymmetrical approach flow conditions	86
Table 5.7 Summary of performances of floating rafts for symmetrical approach flow conditions	101
Table 5.8 Summary of performances of floating rafts for asymmetrical approach flow conditions	103
Table A.1 Experimental results of critical submergence and related important flow parameters for $b= 60$ cm at single water intake structure	113
Table A.2 Experimental results of critical submergence and related important flow parameters for $b= 80$ cm at single water intake structure	114
Table A.3 Experimental results of critical submergence and related important flow parameters for $b= 120$ cm at single water intake structure	114
Table A.4 Experimental results of critical submergence and related important flow parameters for $b= 140$ cm at single water intake structure	114

Table A.5 Experimental results of critical submergence and related important flow parameters for $b= 70$ cm at double water intake structure	114
Table A.6 Experimental results of critical submergence and related important flow parameters for $b= 80$ cm at double water intake structure	115
Table A.7 Experimental results of critical submergence and related important flow parameters for $b= 90$ cm at double water intake structure	115
Table A.8 Experimental results of critical submergence and related important flow parameters for $b= 100$ cm at double water intake structure	115
Table A.9 Experimental results of critical submergence and related important flow parameters for $b= 110$ cm at double water intake structure	116
Table A.10 Experimental results of critical submergence and related important flow parameters for $b= 120$ cm at double water intake structure	116
Table A.11 Experimental results of critical submergence and related important flow parameters for $b= 120$ cm at triple water intake structure	116
Table A.12 Experimental results of critical submergence and related important flow parameters for $b= 140$ cm at triple water intake structure	117
Table B.1 Experimental results of critical submergence and related important flow parameters for $b_1= 40$ cm. $b_2= 80$ cm cm at single water intake structure	119
Table B.2 Experimental results of critical submergence and related important flow parameters for $b_1= 40$ cm. $b_2= 120$ cm cm at single water intake structure	120
Table B.3 Experimental results of critical submergence and related important flow parameters for $b_1= 60$ cm. $b_2= 100$ cm cm at single water intake structure	120
Table B.4 Experimental results of critical submergence and related important flow parameters for $b_1= 60$ cm. $b_2= 140$ cm cm at single water intake structure	120

Table B.5 Experimental results of critical submergence and related important flow parameters for $b_1= 100$ cm. $b_2= 160$ cm cm at single water intake structure	121
Table B.6 Experimental results of critical submergence and related important flow parameters for $b_1= 120$ cm. $b_2= 160$ cm cm at single water intake structure	121
Table B.7 Experimental results of critical submergence and related important flow parameters for $b_1= 70$ cm. $b_2= 80$ cm cm at double water intake structure	121
Table B.8 Experimental results of critical submergence and related important flow parameters for $b_1= 70$ cm. $b_2= 90$ cm cm at double water intake structure	121
Table B.9 Experimental results of critical submergence and related important flow parameters for $b_1= 70$ cm. $b_2= 100$ cm cm at double water intake structure	122
Table B.10 Experimental results of critical submergence and related important flow parameters for $b_1= 70$ cm. $b_2= 110$ cm cm at double water intake structure	122
Table B.11 Experimental results of critical submergence and related important flow parameters for $b_1= 70$ cm. $b_2= 120$ cm cm at double water intake structure	122
Table B. 12 Experimental results of critical submergence and related important flow parameters for $b_1= 80$ cm. $b_2= 90$ cm cm at double water intake structure	123
Table B.13 Experimental results of critical submergence and related important flow parameters for $b_1= 80$ cm. $b_2= 100$ cm cm at double water intake structure	123
Table B.14 Experimental results of critical submergence and related important flow parameters for $b_1= 80$ cm. $b_2= 110$ cm cm at double water intake structure	123

Table B.15 Experimental results of critical submergence and related important flow parameters for $b_1= 80$ cm. $b_2= 120$ cm cm at double water intake structure	124
Table B.16 Experimental results of critical submergence and related important flow parameters for $b_1= 90$ cm. $b_2= 100$ cm cm at double water intake structure	124
Table B.17 Experimental results of critical submergence and related important flow parameters for $b_1= 90$ cm. $b_2= 110$ cm cm at double water intake structure	124
Table B.18 Experimental results of critical submergence and related important flow parameters for $b_1= 90$ cm. $b_2= 120$ cm cm at double water intake structure	125
Table B.19 Experimental results of critical submergence and related important flow parameters for $b_1= 100$ cm. $b_2= 110$ cm cm at double water intake structure	125
Table B.20 Experimental results of critical submergence and related important flow parameters for $b_1= 100$ cm. $b_2= 120$ cm cm at double water intake structure	125
Table B.21 Experimental results of critical submergence and related important flow parameters for $b_1= 110$ cm. $b_2= 120$ cm cm at double water intake structure	126
Table B.22 Experimental results of critical submergence and related important flow parameters for $b_1= 120$ cm. $b_2= 140$ cm cm at triple water intake structure	126
Table B.23 Experimental results of critical submergence and related important flow parameters for $b_1= 120$ cm. $b_2= 160$ cm cm at triple water intake structure	126
Table B.24 Experimental results of critical submergence and related important flow parameters for $b_1= 140$ cm. $b_2= 160$ cm cm at triple water intake structure	127

Table B.25 Experimental results of critical submergence and related important flow parameters for $b_1= 140$ cm. $b_2= 170$ cm cm at triple water intake structure 127

Table B.26 Experimental results of critical submergence and related important flow parameters for $b_1= 147$ cm. $b_2= 183$ cm cm at triple water intake structure 127

LIST OF FIGURES

FIGURES

Figure 1.1 Sources of vortices (Durgin & Hecker, 1978)	2
Figure 1.2 Classification of intakes (Knauss, 1987).....	3
Figure 1.3 General look of eddy, dimple and vortex tail	4
Figure 1.4 General ARL Vortex Type Classification (Knauss, 1987)	5
Figure 2.1 Dimensionless plot of data obtained from existing intakes, field installations and model studies (Gulliver and Rindels, 1983).....	13
Figure 2.2 Recommended submergence for intakes with proper approach flow conditions, (Knauss, 1987).....	14
Figure 3.1 A sketch of a horizontal intake structure with related parameters..	23
Figure 4.1 View of the model from downstream	28
Figure 4.2 Hollow bricks and coarse screens which are located at the entrance of the model.....	28
Figure 4.3 Close view of the triple water intake structure from downstream..	29
Figure 4.4 General plan view of the triple water intake structure (dimensions are in cm).....	30
Figure 4.5 Section view of the triple water intake structure (dimensions are in cm).....	31
Figure 4.6 Detailed plan view of the triple water intake structure with the intake numbers and locations of them with respect to each other (dimensions are in cm).....	32
Figure 4.7 View of the electromagnetic flowmeters mounted on the water intake pipes.....	33

Figure 4.8 Sketch of the locations of adjustable right and left approach-channel side walls for symmetrical and asymmetrical approach flow conditions when only one intake structure, Intake- II, is in operation	36
Figure 4.9 Sketch of the locations of adjustable right and left approach-channel side walls for symmetrical and asymmetrical approach flow conditions when two intake structures, Intake- II and Intake- III, are in operation	37
Figure 4.10 Sketch of the locations of adjustable right and left approach-channel side walls for symmetrical and asymmetrical approach flow conditions when all of three intake structures are in operation	38
Figure 4.11 Vortex formation in front of single water intake structure ($Q=110$ lt/s)	39
Figure 4.12 Vortex formation in front of double water intake structure ($Q=110.51$ lt/s)	39
Figure 4.13 Vortex formation in front of double water intake structure ($Q=111.51$ lt/s)	40
Figure 4.14 Vortex formation in front of triple water intake structure ($Q=96.20$ lt/s)	40
Figure 4.15 Top view of floating rafts which is used at vortex prevention during experiments (dimensions are in cm)	41
Figure 4.16 Top view of floating rafts which is used at vortex prevention during experiments (dimensions are in cm)	41
Figure 5.1 Variation of S_c/D_i with Fr for symmetrical approach flow conditions at single water intake	45
Figure 5.2 Variation of S_c/D_i with Re for symmetrical approach flow conditions at single water intake	45
Figure 5.3 Variation of S_c/D_i with We for symmetrical approach flow conditions at single water intake	46
Figure 5.4 Variation of S_c/D_i with Fr for data of present study ($D_i.=26.5$) cm and Göğüş et al.'s (2015) study ($D_i.=25$) cm	47

Figure 5.5 Variation of S_c/D_i with Re for data of present study ($D_i=26.5$) cm and Göğüş et al.'s (2015) study ($D_i=25$ cm)	47
Figure 5.6 Variation of S_c/D_i with We for data of present study ($D_i=26.5$) cm and Göğüş et al.'s (2015) ($D_i=25$ cm)	48
Figure 5.7 Comparison of $(S_c/D_i)_{calculated}$ data obtained from Equation 5.1, with $(S_c/D_i)_{measured}$ data for single water intake structure under symmetrical approach flow conditions	49
Figure 5.8 Comparison of $(S_c/D_i)_{calculated}$ data obtained from Equation 5.2, with $(S_c/D_i)_{measured}$ data for single water intake structure under symmetrical approach flow conditions	50
Figure 5.9 Comparison of $(S_c/D_i)_{calculated}$ data obtained from Equation 5.3, with $(S_c/D_i)_{measured}$ data for single water intake structure under symmetrical approach flow conditions	51
Figure 5.10 Comparison of $(S_c/D_i)_{calculated}$ data obtained from Equation 5.4, with $(S_c/D_i)_{measured}$ data for single water intake structure under symmetrical approach flow conditions	51
Figure 5.11 Comparison of $(S_c/D_i)_{measured}$ of the present study with $(S_c/D_i)_{calculated}$ from Equation 2.15 proposed by Göğüş. et al (2015) for symmetrical approach flow conditions.....	53
Figure 5.12 Comparison of $(S_c/D_i)_{measured}$ of the present study with $(S_c/D_i)_{calculated}$ from Equation 2.16 proposed by Göğüş et al. (2015) for symmetrical approach flow conditions.....	53
Figure 5.13 Comparison of $(S_c/D_i)_{measured}$ of the present study with $(S_c/D_i)_{calculated}$ from Equation 2.17 proposed by Göğüş et al. (2015) for symmetrical approach flow conditions.....	54
Figure 5.14 Comparison of $(S_c/D_i)_{measured}$ of the present study with $(S_c/D_i)_{calculated}$ from Equation 2.18 proposed by Göğüş et al. (2015) for symmetrical approach flow conditions.....	54
Figure 5.15 Variation of S_c/D_i with Fr for asymmetrical approach flow conditions at single water intake	56

Figure 5.16 Variation of S_c/D_i with Re for asymmetrical approach flow conditions at single water intake	56
Figure 5.17 Variation of S_c/D_i with We for asymmetrical approach flow conditions at single water intake	57
Figure 5.18 Variation of S_c/D_i with Fr for the present study ($D_i=26.5$) cm and Göğüş et al.'s (2015) study ($D_i=25$) cm	59
Figure 5.19 Variation of S_c/D_i with Re for the present study ($D_i=26.5$) cm and Göğüş et al.'s (2015) study ($D_i=25$) cm	60
Figure 5.20 Variation of S_c/D_i with We for the present study ($D_i=26.5$) cm and Göğüş et al.'s (2015) study ($D_i=25$) cm	61
Figure 5.21 Comparison of $(S_c/D_i)_{\text{calculated}}$ data obtained from Equation 5.5, with $(S_c/D_i)_{\text{measured}}$ data for single water intake structure under asymmetrical approach flow conditions.....	62
Figure 5.22 Comparison of $(S_c/D_i)_{\text{calculated}}$ data obtained from Equation 5.6, with $(S_c/D_i)_{\text{measured}}$ data for single water intake structure under asymmetrical approach flow conditions.....	63
Figure 5.23 Comparison of $(S_c/D_i)_{\text{calculated}}$ data obtained from Equation 5.7, with $(S_c/D_i)_{\text{measured}}$ data for single water intake structure under asymmetrical approach flow conditions.....	64
Figure 5.24 Comparison of $(S_c/D_i)_{\text{calculated}}$ data obtained from Equation 5.8, with $(S_c/D_i)_{\text{measured}}$ data for single water intake structure under asymmetrical approach flow conditions.....	64
Figure 5.25 Comparison of $(S_c/D_i)_{\text{measured}}$ of the present study with $(S_c/D_i)_{\text{calculated}}$ from Equation 2.19 proposed by Göğüş et al. (2015) for symmetrical approach flow conditions.....	66
Figure 5.26 Comparison of $(S_c/D_i)_{\text{measured}}$ of the present study with $(S_c/D_i)_{\text{calculated}}$ from Equation 2.20 proposed by Göğüş et al. (2015) for symmetrical approach flow conditions.....	66

Figure 5.27 Comparison of $(S_c/D_i)_{\text{measured}}$ of the present study with $(S_c/D_i)_{\text{calculated}}$ from Equation 2.21 proposed by Göğüş et al. (2015) for symmetrical approach flow conditions.....	67
Figure 5.28 Comparison of $(S_c/D_i)_{\text{measured}}$ of the present study with $(S_c/D_i)_{\text{calculated}}$ from Equation 2.22 proposed by Göğüş et al. (2015) for symmetrical approach flow conditions.....	67
Figure 5.29 Variation of S_c/D_i with Fr for symmetrical approach flow conditions at double water intake structure	69
Figure 5.30 Variation of S_c/D_i with Re for symmetrical approach flow conditions at double water intake structure	69
Figure 5.31 Variation of S_c/D_i with We for symmetrical approach flow conditions at double water intake structure	70
Figure 5.32 Comparison of $(S_c/D_i)_{\text{calculated}}$ data obtained from Equation 5.9, with $(S_c/D_i)_{\text{measured}}$ data for double water intake structure under symmetrical approach flow conditions	71
Figure 5.33 Comparison of $(S_c/D_i)_{\text{calculated}}$ data obtained from Equation 5.10, with $(S_c/D_i)_{\text{measured}}$ data for double water intake structure under symmetrical approach flow conditions	72
Figure 5.34 Comparison of $(S_c/D_i)_{\text{calculated}}$ data obtained from Equation 5.11, with $(S_c/D_i)_{\text{measured}}$ data for double water intake structure under symmetrical approach flow conditions	73
Figure 5.35 Comparison of $(S_c/D_i)_{\text{calculated}}$ data obtained from Equation 5.12, with $(S_c/D_i)_{\text{measured}}$ data for double water intake structure under symmetrical approach flow conditions	73
Figure 5.36 Variation of S_c/D_i with Fr for asymmetrical approach flow conditions at double water intake structure	75
Figure 5.37 Variation of S_c/D_i with Re for asymmetrical approach flow conditions at double water intake structure	75
Figure 5.38 Variation of S_c/D_i with We for asymmetrical approach flow conditions at double water intake structure	76

Figure 5.39 Comparison of $(S_c/D_i)_{\text{calculated}}$ data obtained from Equation 5.13, with $(S_c/D_i)_{\text{measured}}$ data for double water intake structure under asymmetrical approach flow conditions.....	77
Figure 5.40 Comparison of $(S_c/D_i)_{\text{calculated}}$ data obtained from Equation 5.14, with $(S_c/D_i)_{\text{measured}}$ data for double water intake structure under asymmetrical approach flow conditions.....	78
Figure 5.41 Comparison of $(S_c/D_i)_{\text{calculated}}$ data obtained from Equation 5.15, with $(S_c/D_i)_{\text{measured}}$ data for double water intake structure under asymmetrical approach flow conditions.....	79
Figure 5.42 Comparison of $(S_c/D_i)_{\text{calculated}}$ data obtained from Equation 5.16, with $(S_c/D_i)_{\text{measured}}$ data for double water intake structure under asymmetrical approach flow conditions.....	79
Figure 5.43 Variation of S_c/D_i with Fr for symmetrical approach flow conditions at triple water intake structure.....	81
Figure 5.44 Variation of S_c/D_i with Re for symmetrical approach flow conditions at triple water intake structure.....	81
Figure 5.45 Variation of S_c/D_i with We for symmetrical approach flow conditions at triple water intake structure.....	82
Figure 5.46 Comparison of $(S_c/D_i)_{\text{calculated}}$ data obtained from Equation 5.17, with $(S_c/D_i)_{\text{measured}}$ data for triple water intake structure under symmetrical approach flow conditions.....	83
Figure 5.47 Comparison of $(S_c/D_i)_{\text{calculated}}$ data obtained from Equation 5.18, with $(S_c/D_i)_{\text{measured}}$ data for triple water intake structure under symmetrical approach flow conditions.....	84
Figure 5.48 Comparison of $(S_c/D_i)_{\text{calculated}}$ data obtained from Equation 5.19, with $(S_c/D_i)_{\text{measured}}$ data for triple water intake structure under symmetrical approach flow conditions.....	85
Figure 5.49 Comparison of $(S_c/D_i)_{\text{calculated}}$ data obtained from Equation 5.20, with $(S_c/D_i)_{\text{measured}}$ data for triple water intake structure under symmetrical approach flow conditions.....	85

Figure 5.50 Variation of S_c/D_i with Fr for asymmetrical approach flow conditions at triple water intake structure	87
Figure 5.51 Variation of S_c/D_i with Re for asymmetrical approach flow conditions at triple water intake structure	87
Figure 5.52 Variation of S_c/D_i with We for asymmetrical approach flow conditions at triple water intake structure	88
Figure 5.53 Comparison of $(S_c/D_i)_{\text{calculated}}$ data obtained from Equation 5.21, with $(S_c/D_i)_{\text{measured}}$ data for triple water intake structure under asymmetrical approach flow conditions	89
Figure 5.54 Comparison of $(S_c/D_i)_{\text{calculated}}$ data obtained from Equation 5.22, with $(S_c/D_i)_{\text{measured}}$ data for triple water intake structure under asymmetrical approach flow conditions	90
Figure 5.55 Comparison of $(S_c/D_i)_{\text{calculated}}$ data obtained from Equation 5.23, with $(S_c/D_i)_{\text{measured}}$ data for triple water intake structure under asymmetrical approach flow conditions	91
Figure 5.56 Comparison of $(S_c/D_i)_{\text{calculated}}$ data obtained from Equation 5.24, with $(S_c/D_i)_{\text{measured}}$ data for triple water intake structure under asymmetrical approach flow conditions	91
Figure 5.57 Comparison of S_c/D_i equations obtained from the present study and Göğüş et al.'s (2015) study which are only dependent on Froude Number for symmetrical approach flow conditions	92
Figure 5.58 Comparison of S_c/D_i equations obtained from the present study and Göğüş et al.'s (2015) study which are only dependent on Froude Number for asymmetrical approach flow conditions	95
Figure 5.59 Comparison of S_c/D_i equations obtained from the present study and Göğüş et al.'s (2015) Study which are only dependent on Froude Number for both symmetrical and asymmetrical approach flow conditions	98

LIST OF SYMBOLS

a	Intake gate height
b	Horizontal distance from the center of the intake to a side wall of the reservoir
b ₁	Horizontal distance from the center of the intake to the right- side plexiglass wall
b ₂	Horizontal distance from the center of the intake to the left- side plexiglass wall
c	Vertical distance between the lowest point of the intake pipe and reservoir bottom
c ₁	Regression variable
c ₂	Regression variable
c ₃	Regression variable
c ₄	Regression variable
D _i	Intake diameter
Fr	Intake Froude number
g	Gravity acceleration
h	The depth of water above centerline of the intake
H	Submergence for vertical intakes
K _o	Intake Kolf number
Γ	Average circulation imposed to flow
Q _i	Intake discharge
R	Correlation coefficient
Re	Intake Reynolds number
Re _R	Radial Reynolds number
S _c	Critical submergence measured from the summit point of horizontal intakes

S_{c^*}	Critical submergence measured from the center of horizontal intakes
V_i	Average velocity of the flow at the intake pipe
ν	Kinematic viscosity of water
ρ	Density of the fluid
μ	Dynamic viscosity of the fluid
β_s	Scale effect correction coefficient for symmetrical approach flow conditions
β_a	Scale effect correction coefficient for asymmetrical approach flow conditions
σ	Surface tension of the fluid
ψ	Representation of geometrical parameter for asymmetrical approach flow conditions
We	Intake Weber number

CHAPTER 1

INTRODUCTION

1.1 Introductory Remarks on the Intake Vortex and Critical Submergence

Water has been used by humans for power generation, irrigation, domestic and industrial purposes from seas, lakes, rivers or from reservoirs through intakes. However, in modern era, water resources are started to dry up and humans are faced with a serious waste water problem, so it is important to use water resources effectively and carefully. For this reason, more efficient design criteria should be applied for water intake structures to minimize cost and operational problems. One of these problems is air-entraining vortices which were created by swirling flows on the intake. The position of the intake should be justified for the most critical scenario which is the case when the reservoir is at dead or at minimum storage level, water level should be sufficiently above from the intake to provide a vortex free flow. By the way, the intake has to be located close to the water surface so as to decrease cost of construction.

Distance between the free surface and the intake is called as submergence. When this submergence falls to a critical level which is called "critical submergence", air-entraining vortices start to occur on the free surface. For an effective intake, the submergence should be large enough to prevent inducing air-entraining vortices extending from the free surface down to the intake

entrance. Occurrence of air-entraining vortices causes serious problems such as; increasing loss of hydraulic load and loss of discharge at water intake structures, loss of efficiency, operational problems, cavitation and vibration problems in hydraulic machines.

1.2 Sources of Vortex Formation on Free Surface

According to Durgin & Hecker (1978), vortices can be formed by three fundamental reasons as shown in Figure 1.1. These reasons are listed as:

- a) Eccentric orientation of the intake relative to a symmetric approach flow area
- b) Approach flow conditions due to irregularities in boundary lining
- c) Unfavorable effects of obstructions such as offsets, piers or dividing walls, non-uniform velocity distribution caused by boundary layer separation

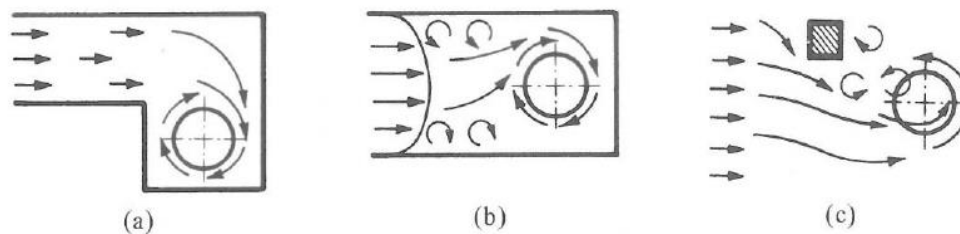


Figure 1.1 Sources of vortices (Durgin & Hecker, 1978)

1.3 Types of Intakes

In the theory and practice, many intake types can be seen. To make a straight classification, two differences can be taken into the consideration. First one is intake direction; the second one is structural differences which are location of

intake according to walls and floor of reservoir. Classification of intakes can be seen in Figure 1.2.

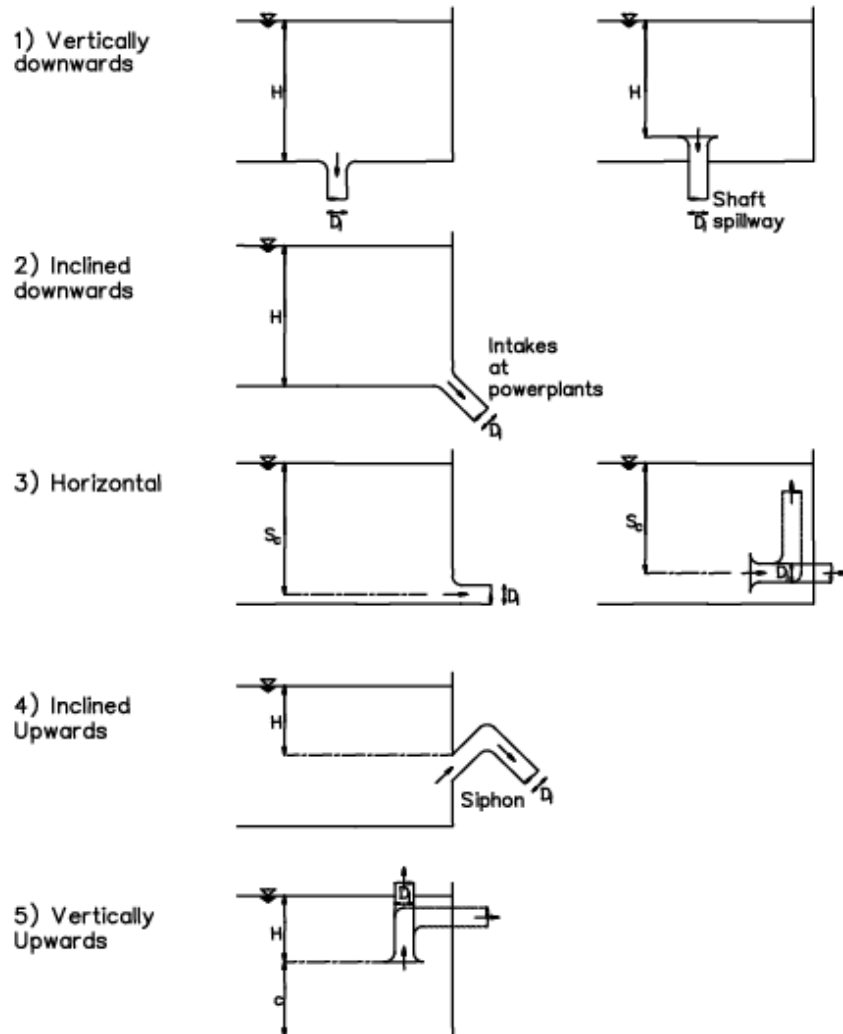


Figure 1.2 Classification of intakes (Knauss, 1987)

1.4 Types of Vortices

Vortices can be classified according to their zones such as surface vortices and subsurface vortices. Surface vortices are responsible from swirl motion and air bubble. On the other hand, subsurface vortices are responsible from air core.

To make a clear classification, some visual measuring techniques are used. Alden Research Laboratory, ARL, have classified vortex types according to their outlook. Before explaining these types, some visual concepts such as swirl, eddy, dimple and vortex tail should be explained.

Swirl, eddy, dimple and vortex tail are used to explain appearance of water surface according to vortex type which is seen in Figure 1.3. Occurrence of vortices is started by swirl motion which is only seen by reflecting light. After gaining strength, it turns into dimple then it takes the form of vortex tail into the intake.

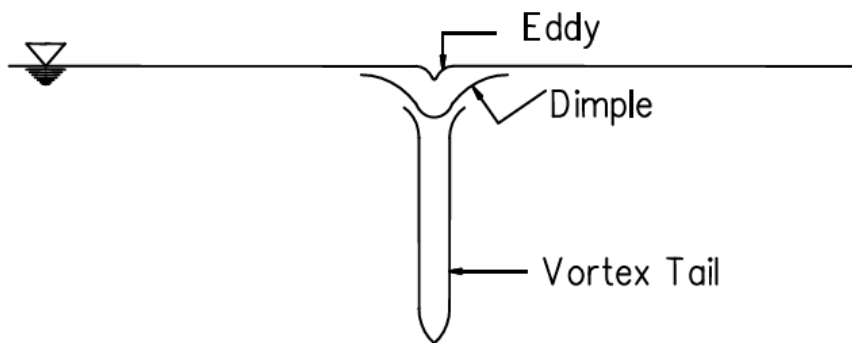


Figure 1.3 General look of eddy, dimple and vortex tail

Vortices are classified according to their appearance at the Alden Research Laboratory of WPI includes the following steps (Figure 1.4, Knauss, 1987):

- 1) Formation of weak vortices can be seen without air core, only swirl motion is occurred on the free surface.
- 2) Swirl motion starts to turn into a dimple formation.
- 3) A tail develops on the dimple through intake which does not pull in air- entrainment or air bubbles to the intake, can be seen by adding dye to water. Type 3 vortex is called dye core to intake.

- 4) Strength of vortices is larger than Type 3 in Type 4 and vortices start to pull in some objects which are floating in the reservoir, but there is no air- entrainment occurrence.
- 5) By increasing strength of vortices, air bubble form of vortices can be pulled in to the intake.
- 6) Strongest and most dangerous type of vortices has seen in this type, air is pulled in to the intake by formation of continuous air cores.

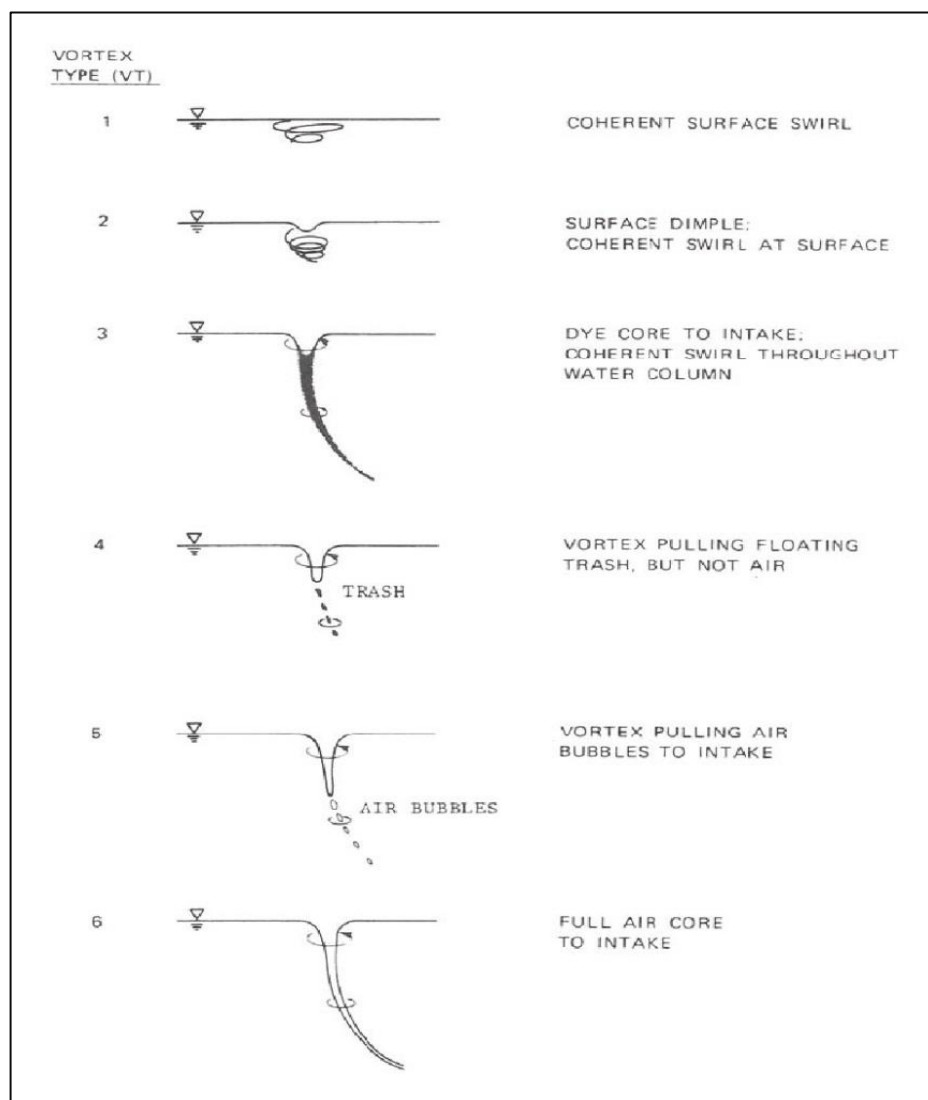


Figure 1.4 General ARL Vortex Type Classification (Knauss, 1987)

1.5 Prevention of Vortices

Vortices form due to eccentric orientation, irregularities in boundary line and unfavorable effects of obstructions that it is mentioned before. Although, intakes are designed by considering vortices, it cannot be prevented due to approach flow conditions, submergence and financial problems. To prevent vortices, some structural changes can be considered. Some suggestions are developed by Volkart and Rutschmann (1986), these are: extending flow lines between surface and intake, correction of flow conditions and using some anti-vortex devices to prevent asymmetric flow conditions.

1.6 Scope of the Study

Scope of the study is to investigate the formation of air- entraining vortices at single and multiple horizontal intakes of diameters $D_i=0.265$ m at a wide range of discharges with varying side wall clearances. By using dimensional analysis empirical equations are developed for critical submergence for single and multiple unit operation cases. By using these equations it will be possible to determine the required critical submergences above which there will be no air-entraining vortices, at single and multiple- horizontal intakes. Moreover, the results of the study are compared with those of similar past studies.

Literature review about vortex phenomena in water intakes is given in Chapter 2. In Chapter 3, theoretical concepts and modeling process of air- entrainment vortices are explained. Process of experiment and experimental setup are described in Chapter 4. Results of experiments and considerations are given in Chapter 5. Finally, in Chapter 6, conclusions and recommendations are presented.

CHAPTER 2

LITERATURE REVIEW

Anwar (1967) presented an investigation for various types of flows occurring at an intake and the prevention of vortices according to theoretical and experimental results. Experiments were carried out in a circular tank of which the top was closed. Anwar claimed that using floating rafts where vortices are occurred can successfully prevent vortex formation.

Anwar (1968) made another research about vortex formation at low- head intakes. Both theoretical and experimental studies were conducted for different types of flows and prevention of swirl and vortex occurrence. It was mentioned that the location of intakes is an important parameter to prevent vortex occurrence and also submergence of intake must be adequate to prevent vortex formation. Moreover, Anwar stated that when the radial Reynolds number, Re_R , was larger than 10^3 , deep dimples and weak vortices were not dependent on radial Reynolds number. In addition, Anwar also stated that increasing the radial Reynolds number by increasing roughness at the rigid boundaries could block vortex formation at intakes. Roughness can be increased by using floating rafts.

Gordon (1970) studied on the data of 29 different hydroelectric intakes and claimed that three important parameters affecting the formation of vortex are; velocity at the intake, V_i , submergence, S_c , and the diameter of intake, D_i .

Moreover, the relationship of these parameters was formulized by Gordon to calculate the critical submergence for both symmetrical and asymmetrical flow conditions.

$$\frac{S_c}{D_i} = 1.70 Fr \quad 2.1$$

for symmetrical, and

$$\frac{S_c}{D_i} = 2.27 Fr \quad 2.2$$

for asymmetrical approaching flow conditions. In these formulas, Fr is the Froude number ($=V_i/\sqrt{gD_i}$), S_c is the critical submergence which is the vertical distance between free surface and top point of the intake.

Johnson (1972) conducted some experiments to increase approach flow conditions at Mt. Elbert Pumped- Storage Powerplant to prevent some unwanted situations such as vortex occurrence, vibration and system fail. To increase approach flow conditions, a deflector was located to the model and it was discovered that the deflector can prevent unwanted situations. Moreover, two different devices were also tested to prevent vortex formation at extraordinary conditions. Even these devices could not prevent vortex formation, they prevented accessing of vortices into the intake, so it was accepted that experiments were successful.

Reddy and Pickford (1972) claimed that approach flow conditions at intake zone is the most important factor for vortex occurrence and this situation is a free surface phenomenon, so the Reynolds number can be eliminated from the parameters which affect vortex formation. By using both experimental and field data, it was stated that the critical submergence should be greater than the Froude number to prevent vortex formation. Moreover two formulas were generated for two different conditions by using these data.

If vortex prevention devices are not located to the intake;

$$S_c/D_i=Fr \quad 2.3$$

If vortex prevention devices are located to the intake;

$$S_c/D_i=1+Fr \quad 2.4$$

Dagget and Keulegan (1974) had studied effects of surface tension and viscosity on occurrence, shape, size of vortices and also efficiency of the intake when vortices occur. Experiments were conducted by two cylindrical tanks. Water- glycerin and different oil mixtures which had different surface tension and kinematic viscosity were used on the experiments. In the result of the study it was mentioned that viscosity can be negligible when the Reynolds number is larger than 5×10^5 and also surface tension can be negligible when the Radial Reynolds number is larger than 3×10^3 .

Zeigler (1976) had conducted some experiments on scaled model of Grand Coulee Third Power plant to research air- entraining vortices and determine effects of vortex prevention devices. Experiments were conducted with and without using thrash racks. In the results of the study it was stated that the intensity of vortices were larger when thrash racks were not used, compared to the cases where the thrash racks were used. Three different sizes of thrash racks were used and it was seen that smaller thrash racks have more effect on prevention of vortices. In addition, experiments were also conducted with using floating and sinking rafts and it was presented that sinking rafts were more successful than floating rafts to prevent occurrence of vortices.

Durgin and Hecker (1978) presented a method which is called vortex projection technique to explain scale effects on free surface vortices. With the help of this method, a projection can be investigated to prototype operating conditions. This method was applied to research potential vortices in the sump of the Emergency Core Cooling System (ECCS) of nuclear reactors. In this

experiment, vorticity sources are classified as three different types: obstruction, velocity gradients, and offset introduction. First and second types are related to viscous effects, so the Reynolds number could not be thought as independent. Moreover, vortices were classified as 6 different types in this study were presented in the first part. In the result of study, it was claimed that the Reynolds numbers cannot be independent due to viscous effects on vortices. In addition, if Weber number is larger than 1, scale effects have no effect on vortex formation, so it can be negligible. Since surface tension parameter will be important, the Weber number will be important on scale effects when Weber number is smaller than 1. Moreover, intensity of vortex was dependent on the Froude number, geometry and less on Reynolds number.

Anwar et al. (1978) had studied on beginning of air- entrainment vortices at horizontal intakes. It was presented that air- entrainment vortices can not be affected from surface tension, viscosity, radial Reynolds number which is larger than 3×10^4 and Weber number which is larger than 10^4 . Moreover, it was shown that the type of entrance of intake structure has no effect on critical submergence. However, flush mounted intakes are more efficient than bell mouth intakes due to lower circulation at the intake.

Jain et al. (1978) had conducted experiments by using two geometrically similar models of circular vortex tanks to determine effects of surface tension, viscosity and model ratio to vortex formation. This study was separated from past studies, because it was assumed that equality of Froude number was not enough to ensure dynamic similarity of model and prototype for vortex formation. Moreover, critical submergence was determined independent from the surface tension and viscosity. As a result of the study, it was mentioned that when the Weber number is in the range of $1.2 \times 10^2 < We < 3.4 \times 10^4$, the Weber number has no effect on the occurrence of vortices. Due to reduction of circulation by increasing kinematic viscosity, critical submergence will result at lower levels. Also, it was mentioned that geometric similarity is provided

according to a case where circulation parameter is constant. So, for the Froude scaled models, irregularities came from only the difference between the Reynolds number of the model and prototype. To prevent those irregularities, a correction factor, K , was involved in calculations by multiplying it with model's critical submergence. In addition, it was stated that surface tension has no influence on the critical submergence when the Weber number is larger than 120.

Hecker (1981) studied on model- prototype comparison of free surface vortices. It was stated that even inertial and gravitational forces can be reduced in Froude- scaled flows, viscous and surface tension forces cannot be reduced similarly as inertial and gravitational forces, this is called scale effect. Moreover, some conditions such as topography, boundary roughness in model, small structural changes in model and wind induced currents can change the vortex activity. For these reasons, it was claimed that old studies which were based on higher Froude- scaled flows were non- acceptable. To examine and solve scale effect problem, data was collected from 65 different water structures which have occurrence of vortex problem. According to these data, it was mentioned that the Weber and Reynolds numbers should be above critical numbers to reduce the scale effects. Also, when vortex frequency was simulated to air core vortices, the scale effects would be important for Froude- scaled flows and to overcome scale effect larger Froude scaled values could be used. But it cannot be too large which can distort the approach flow. Finally, for Froude-scaled models which have occurrence of swirls and surface dimples but no occurrence of air core vortices, the scale effect could be ignored. In addition, the following recommendations were given. Topography and boundary roughness should be considered in scaling the prototype correctly, also in tests vortex data should be taken carefully such as vortex types, location and vortex prevention devices which are used in the prototype tests should be

considered in terms of the Reynolds number due to energy dissipation difference between model and prototype.

Rindels and Gulliver (1983) collected available past data from Gordon (1970) and Reddy and Pickford (1972) studies to find the most correct critical submergence value for a known discharge. These data were given in Figure 2.1. It is seen from the figure that neither Gordon (1970) nor Reddy and Pickford (1972) studies can not provide vortex problem. Furthermore, there is a zone where dimensionless critical submergence is larger than 0.7 and Froude number is smaller than 0.5 has less free surface vortex problem, but if approach flow conditions are terrible, there will be probability occurrence of vortices in that safety zone.

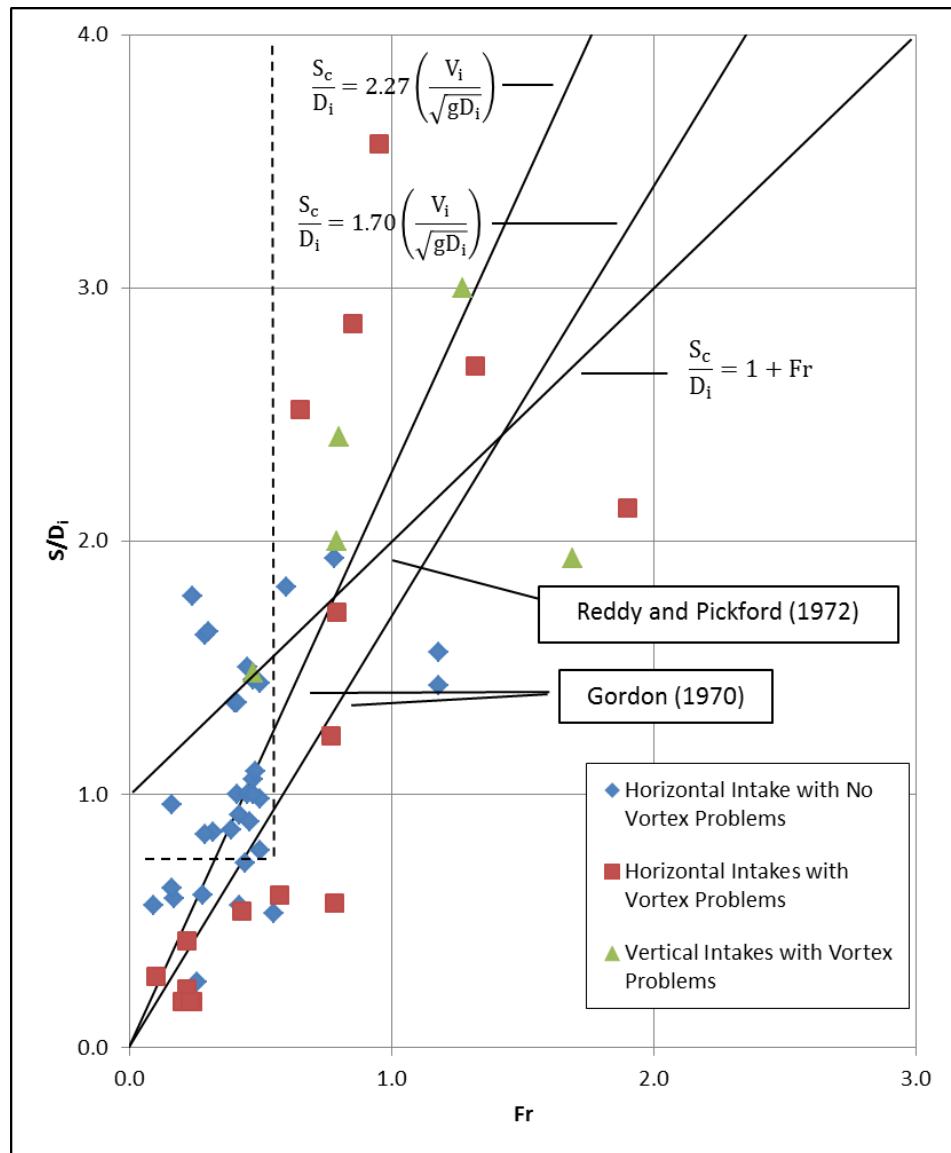


Figure 2.1 Dimensionless plot of data obtained from existing intakes, field installations and model studies (Gulliver and Rindels, 1983)

Padmanabhan and Hecker (1984) conducted experiments with using one full sized and two reduced scale models of a pump sump which have geometric scales of 1: 2 and 1: 4 to detect scale effects of free surface vortices. Experiments which were conducted according to Froude similarity and geometric scales of 1: 2 and 1: 4 have shown that scale effect had no effect on

the formation of free surface vortices. Main reason of this situation is that full-size and reduced scale models are compared with vortex types according to ARL instead of critical submergence. As a result of this study, it was stated that when $Re_R > 1.5 \times 10^4$, $Re > 7.7 \times 10^4$ and $We > 600$, viscosity and surface tension can be negligible. Moreover, when $Re > 1 \times 10^5$, hydraulic losses at the intake of model can be determined from reduced scale models.

Knauss (1987) analyzed critical submergence of some large size intakes of powerplants and recommended a submergence of 1 up to 1.5 times of the intake diameter. It is given that the submergence requirements may be found using the formula given in Figure 2.2.

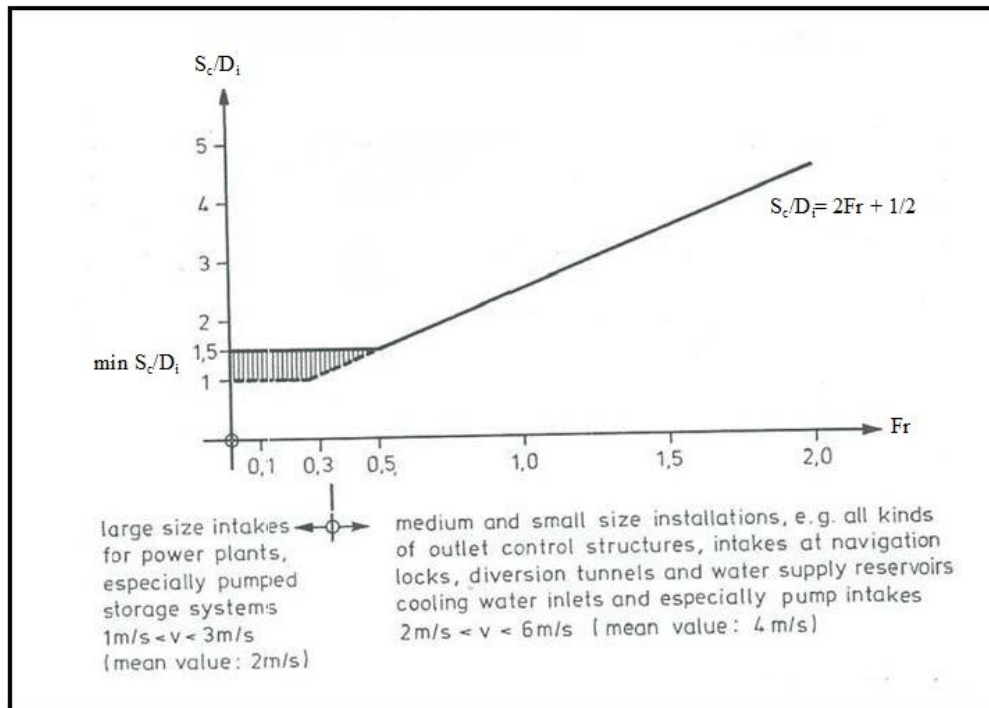


Figure 2.2 Recommended submergence for intakes with proper approach flow conditions, (Knauss, 1987)

Yıldırım and Kocabaş (1995) investigated critical submergence of air-entraining vortices at intakes in a uniform canal flow both in theory and experimental. Potential approach flow were used to solve vortex problem by combining point sink and uniform flow approach which is known Rankine's half body of revolution. According to this theory, it is assumed that critical submergence is equal to radius of an imaginary spherical sink surface and it is called critical spherical sink surface. As a result of the study a dimensionless formula was presented for critical submergence which is shown below.

$$\frac{S_c}{D_i} = \frac{1}{2\sqrt{2}} \left(C_d \frac{V_i}{U_\infty} \right)^{1/2} \quad 2.5$$

where V_i = velocity in intake pipe, C_d = discharge coefficient of the intake in a uniform canal flow, U_∞ = velocity of uniform canal flow at upstream of the intake.

Jiming et al. (2000) conducted experiments to determine minimum critical submergence of large- scaled models of double entrance pressure intakes. By comparing single and double entrance pressure intakes, it was stated that air-entrainment vortices were occurred in single entrance pressure intakes; by contrast air- entrainment vortices did not occur in double entrance pressure intakes. As a result of the study, two empirical formulas investigated to find critical submergence for double entrance pressure intakes are shown below.

For symmetrical approach flow conditions;

$$\frac{S_c}{a} = 2.39Fr - 0.001 \quad 2.6$$

For asymmetrical approach flow conditions;

$$\frac{S_c}{a} = 3.17Fr - 0.001 \quad 2.7$$

where a = height of the water intake gate.

Yıldırım et al. (2000) studied on flow boundary effects on water intake pipe to make a better investigation for critical submergence. Experiments were conducted in a horizontal rectangular flume located at the dead-end wall of a canal. It was stated that when the distance between the pipe of water intake and the dead-end wall is smaller than critical submergence, the difference between theoretical and analytical results increases. Thus, potential solution is acceptable when this distance is smaller. As a result of the study, it was expressed that the distance between the pipe of water intake and dead-end wall plays an important role for vortex formation.

Gürbüzdal (2009) conducted experiments by using horizontal intakes having different diameters to investigate the effect of the model scales on the formation of air- entraining vortices. It was mentioned that the basic parameters which affect the vortex formation are Reynolds number, Froude number and side wall clearance, $2b$, which is defined as the distance between two walls of the approach flow channel and then an empirical formula was developed to calculate critical submergence (Equation 2.8).

$$\frac{S_c}{D_i} = Fr^{0.865} \left(\frac{b}{D_i}\right)^{-0.565} Re^{0.0424} \quad 2.8$$

The above formula is valid for the following conditions;

$$0.51 \leq Fr \leq 4.03, 1.597 \leq b/D_i \leq 5.147 \text{ and } 2.96 \times 10^4 \leq Re \leq 2.89 \times 10^5$$

In addition, it was observed that S_c/D_i becomes independent of b/D_i for $b/D_i \geq 6$.

Yıldırım et al. (2009) studied the effects of size and location of two vertical intakes to critical submergence by using dimensional analyses and potential flow solution. It was stated that critical submergence of dual intakes is higher than critical submergence of single intake due to increment of irregularities on dual intakes.

Taştan and Yıldırım (2010) studied on the effects of dimensionless parameters and boundary friction on air- entraining vortices and the critical submergence of an intake located in no-circulation imposed cross-flow and still water. It was stated that vortices and critical submergence are affected by limiting values of the flow and geometrical conditions. Moreover, it was mentioned that for the cross flow; there are limiting values for the Reynolds number, Froude number and Weber number. When these limiting values are exceeded, critical submergence is independent of them.

Baykara (2013) conducted experiments at METU Hydromechanics Laboratory to investigate vortex formation under symmetrical approach flow conditions with different side wall distances and also to generate empirical formulas as a function of Reynolds number, Froude number, Weber number and geometrical parameters. In the experiments, 6 different pipe diameters were used with variations of different side wall distances and discharges. Moreover, floating raft experiments were done to prevent vortex formation. In addition, the data set was separated into three groups as maximum minimum and intermediate values of S_c/D_i and the following empirical equations were presented;

For maximum values of S_c/D_i , $1.33 \leq 2b/D_i \leq 4.00$,

$$\frac{S_c}{D_i} = Fr^{5.792} Re^{3.246} We^{-4.333} \left(\frac{2b}{D_i}\right)^{-3.489} \quad 2.9$$

For minimum values of S_c/D_i , $2.00 \leq 2b/D_i \leq 8.00$,

$$\frac{S_c}{D_i} = Fr^{0.039} Re^{-0.357} We^{-0.425} \left(\frac{2b}{D_i}\right)^{-0.602} \quad 2.10$$

For intermediate values of S_c/D_i , $3.33 \leq 2b/D_i \leq 12.00$,

$$\frac{S_c}{D_i} = Fr^{0.336} Re^{-0.229} We^{0.401} \left(\frac{2b}{D_i}\right)^{-0.261} \quad 2.11$$

By disregarding the effect of Re and We on S_c/D_i , Equation 2.12 was presented for S_c/D_i as a function of only Fr ,

$$\frac{S_c}{D_i} = Fr^{0.639} \quad 2.12$$

In the region of the data where S_c/D_i is independent of $2b/D_i$, the general formula of S_c/D_i was presented as below,

$$\frac{S_c}{D_i} = Fr^{0.324} Re^{-0.176} We^{0.282} \quad 2.13$$

The most simplified equation of S_c/D_i as a function of Fr was derived as given in Equation 2.14.

$$\frac{S_c}{D_i} = 1.278 Fr^{0.558} \quad 2.14$$

Taştan and Yıldırım (2014) conducted a study according to semi-theoretical approach, which is based on principle of flow continuity, and published experimental data to research the effects of Froude, Reynolds and Weber numbers on air-entraining vortices. It was stated that models relating to the identical ratio of the critical submergence to the intake diameter should be specified according to kinematic similarity to avoid scale effects. It was also concluded that for intakes which have the same identical ratio of the intake velocity to the velocity at critical spherical sink surface, the ratio of the critical submergence to the diameter of intake is identical and is independent of the flow and geometrical conditions. If identical ratio of the critical submergence to the diameter of intake is concern, only kinematic similarity should be considered instead of the similarities of Froude, Reynolds and Weber numbers. When the ratio of the intake velocity to the velocity at critical spherical sink surface is identical, overall scale effects because of Froude, Reynolds and Weber numbers on the ratio of the critical submergence to the diameter of the pipe will be identical.

Göğüş et al. (2015) conducted experiments at METU Hydromechanics Laboratory to investigate vortex formation for symmetrical and asymmetrical approach flow conditions at the horizontal intakes. A wide range of discharges were examined with different combinations of channel side wall clearances by using 6 different intake diameters. Based on the experimental results it was concluded that the dimensionless critical submergence increases with the increase in dimensionless flow parameters; Froude, Reynolds and Weber numbers. After comparing their data with those of Gordon (1970), Reddy and Pickford (1972) and Baykara (2013), it was stated that their study underestimates the critical submergence according to past studies due to the scale effects on the model. Floating rafts experiments were also done to investigate about vortex prevention methods. Empirical formulas were derived for critical submergence ratio based on regression analysis, as a function of Froude, Reynolds, Weber numbers and geometrical parameter. These equations are shown below in a row starting from the most general one to the most simplified form;

For symmetrical approach flow conditions;

$$(S_c/D_i) = Fr^{0.193} Re^{-0.331} We^{0.544} (2b/D_i)^{-0.241} \quad 2.15$$

$$(S_c/D_i) = Fr^{-0.066} Re^{-0.503} We^{0.747} \quad 2.16$$

$$(S_c/D_i) = Fr^{0.580} Re^{0.00795} \quad 2.17$$

and

$$(S_c/D_i) = Fr^{0.609} \quad 2.18$$

For asymmetrical approach flow conditions the general equation of S_c/D_i was expressed as given below as a function of all the dimensionless parameters involved in the phenomenon.

$$(S_c/D_i) = Fr^{0.154} Re^{-0.315} We^{0.462} \psi^{0.071} \quad 2.19$$

where $\psi = (b_1 + b_2) / (D_i) \cdot (b_1 / b_2)$

After removing the independent dimensionless terms; ψ , We and Re , in a row, the following equations for S_c/D_i were presented, respectively.

$$(S_c/D_i) = Fr^{0.209} Re^{-0.281} We^{0.421} \quad 2.20$$

$$(S_c/D_i) = Fr^{0.555} Re^{0.0025} \quad 2.21$$

and

$$(S_c/D_i) = Fr^{0.564} \quad 2.22$$

Based on the experimental results it was stated that for symmetrical approach flow conditions, critical submergence increases with the increase of Froude, Reynolds and Weber number, but when the limit values of these parameters are exceeded, critical submergence becomes independent of geometrical parameters. For asymmetrical flow conditions, critical submergence also increases with the increase of Froude, Reynolds and Weber number. However, there is no limiting value to consider dependency of critical submergence on geometrical parameter.

CHAPTER 3

MODELLING OF AIR ENTRAINING VORTICES

3.1 Introduction

In hydraulics, many concepts can not be explained by computational and theoretical studies due to complexity of problem and also these studies can not provide realistic results for many hydraulic concepts. Moreover, scaled models of many hydraulic structures have to be constructed and tested to solve potential problems before real construction due to high cost and to by-pass financial risks. By modeling, complex studies can be simplified and problems can be seen well in that concept by conducting some tests on scaled models in laboratory. Moreover, better solutions can be obtained by modeling.

Occurrence of vortices is one of the complex flow phenomena in hydraulics. It depends on condition of the approaching flow to the intake, geometrical properties of the system, intake velocity of the flow and fluid properties which are used in the experiment. Modeling of vortices is necessary by conducting laboratory experiments to explain and present reliable solutions about vortex phenomena.

3.2 Application of Dimensional Analysis to the Related Parameters

General parameters should be collected and investigated properly which are related with vortex phenomena, before conducting vortex formation experiments. These parameters are classified into three main groups;

- Flow Properties: Average velocity of flow in the intake pipe (V_i), average circulation exposed to flow (Γ) and gravity acceleration (g).
- Fluid Properties: Fluid density (ρ), dynamic viscosity of the fluid (μ) and surface tension of the fluid (σ).
- Geometric Properties of the Intake and Reservoir: Intake pipe diameter (D_i), right and left approach channel side wall distances (with respect to flow direction) of the intake structure to the intake center axis b_1 and b_2 , respectively, and the vertical distance between the bottom point of the intake and the base of the reservoir (c).

Consider the common type of a horizontal intake as shown in Figure 3.1, S_c is the critical submergence, which is the distance between the free surface level and the intake at which air- entraining vortex form. So, S_c can be described as a function of the independent variables as given below;

$$S_c = f_1 (\rho, \mu, \sigma, g, V_i, \Gamma, D_i, c, b_1, b_2) \quad 3.1$$

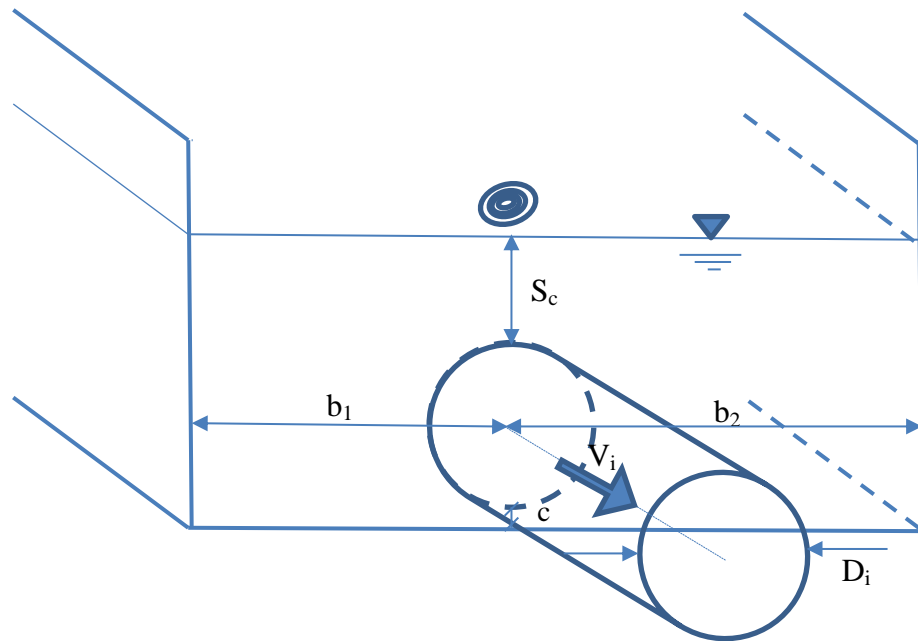


Figure 3.1 A sketch of a horizontal intake structure with related parameters

From the application of Buckingham's π theorem to the parameters given in Equation 3.1 the following dimensionless terms are obtained ;

$$\frac{S_c}{D_i} = f_2 \left(\frac{b_1}{D_i}, \frac{b_2}{D_i}, \frac{c}{D_i}, Re, Fr, We, K_o \right) \quad 3.2$$

where

$$\frac{b_1}{D_i} = \text{Aspect ratio of right side wall clearance to intake diameter}$$

$$\frac{b_2}{D_i} = \text{Aspect ratio of left side wall clearance to intake diameter}$$

$$\frac{c}{D_i} = \text{Aspect ratio of bottom clearance to intake diameter}$$

$$Re = \text{Intake Reynolds number} = \frac{V_i D_i \rho}{\mu}$$

$$Fr = \text{Intake Froude number} = \frac{V_i}{\sqrt{gD_i}}$$

$$We = \text{Intake Weber number} = \frac{\rho V_i^2 D_i}{\sigma}$$

$$K_o = \text{Intake Kolf number} = \frac{\Gamma}{V_i D_i}$$

In this study, the vertical distance between the intake pipe and bottom of the reservoir, called as bottom clearance c , is zero. Thus, $\frac{c}{D_i}$ parameter can be neglected from Equation 3.2. Equation 3.2 can be expressed in the form of Equation 3.3 which can be used for both symmetrical and asymmetrical approach flow conditions.

$$\frac{S_c}{D_i} = f_2 \left[\frac{(b_1+b_2)}{D_i} \cdot \left(\frac{b_1}{b_2}\right), Re, Fr, We, K_o \right] \quad 3.3$$

If the approach flow is symmetrical, $b_1=b_2=b$ and also the term of $(b_1+b_2)/D_i \cdot (b_1/b_2)$ is converted to $2b/D_i$. On the other hand, $(b_1+b_2)/D_i \cdot (b_1/b_2)$ becomes the dimensionless term of the asymmetry of the approach flow and it is shown by “ ψ ” in this study.

$$\frac{S_c}{D_i} = f_2 \left(\frac{2b}{D_i}, Re, Fr, We, K_o \right) \quad 3.4$$

for symmetrical approach flow and,

$$\frac{S_c}{D_i} = f_2 \left[\frac{(b_1+b_2)}{D_i} \cdot \frac{b_1}{b_2}, Re, Fr, We, K_o \right] \quad 3.5$$

for asymmetrical approach flow conditions. In the following analysis b_1 and b_2 will be considered as the small and large wall clearances, respectively, instead of considering them as the clearances of the right and left wall, so that b_1/b_2 becomes less than unity all the time.

If a model of a prototype is to be constructed, complete similarity between the model and prototype have to be provided. However, to provide complete similarity, all of the similar dimensionless parameters given in the expression of S_c/D_i has to be written for model and prototype, Equations 3.4 and 3.5, must be the same. This condition, which results in model length ratio $L_r=1$, can not be satisfied in practice. For this reason, the parameters related with vortex formation, which are less important, should be omitted from the equation and one of the parameters, which is still in the equation, should be selected as the main parameter to make a proper modelling. In this study, equality of Reynolds and Weber numbers are neglected and Froude number is selected as the main parameter, because vortex formation is a free surface phenomena and it is affected by gravity.

3.3 Effect of Froude Number

Most of past studies about vortex formation states that the most important dimensionless parameter for vortex formation is Froude number. In these studies, for instance Gordon (1970), critical submergence was only described as parameter of Froude number. For this reason, Froude similitude law is used for modelling of air- entraining vortices. However, it creates incomplete similarity between model and prototype which causes scale effect. Moreover, limit values were stated for Reynold and Weber numbers in most of the past studies to neglect viscous and surface tension forces.

3.4 Effect of Reynolds Number

Reynold number is an important dimensionless parameter for pipe flow which shows the viscous effect of flow. In the past studies, it was stated that Reynold number has no effect for vortex formation when a specific limit is exceeded. Anwar (1977) stated that when $Re_R > 3 \times 10^4$, it can be neglected for vortex formation. Moreover, Jain (1978) specified this limit as $Re > 2.5 \times 10^3$.

3.5 Effect of Weber Number

Weber number is a dimensionless parameter which reflects surface tension forces in the flow. Similarity of Weber number is necessary to prevent scale effect on dynamic similarity of models. However, similarity of Weber number can not be used in small scaled models which are modelled by using Froude similtude law. Scale effect problems which are caused by neglecting Weber number, were studied by many researchers. Some limiting values were recommended for Weber number and it was shown that surface tension can be neglected above these limits. Anwar (1977) stated that vortex formation at high Weber number is independent from surface tension forces. Jain (1978) and Padmanabhan and Hecker (1987) gave limit Weber numbers as 1.2×10^2 and 600, respectively.

3.6 Effect of Kolf Number

Kolf number is a dimensionless parameter which shows effect of circulation on the flow. Approach flow conditions, geometry of water intake and discharge of flow are the main parameters for circulation. All these parameters are shown in Equations 3.4 and 3.5. Since an unnatural circulation is not created by an external response in this study, circulation parameter, Γ , can be removed from these equations. The final forms of the equations are shown below;

For symmetrical approach flow;

$$\frac{S_c}{D_i} = f_2 \left(\frac{2b}{D_i}, Re, Fr, We \right) \quad 3.6$$

For asymmetrical approach flow;

$$\frac{S_c}{D_i} = f_2 \left[\frac{(b_1+b_2)}{D_i} \cdot \frac{b_1}{b_2}, Re, Fr, We \right] \quad 3.7$$

CHAPTER 4

EXPERIMENTAL SETUP AND METHODOLOGY

4.1 Experimental Setup

The experimental setup used in this study is composed of a large reservoir and three horizontal intake structures having the same dimensions. The photographs of the setup taken from different points are shown in Figures 4.1-4.3. The general plan view, longitudinal section and detailed plan view of the experimental setup are presented in Figures 4.4- 4.6, respectively. The width, length and height of the reservoir are 6.35 m, 6.7 and 2.05 m respectively. At the upstream section of the reservoir there is an energy dissipater structure where the energy of incoming water from the inlet pipe is dissipated. Three identical horizontal intake structure are followed by three pipes of the same diameter, $D_i=26.5$ cm, which discharge the flow into the discharge channel. The fourth intake structure seen in the photograph and in Figure 4.4 has a pipe diameter of $D_i=10.9$ cm, which was available in the original model, was not used within the scope of this study and was kept closed. Each intake structure pipe has an electromagnetic flow meter for discharge measurement.



Figure 4.1 View of the model from downstream



Figure 4.2 Hollow bricks and coarse screens which are located at the entrance of the model



Figure 4.3 Close view of the triple water intake structure from downstream

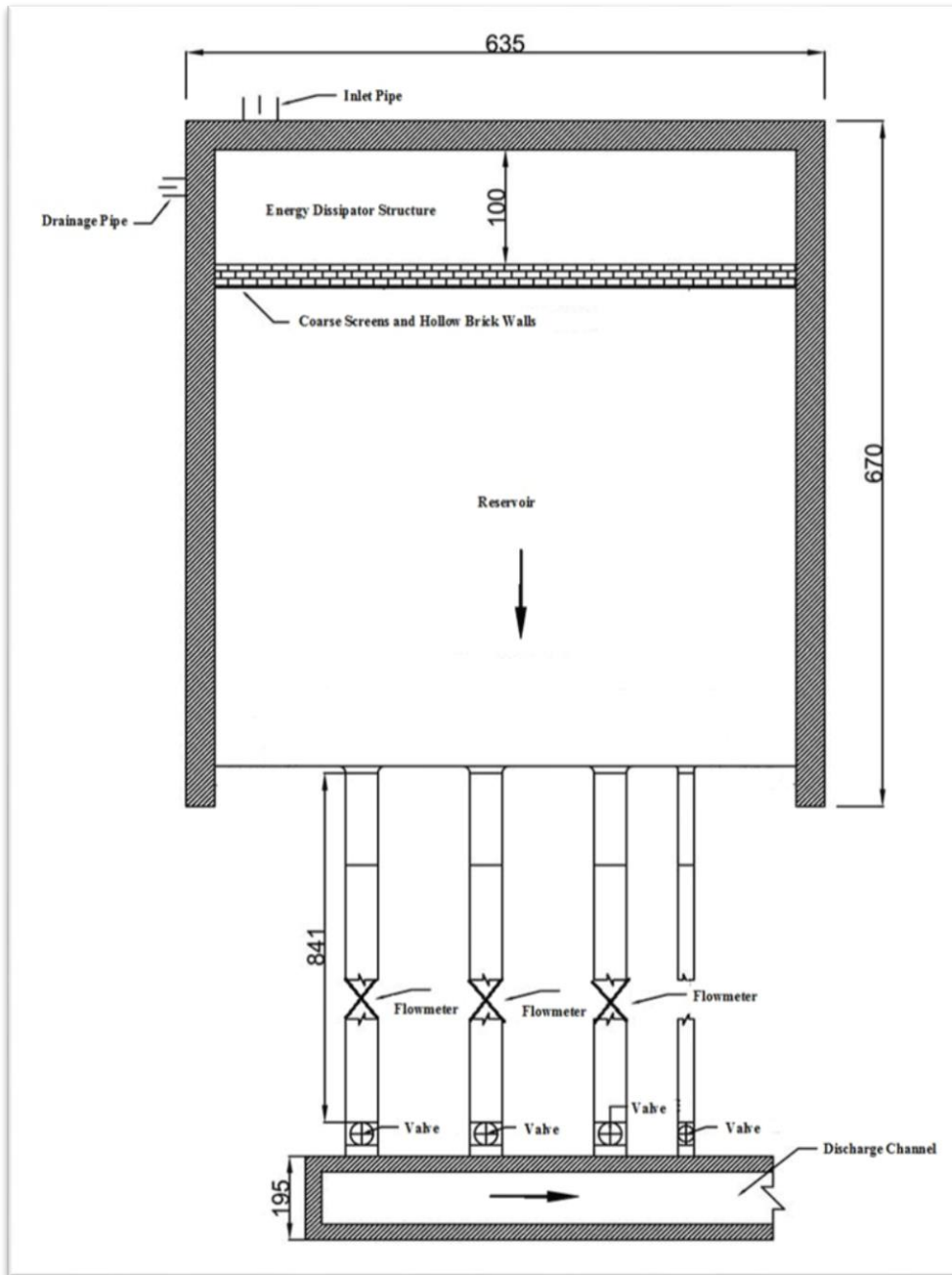


Figure 4.4 General plan view of the triple water intake structure (dimensions are in cm)

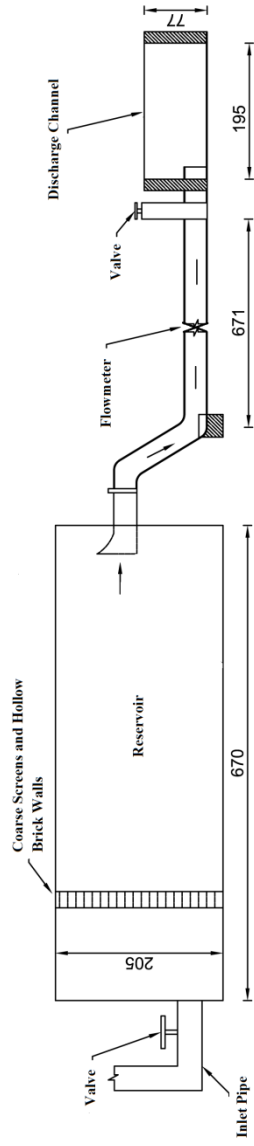


Figure 4.5 Section view of the triple water intake structure
(dimensions are in cm)

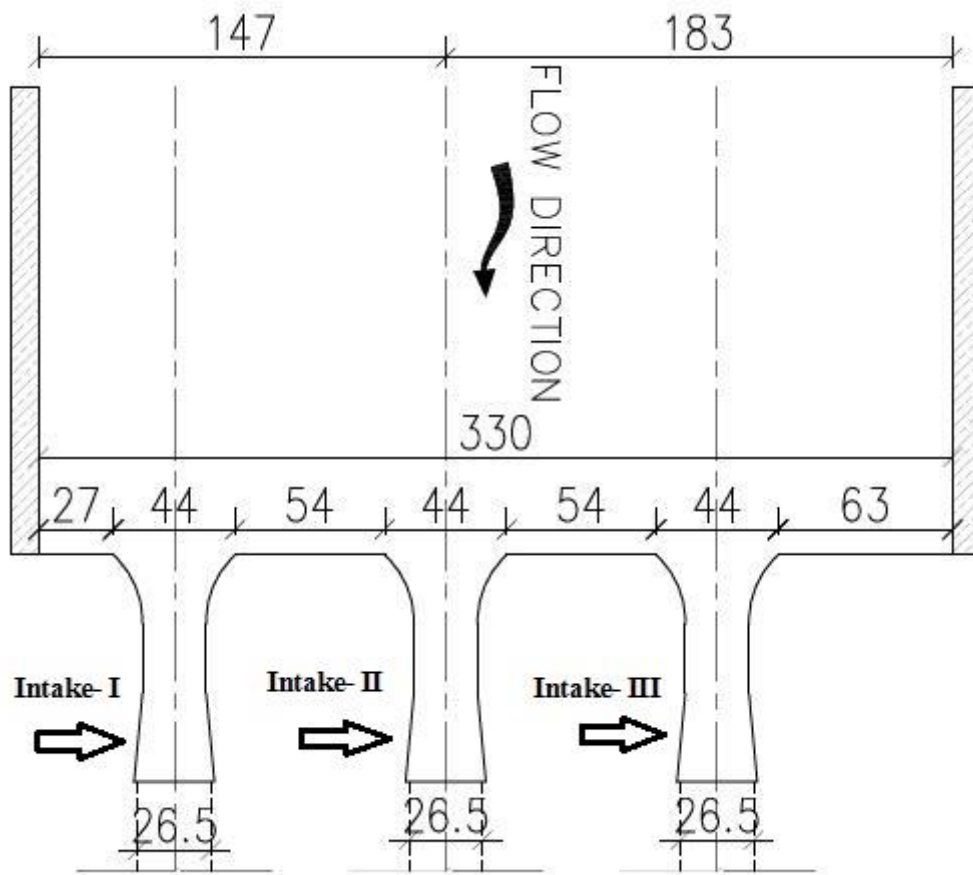


Figure 4.6 Detailed plan view of the triple water intake structure with the intake numbers and locations of them with respect to each other (dimensions are in cm)

4.2 Methodology of the Experiments

Water is conveyed to the reservoir by an intake pipe of 30 cm diameter, from the constant-head water tank of the laboratory. Then, water enters the energy dissipator and passes through the hollow bricks and coarse screens where the energy of the incoming water is dissipated, and therefore, a calm water surface is provided in the reservoir. Discharges passing through the water intake pipes are measured by the help of electromagnetic flowmeters mounted on them (Figure 4.7).



Figure 4.7 View of the electromagnetic flowmeters mounted on the water intake pipes

In this study, experiments were conducted for three different combinations of the intake structures: Single, double and triple water intakes were operated, respectively. In other words, the operation of modes of the intake structures can be named as; single unit, double unit and triple unit operation. In the first combination, experiments were conducted for single water intake for which Intake- II was selected for the experiments and the exit valves of the other intake pipes were closed to prevent occurrence of flow through these water intakes. Different side wall distances in the approach channels of the intake structures were specified previously to create symmetrical and asymmetrical flow conditions and side walls were located according to these specified distances before each experiment. In the single unit operations, 4 symmetrical and 6 asymmetrical approach flow conditions were investigated. In the double unit operations, two water intakes, Intake- II and Intake- III were operated. In this combination, 6 symmetrical and 15 asymmetrical approach flow conditions

were studied. For the triple unit operations, it was not possible to conduct more experiments due to the limited distances between the intake structures, so only 2 symmetrical and 5 asymmetrical approach flow conditions were done. Sketches of the experimental setup, water intake structures and positions of the right and left approach channel side walls for each combination are shown in Figures 4.9- 4.11.

Firstly, maximum discharge was given to the reservoir of the model and the drainage pipe valve of the water intake was opened slowly to get constant water level in the reservoir. When the access discharge and exit discharge were equal to each other on the system, constant water level was provided. After waiting for about 15- 20 minutes at this reservoir water level and observing the flow conditions in front of the intake structures in operation it was concluded that there would not be vortex formation at this level. Thus, drainage pipe valve of the water intake were opened gradually to reduce the water level in the reservoir and at this new reduced reservoir water level the similar observations were made in front of the water intake structure for another 15- 20 minutes. In the case where air- entraining vortex does not form, the process described above was repeated until air- entraining vortex is formed. After the occurrence of air- entraining vortex, discharge of the flow was measured from the flowmeter for this critical submergence. Then, the valve of the inlet pipe of water intake was closed gradually to reduce the discharge coming into the reservoir and the procedure described above was applied to determine the critical submergence for the reduced inflow. These processes were applied for each single, double and triple water intake structures for both symmetrical and asymmetrical approach flow conditions. For each case, critical submergence and discharge values were obtained. In the experiments of double and triple water intake structures, the same discharge value was passed through each pipe. Each experiment conducted with single, double and triple water intake structures for symmetrical and asymmetrical flow conditions proceeded

between 5- 7 hours. Photographs of some of the vortices observed are shown in Figures 4.12- 4.14. Measured critical submergence values and the other parameters were given in Appendices part.

At different discharge values, vortex prevention experiments were conducted. For these experiments, floating rafts made of timber which was 10 and 20 cm in width, 1 cm in thickness, were used (Figures 4.15 and 4.16). Lengths of the rafts tested according to the side wall distances used in the experiments.

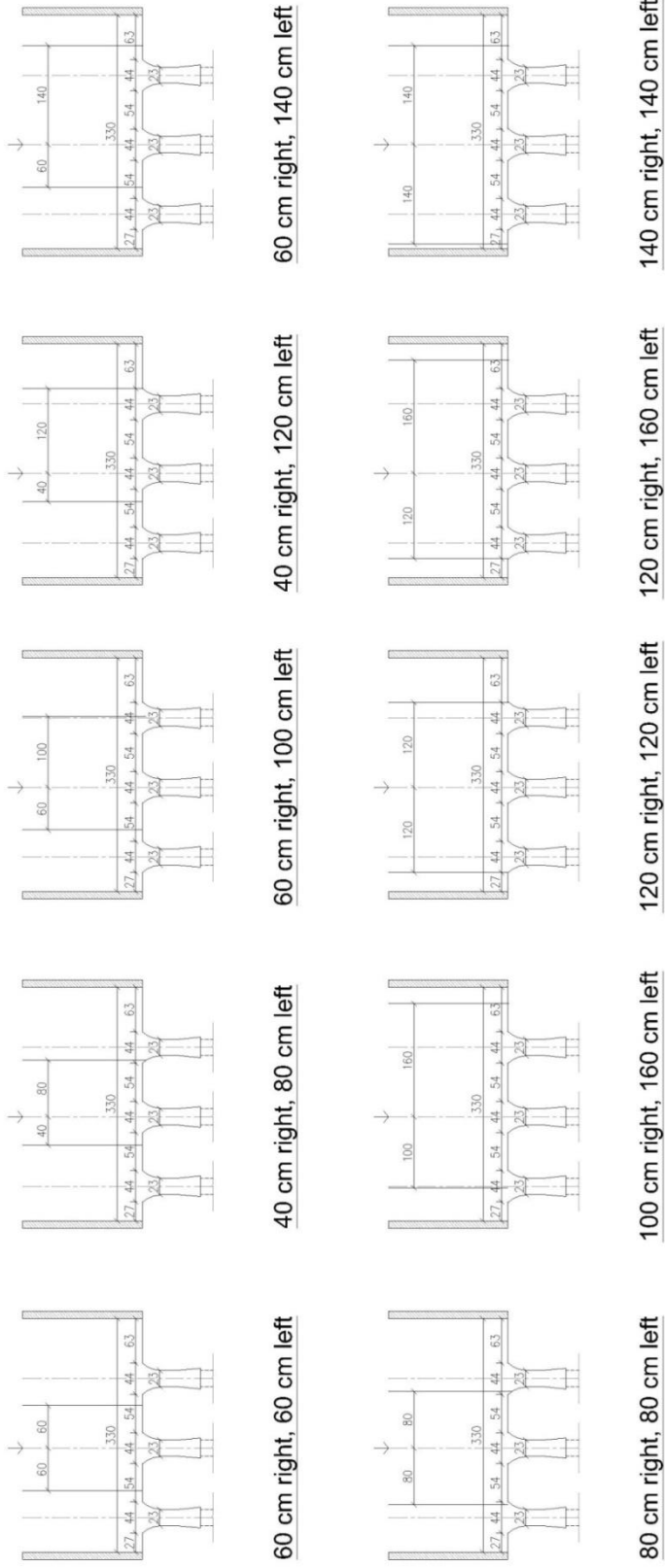


Figure 4.8 Sketch of the locations of adjustable right and left approach- channel side walls for symmetrical and asymmetrical approach flow conditions when only one intake structure, Intake- II, is in operation

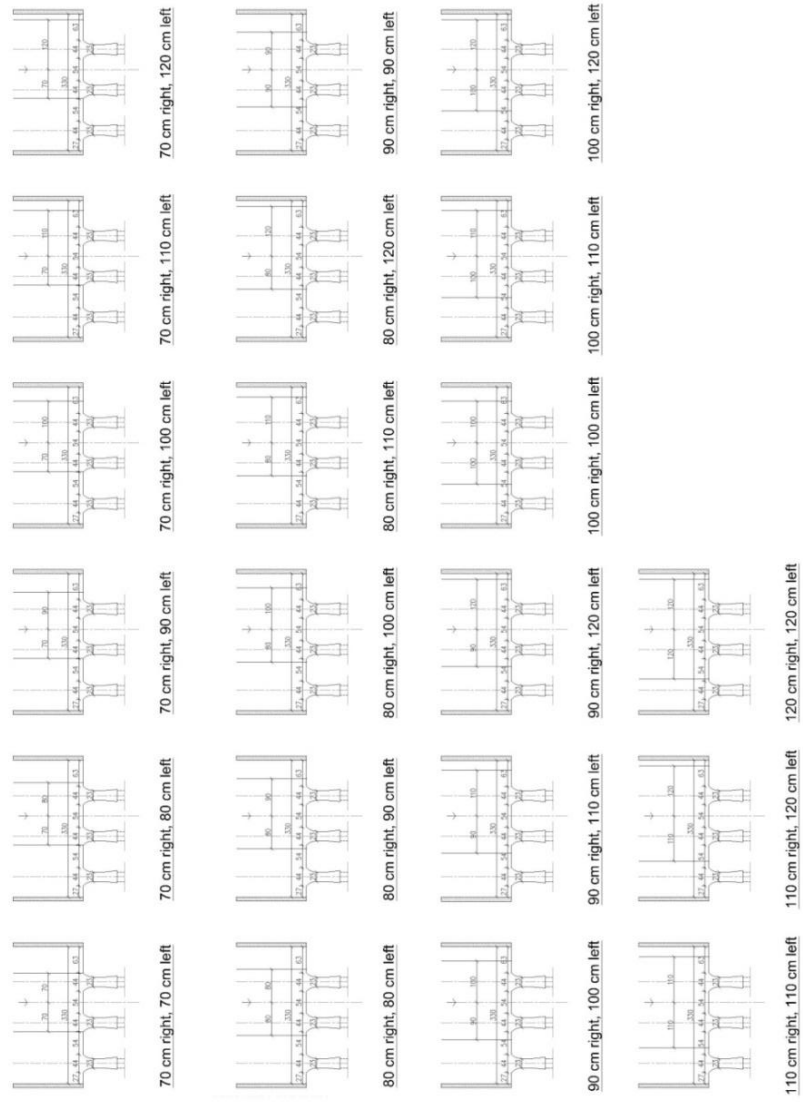
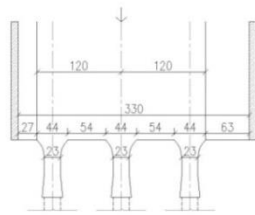
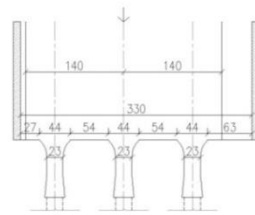


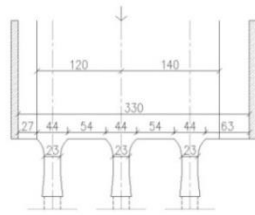
Figure 4.9 Sketch of the locations of adjustable right and left approach- channel side walls for symmetrical and asymmetrical approach flow conditions when two intake structures, Intake- II and Intake- III, are in operation



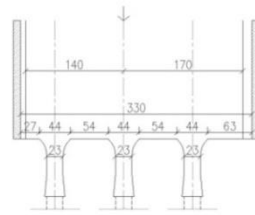
120 cm right, 120 cm left



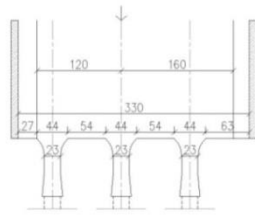
140 cm right, 140 cm left



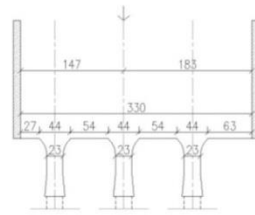
120 cm right, 140 cm left



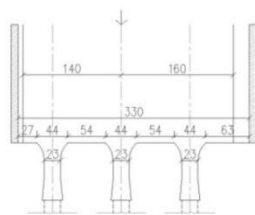
140 cm right, 170 cm left



120 cm right, 160 cm left



147 cm right, 183 cm left



140 cm right, 160 cm left

Figure 4.10 Sketch of the locations of adjustable right and left approach-channel side walls for symmetrical and asymmetrical approach flow conditions when all of three intake structures are in operation



Figure 4.11 Vortex formation in front of single water intake structure ($Q=110$ lt/s)

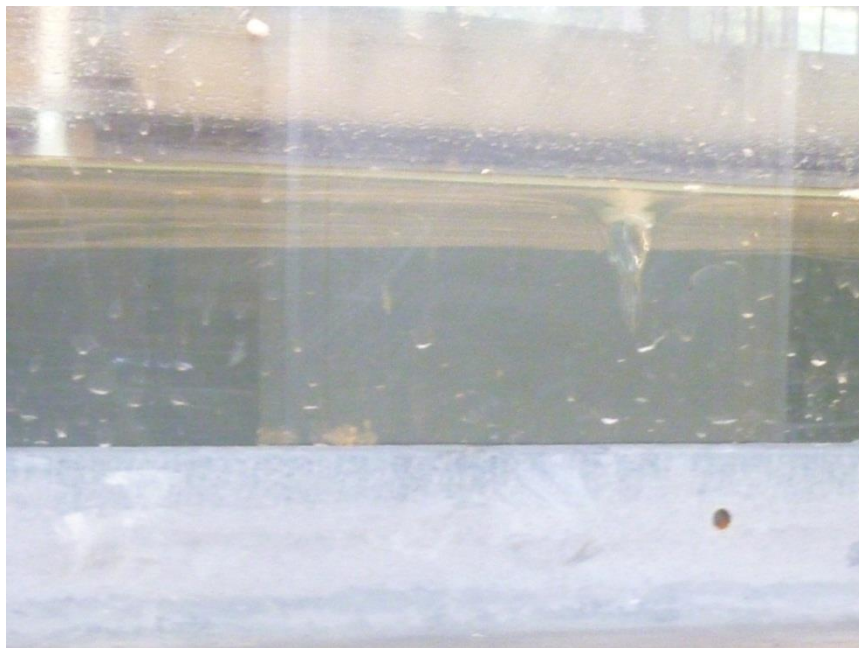


Figure 4.12 Vortex formation in front of double water intake structure ($Q=110.51$ lt/s)



Figure 4.13 Vortex formation in front of double water intake structure
($Q=111.51$ lt/s)



Figure 4.14 Vortex formation in front of triple water intake structure ($Q=96.20$
lt/s)



Figure 4.15 Top view of floating rafts which is used at vortex prevention during experiments (dimensions are in cm)



Figure 4.16 Top view of floating rafts which is used at vortex prevention during experiments (dimensions are in cm)

CHAPTER 5

ANALYSIS AND EVALUATION OF THE EXPERIMENTAL RESULTS

5.1 Introduction

In the following sections the experimental results and their discussions will be presented for single, double and triple water intake structures under the titles of “symmetrical” and “asymmetrical approach flow conditions”. Ranges of the important parameters used in the experiments are given in tables for each approach flow conditions. The variation of measured S_c/D_i values in this study with the related hydraulic parameters; Fr, Re, We as a function of geometrical parameter, ψ , were shown graphically. For symmetrical flow conditions Equation 3.6. was taken as reference. On the other hand, Equation 3.7. was considered as reference for asymmetrical flow conditions. Moreover, empirical equations were derived for variation of S_c/D_i as a function of the related hydraulic parameters; Fr, Re, We and ψ . In addition, the empirical equations obtained by Göğüş et al. (2015) for single intake structure were applied to the data of this study and the results of both studies were compared with each other.

5.2 Single Water Intake Structure

5.2.1 Symmetrical Approach Flow Conditions

Important hydraulic and geometrical parameters used in the experiments and those calculated taking Equation 3.6 as reference are given in Table 5.1.

Table 5.1 The ranges of important hydraulic and geometrical parameters used and calculated in the experiments of symmetrical approach flow conditions

D_i (cm)	Ranges of Parameters						Number of Observations
	Q_i (lt/s)	S_c/D_i	Fr	Re	We	2b/D_i	
26.5	126.83	1.97	1.43	609393	19215	10.57	14
	~	~	~	~	~	~	
	77.53	1.37	0.87	372495	7179	4.53	

5.2.1.1 Variation of S_c/D_i with Dimensionless Flow Parameters under Symmetrical Approach Flow Conditions

Variation of S_c/D_i values with the related hydraulic parameters Fr, Re and We as a function of 2b/D_i are shown in Figures 5.1- 5.3. The following evaluations can be made from these figures: for a given 2b/D_i value, S_c/D_i value increases with increasing Fr, Re and We numbers. For a given Fr, Re and We numbers, when 2b/D_i value increases, S_c/D_i value also increases.

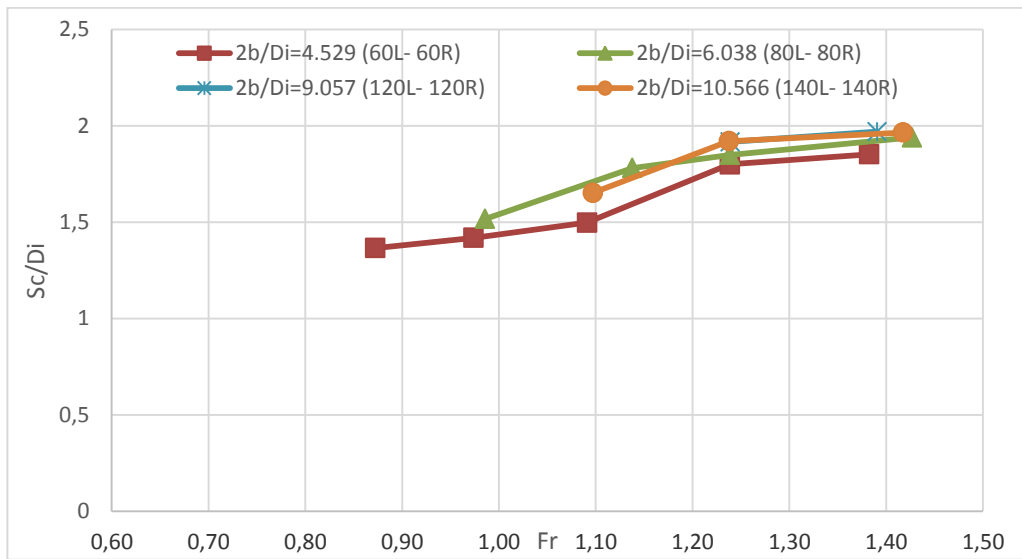


Figure 5.1 Variation of S_c/D_i with Fr for symmetrical approach flow conditions at single water intake

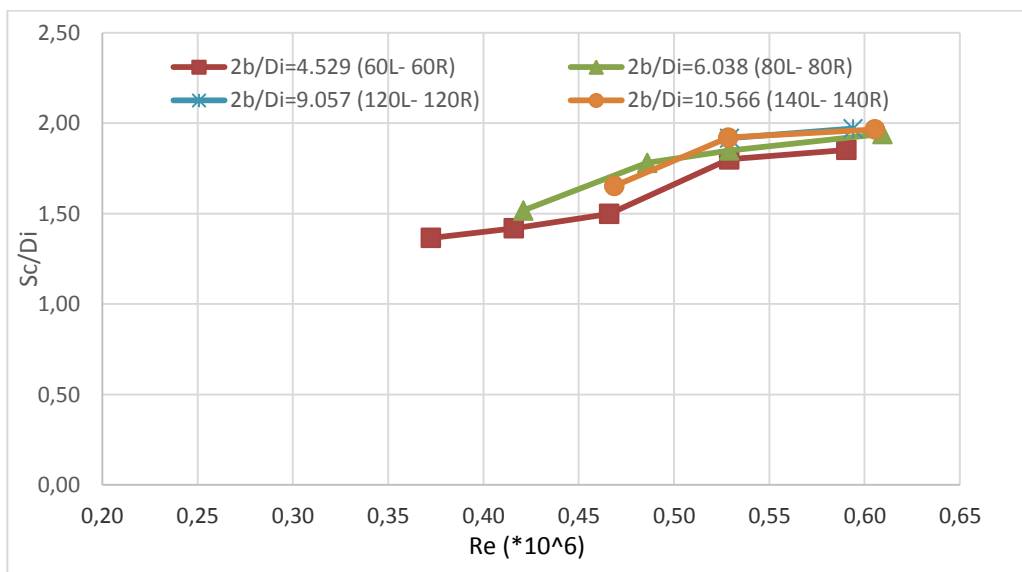


Figure 5.2 Variation of S_c/D_i with Re for symmetrical approach flow conditions at single water intake

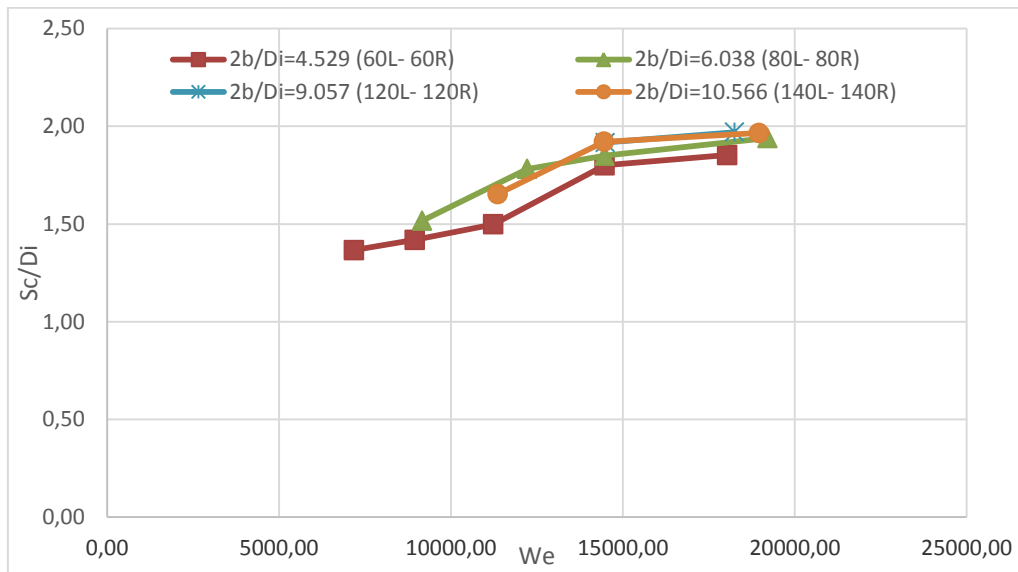


Figure 5.3 Variation of S_c/D_i with We for symmetrical approach flow conditions at single water intake

5.2.1.2 Comparison of Results of Present Study and Gögüş et al.'s (2015) Study

In Gögüş et al.'s (2015) study, six different pipe diameters were used in the experiments to determine the relationships for critical submergence. Whereas in the present study only one type of pipe with a diameter of 26.5 cm was tested. Since the pipe diameter of $D_i=25$ cm was the only one close to the pipe used in the present study, $D_i=26.5$ cm, the experimental results of those two pipes were compared with each other by plotting the values of S_c/D_i with respect to; Fr , Re and We as shown in Figures 5.4- 5.6. Although pipe diameters of both studies are not the same, the general trend of both data groups is approximately similar which indicates that the Fr vs. S_c/D_i relationship proposed by Gögüş at al. (2015) can be used at larger Froude numbers. Also it should not be forgotten that the layouts of the entrance sections of both intake structures are not the same. While the model of the present study has a bell mouth transition at the entrance section between the

reservoir and the pipe of the intake structure, the other one has a sudden contraction with sharp corners. Thus, it should be considered that similar results can not be obtained from these two studies.

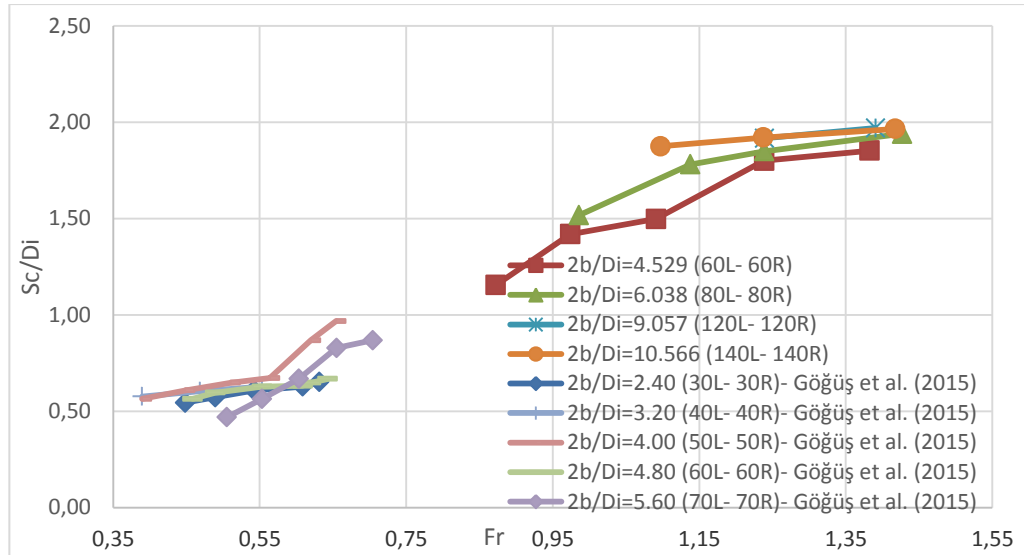


Figure 5.4 Variation of S_c/D_i with Fr for data of present study ($D_i=26.5$ cm) and Göğüş et al.'s (2015) study ($D_i=25$ cm)

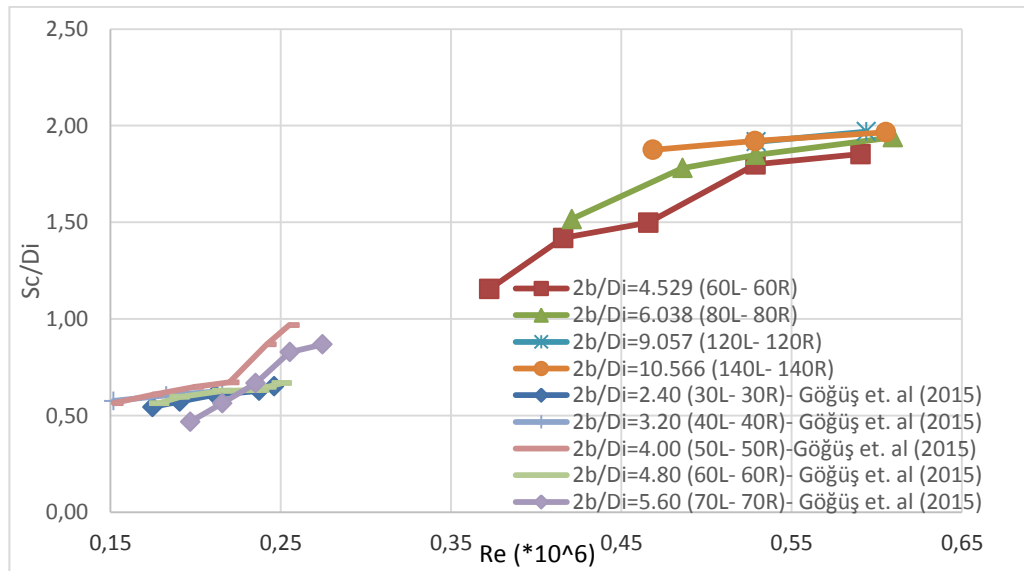


Figure 5.5 Variation of S_c/D_i with Re for data of present study ($D_i=26.5$ cm) and Göğüş et al.'s (2015) study ($D_i=25$ cm)

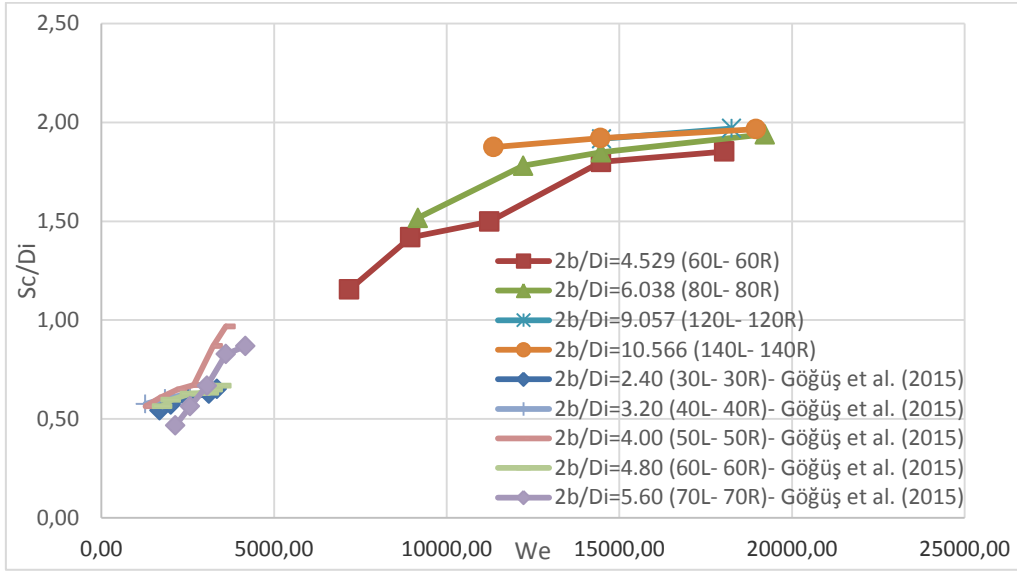


Figure 5.6 Variation of S_c/D_i with We for data of present study ($D_i=26.5$ cm) and Göğüş et al.'s (2015) ($D_i=25$ cm)

5.2.1.3 Derivation of Empirical Equations for Dimensionless Critical Submergence

5.2.1.3.1 The General Case

Variation of S_c/D_i with the related parameters for symmetrical approach flow conditions was given in Equation 3.6. By considering this equation, regression analysis were applied to the data of present study and Equation 5.1 was obtained with $R^2=0.92$.

$$S_c/D_i = Fr^{-0.126} Re^{-0.423} We^{0.629} (2b/D_i)^{0.084} \quad 5.1$$

Figure 5.7 compares the measured S_c/D_i data with those calculated from Equation 5.1 which is valid for the ranges of dimensionless parameters used and presented in Table 5.1 in this study. The calculated data lies between $\pm 10\%$ error lines.

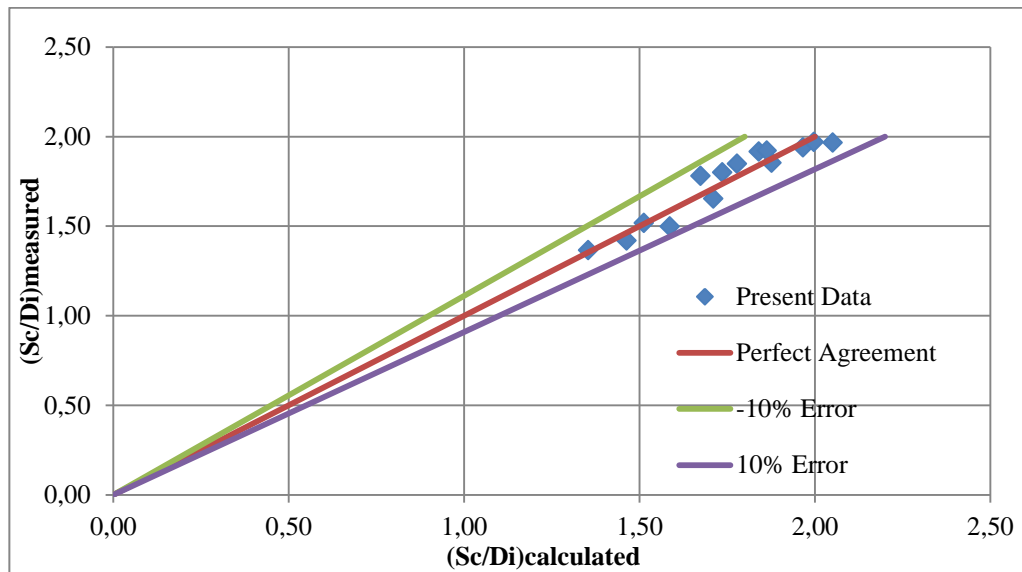


Figure 5.7 Comparison of $(S_c/D_i)_{\text{calculated}}$ data obtained from Equation 5.1, with $(S_c/D_i)_{\text{measured}}$ data for single water intake structure under symmetrical approach flow conditions

5.2.1.3.2 Simplified Empirical Equations for S_c/D_i

To obtain simplified empirical equations for S_c/D_i , the numbers of independent dimensionless parameters; $2b/D_i$, We and Re were reduced one by one from the general equation of S_c/D_i (Equation 3.6) and three empirical equations, Equations 5.2- 5.4, for S_c/D_i were derived using regression analysis. Variation of $(S_c/D_i)_{\text{measured}}$ data with those of calculated from Equations 5.2- 5.4 were shown in Figures 5.8- 5.10 for three different cases.

$$S_c/D_i = Fr^{-0.065} Re^{-0.414} We^{0.632} \quad \text{and } R^2=0.876 \quad 5.2$$

$$S_c/D_i = Fr^{0.753} Re^{0.032} \quad \text{and } R^2=0.876 \quad 5.3$$

$$S_c/D_i = 1.520 * Fr^{0.785} \quad \text{and } R^2=0.876 \quad 5.4$$

The correlation coefficients presented above show that the elimination of $2b/D_i$, We and Re from the original expression of S_c/D_i does not change the value of S_c/D_i . Almost all the S_c/D_i data calculated from Equations 5.2- 5.4

falls between $\pm 15\%$ error lines while the values of error lines were $\pm 10\%$ from Equation 5.1.

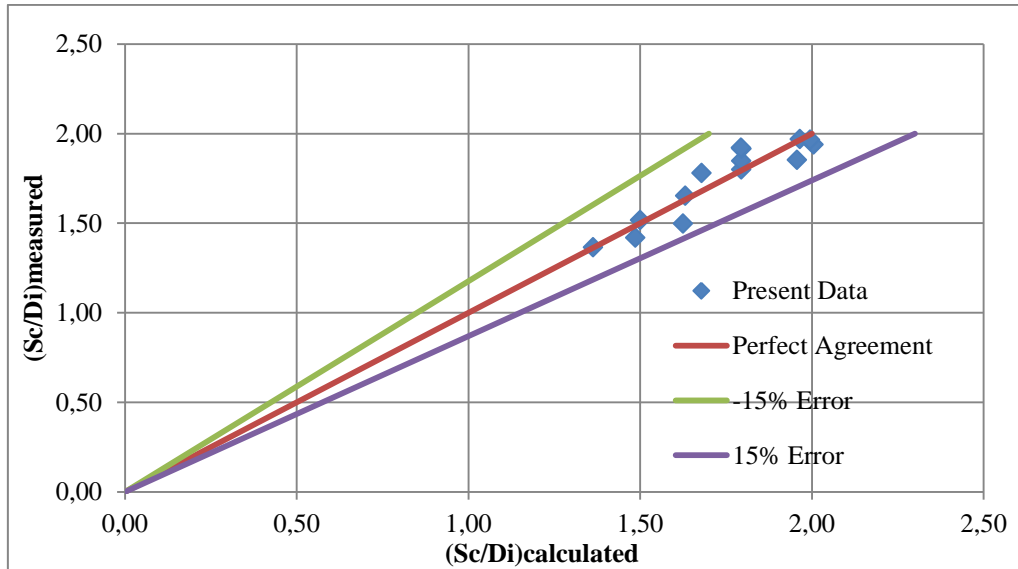


Figure 5.8 Comparison of $(S_c/D_i)_{\text{calculated}}$ data obtained from Equation 5.2, with $(S_c/D_i)_{\text{measured}}$ data for single water intake structure under symmetrical approach flow conditions

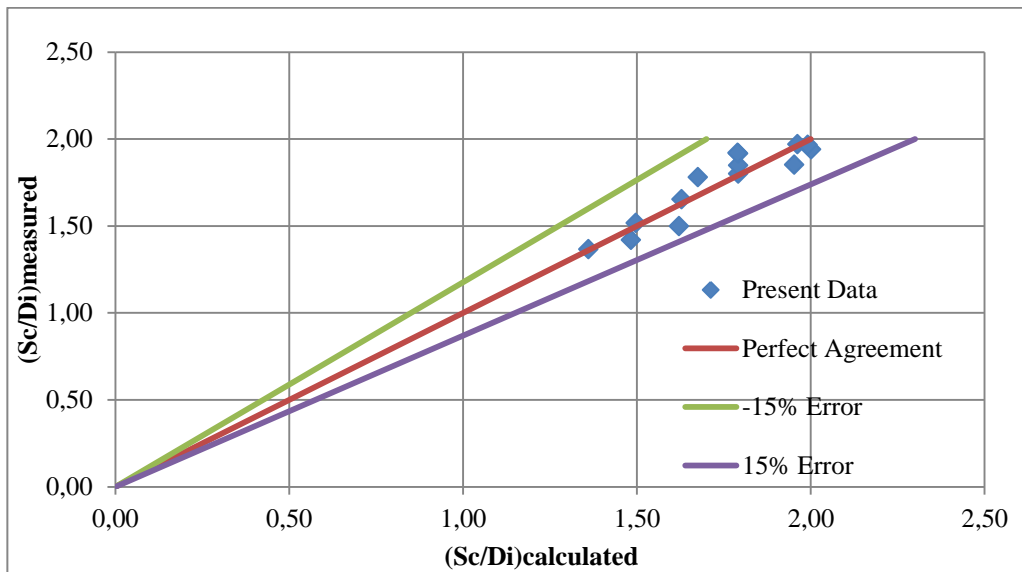


Figure 5.9 Comparison of $(S_c/D_i)_{\text{calculated}}$ data obtained from Equation 5.3, with $(S_c/D_i)_{\text{measured}}$ data for single water intake structure under symmetrical approach flow conditions

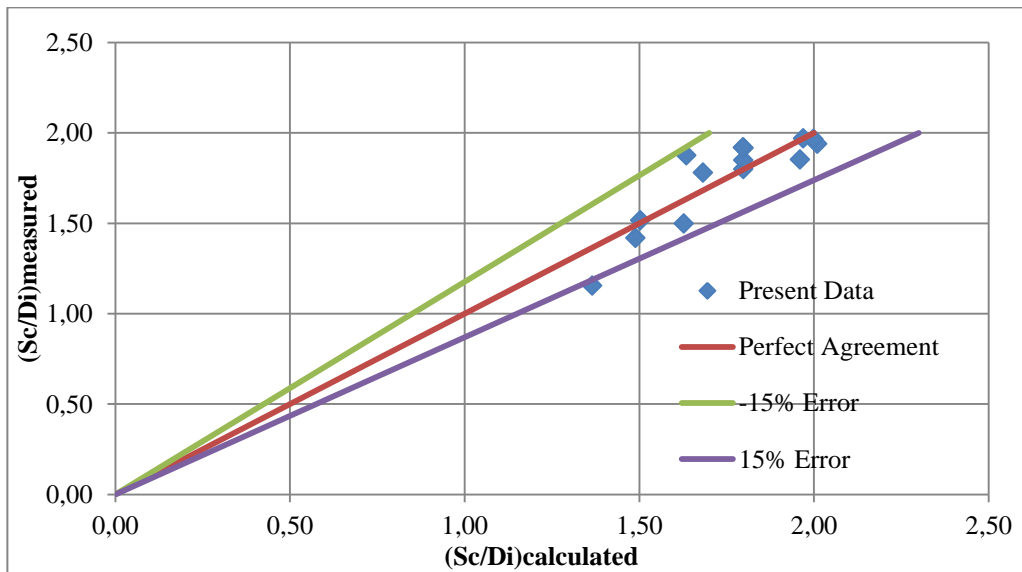


Figure 5.10 Comparison of $(S_c/D_i)_{\text{calculated}}$ data obtained from Equation 5.4, with $(S_c/D_i)_{\text{measured}}$ data for single water intake structure under symmetrical approach flow conditions

5.2.1.4 Comparison of the Results of Present Study with the Empirical Equations Proposed by Göğüş et al. (2015)

In Göğüş et al.'s (2015) study, horizontal water intakes of six different pipe diameters were used to determine the relationships for critical submergence. By using the data of those experiments with Baykara's (2013) data which had been obtained from the same model under symmetrical approach flow conditions, a general empirical equation (Equation 2.15) and simplified empirical equations (Equations 2.16- 2.18) for S_c/D_i were obtained. To see how the data of present study match up with Göğüş et al.'s (2015) study, the data of the present study were applied to those equations to get the corresponding $(S_c/D_i)_{\text{calculated}}$ values. Figures 5.11- 5.14 show the data of $(S_c/D_i)_{\text{measured}}$ with $(S_c/D_i)_{\text{calculated}}$. From these figures it can be stated that the empirical equations for S_c/D_i stated above (Equations 2.15- 2.18), can represent S_c/D_i data of the present study within the $\pm 25\%$ error lines as presented in the figures. In the case of reducing the number of independent dimensionless parameters from the general expression of S_c/D_i as described in the previous section, the ranges of error lines become $\pm 35\%$ in Figures 5.12 and 5.14. In conclusion, it can be said that Equations 2.15 and 2.16 can be used to determine S_c/D_i values for a similar model with the existing error ranges.

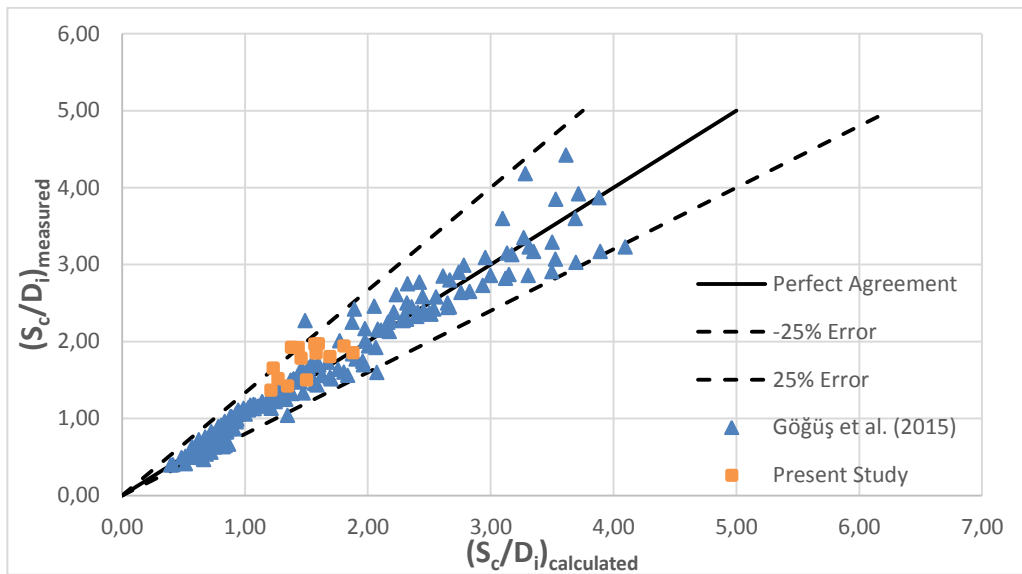


Figure 5.11 Comparison of $(S_c/D_i)_{measured}$ of the present study with $(S_c/D_i)_{calculated}$ from Equation 2.15 proposed by Göğüş. et al (2015) for symmetrical approach flow conditions

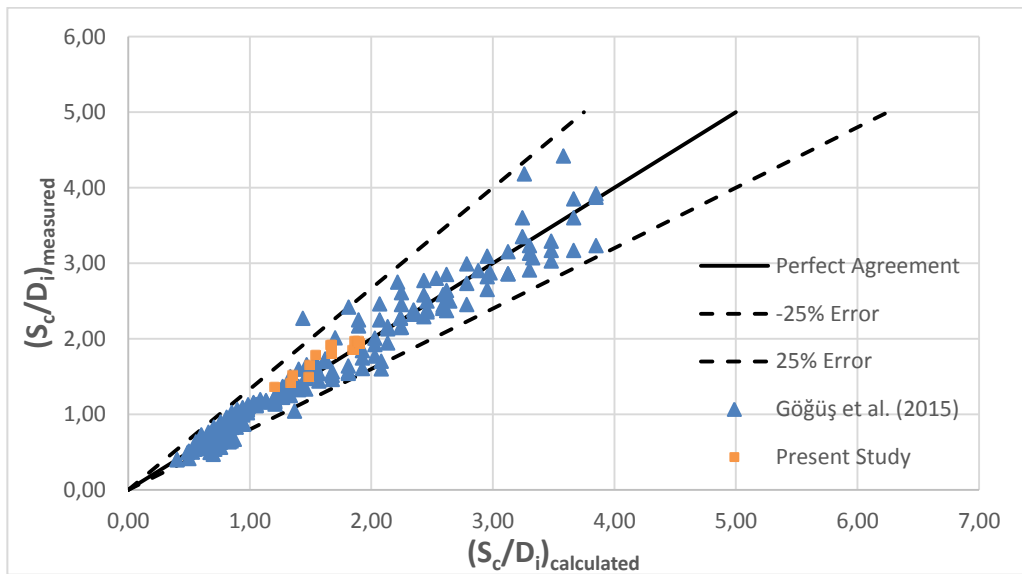


Figure 5.12 Comparison of $(S_c/D_i)_{measured}$ of the present study with $(S_c/D_i)_{calculated}$ from Equation 2.16 proposed by Göğüş et al. (2015) for symmetrical approach flow conditions

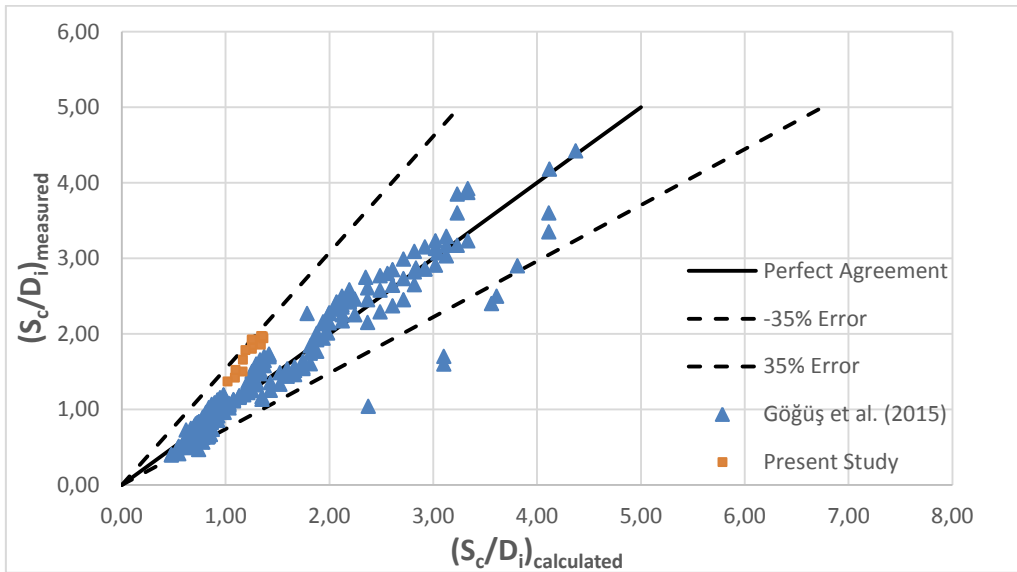


Figure 5.13 Comparison of $(S_c/D_i)_{measured}$ of the present study with $(S_c/D_i)_{calculated}$ from Equation 2.17 proposed by Gögüş et al. (2015) for symmetrical approach flow conditions

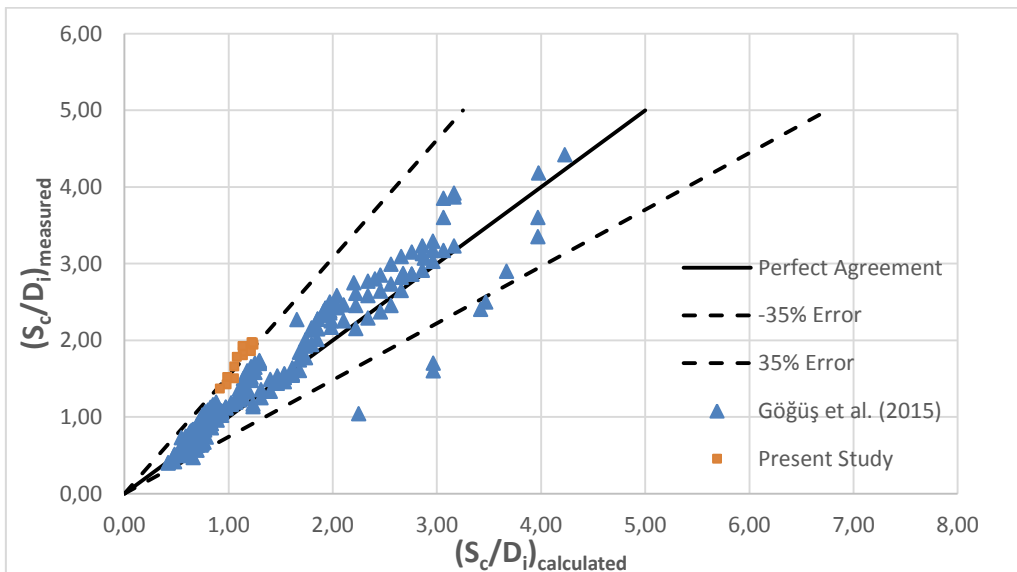


Figure 5.14 Comparison of $(S_c/D_i)_{measured}$ of the present study with $(S_c/D_i)_{calculated}$ from Equation 2.18 proposed by Gögüş et al. (2015) for symmetrical approach flow conditions

5.2.2 Asymmetrical Approach Flow Conditions

Important hydraulic and geometrical parameters used and calculated in the experiments are given in Table 5.2.

Table 5.2 The ranges of important hydraulic and geometrical parameters used and calculated in the experiments of asymmetrical approach flow conditions

D_i (cm)	Ranges of Parameters						Number of Observations
	Q_i (lt/s)	S_c/D_i	Fr	Re	We	ψ	
26.5	126.81	1.94	1.43	609260	19206	7.93	25
	~	~	~	~	~	~	
	68.67	1.17	0.77	329921	5632	2.26	

5.2.2.1 Variation of S_c/D_i with Dimensionless Flow Parameters under Asymmetrical Approach Flow Conditions

Variation of S_c/D_i values with the related hydraulic parameters; Fr, Re and We as a function of ψ are shown in Figures 5.15- 5.17. From these figures it can be stated that for a given ψ , S_c/D_i increases with increasing Fr, Re and We numbers. Similarly for a given Fr, Re and We numbers, S_c/D_i value increases while ψ value increases.

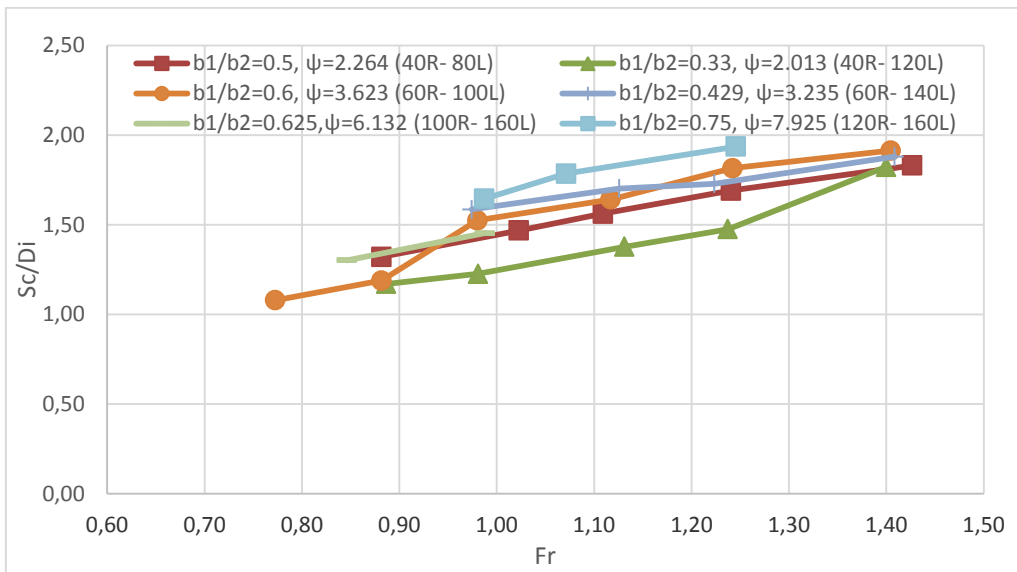


Figure 5.15 Variation of Sc/Di with Fr for asymmetrical approach flow conditions at single water intake

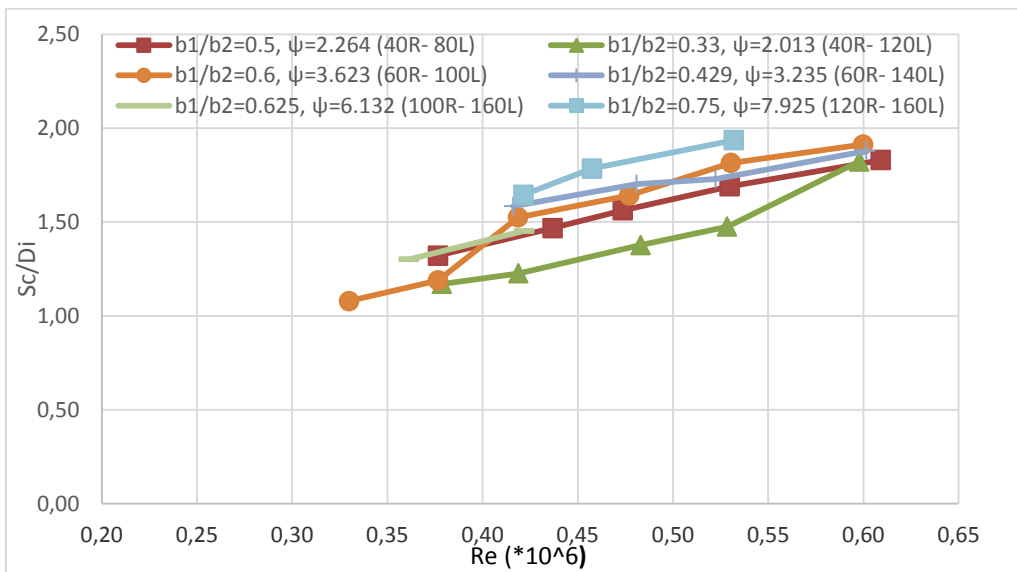


Figure 5.16 Variation of Sc/Di with Re for asymmetrical approach flow conditions at single water intake

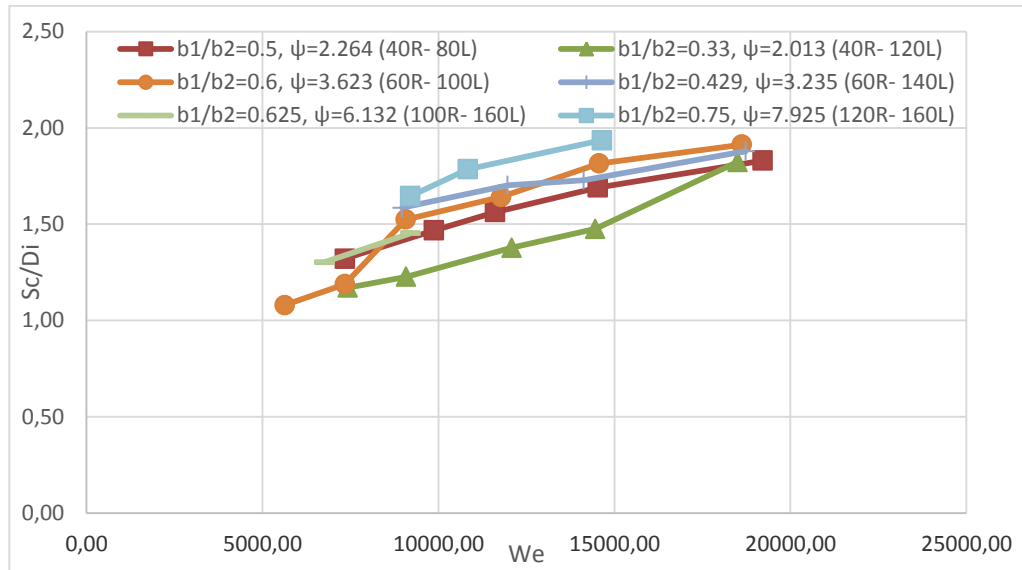


Figure 5.17 Variation of S_c/D_i with We for asymmetrical approach flow conditions at single water intake

5.2.2.2 Comparison of the Results of Present and Göğüş et al.'s (2015) Studies

In Göğüş et al.'s (2015) study, six different pipe diameters were tested in a horizontal water intake structure with various side wall clearances to determine the critical submergence under asymmetrical approach flow conditions. Variation of S_c/D_i data with the related hydraulic parameters; Fr , Re and We are shown in Figures 5.18- 5.20 for the present study and Göğüş et al.'s (2015) study together. Although pipe diameters and the shapes of the intake entrance profiles of both studies are not the same, general trends of both data groups are approximately similar. The ranges of the Fr , Re and We used in the study of Göğüş et al. (2015) are much smaller than those of the present study. Therefore, with these two groups of data a wide range of Fr , Re and We is covered on the given figures. Even though the both models used in the experiments are not exactly similar as stated earlier, there is a good harmony between present and Göğüş et al.'s (2015) data for similar ψ values. However,

evaluation of the results of the present study should be done with its own parameters.

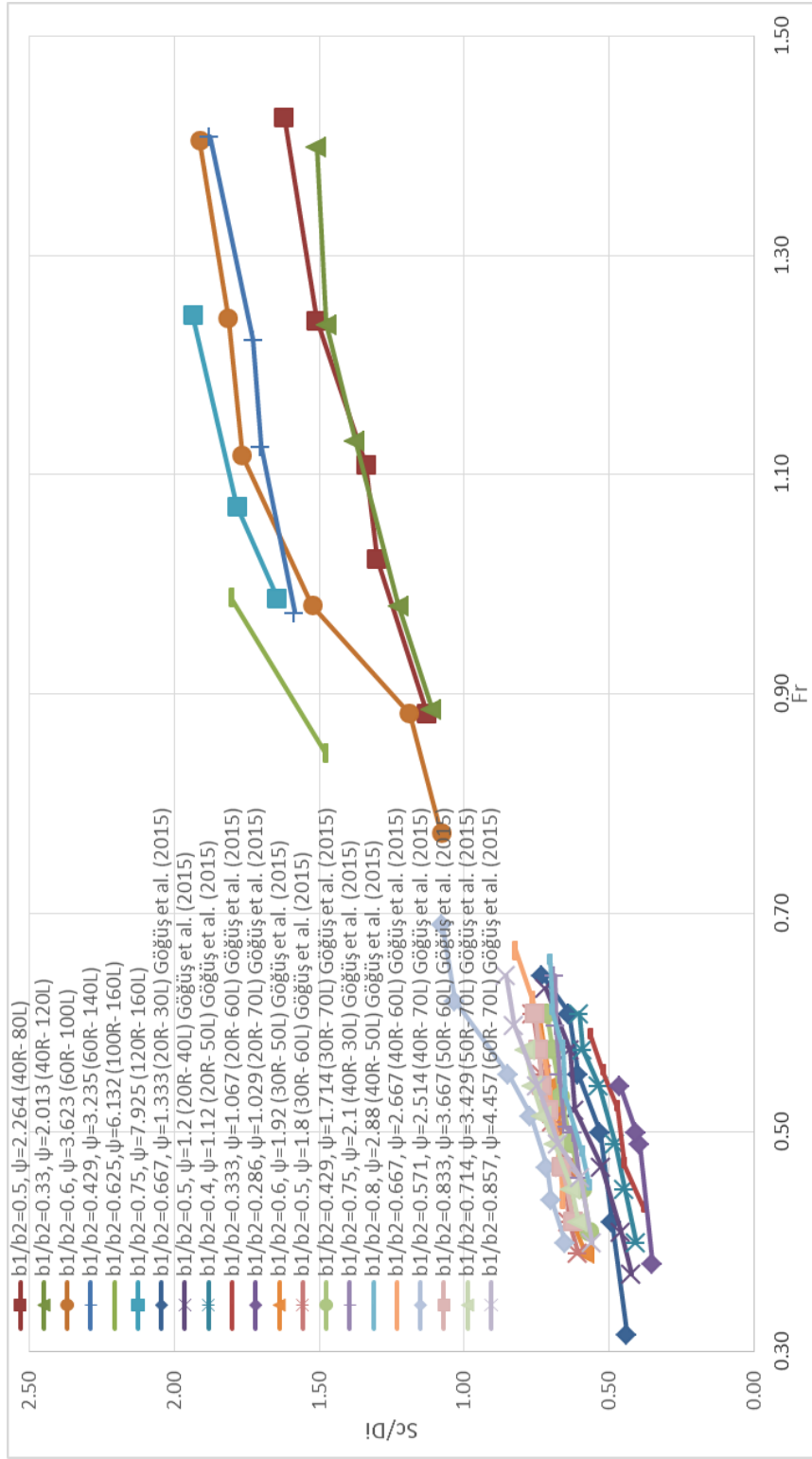


Figure 5.18 Variation of S_c/D_i with Fr for the present study ($D_i=26.5$) cm and Göğüş et al.'s (2015) study ($D_i=25$) cm

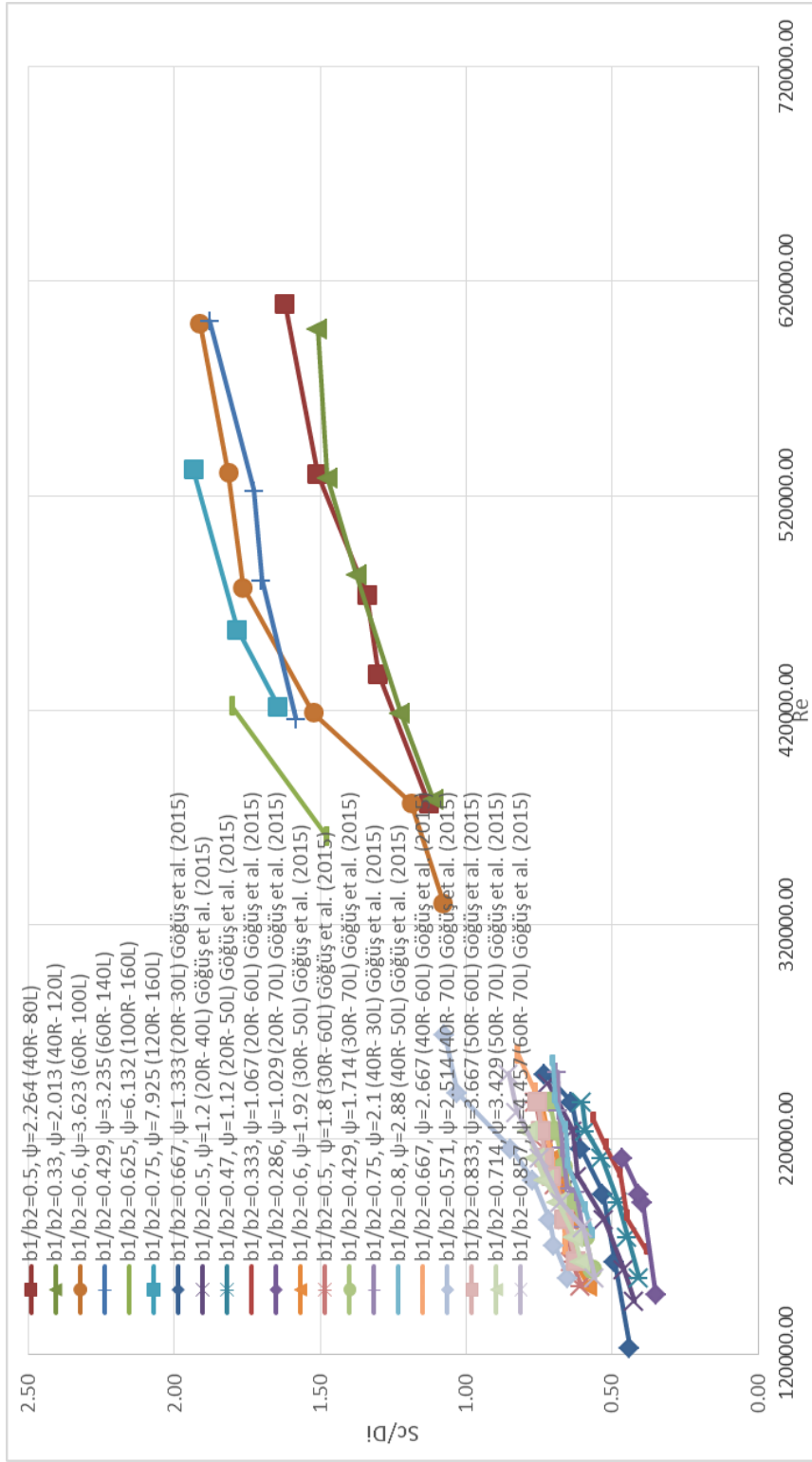


Figure 5.19 Variation of Sc/Di with Re for the present study ($Di=26.5$) cm and Göğüş et al.'s (2015) study ($Di=25$) cm

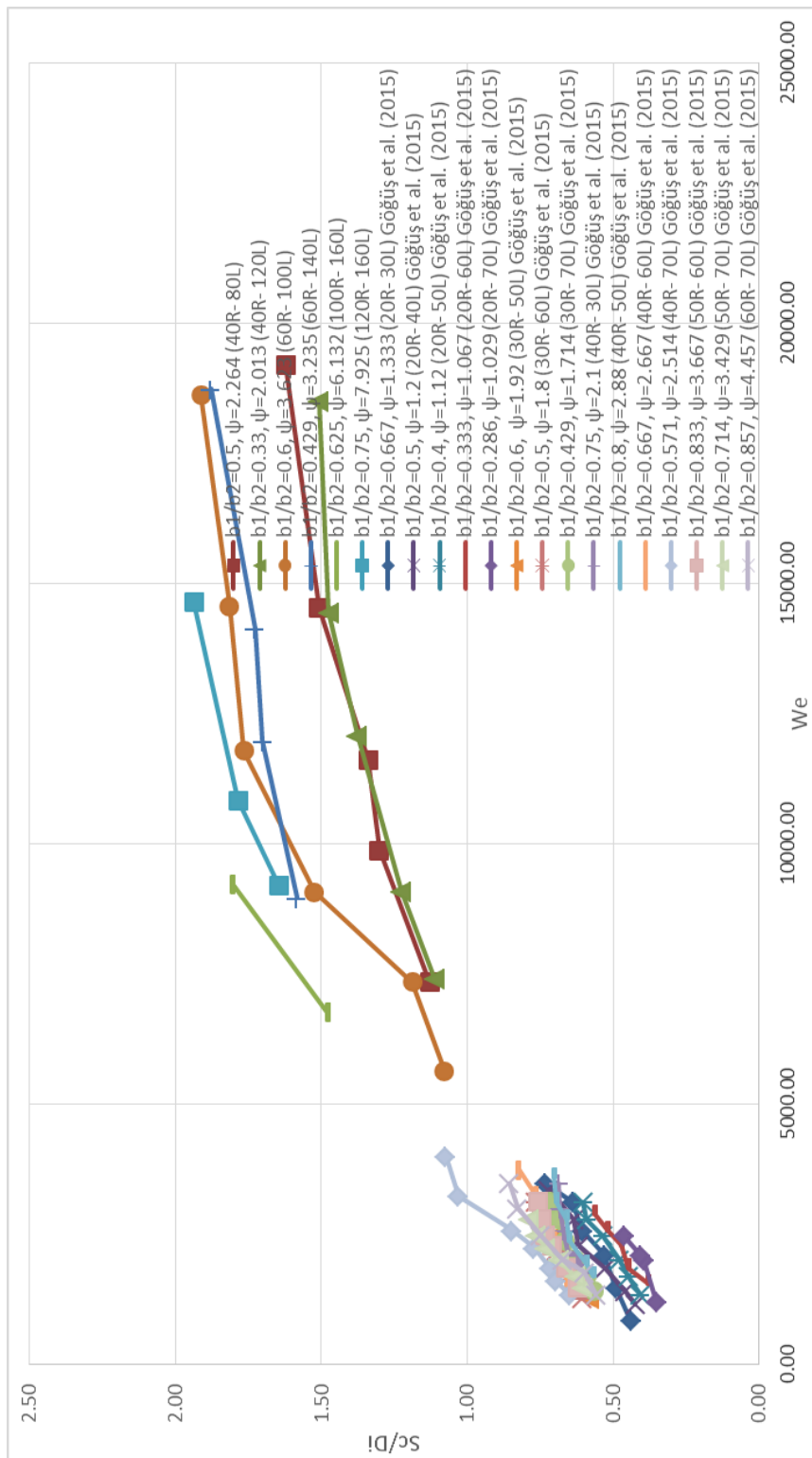


Figure 5.20 Variation of Sc/Di with We for the present study ($D_i=26.5$ cm) and Göğüş et al.'s (2015) study ($D_i=25$ cm)

5.2.2.3 Derivation of Empirical Equations for Dimensionless Critical Submergence

5.2.2.3.1 The General Case

Variation of S_c/D_i with the related parameters for asymmetrical approach flow conditions was given in Equation 3.7. By considering this equation, regression analysis was applied to the data of present study and Equation 5.5 was obtained with $R^2=0.88$.

$$S_c/D_i = Fr^{4.046} Re^{1.741} We^{-2.446} \psi^{0.145} \quad 5.5$$

Figure 5.21 compares the measured S_c/D_i data with those calculated from Equation 5.5, which is valid for the ranges of dimensionless parameters presented in Table 5.2. The calculated data lies between $\pm 10\%$ error lines.

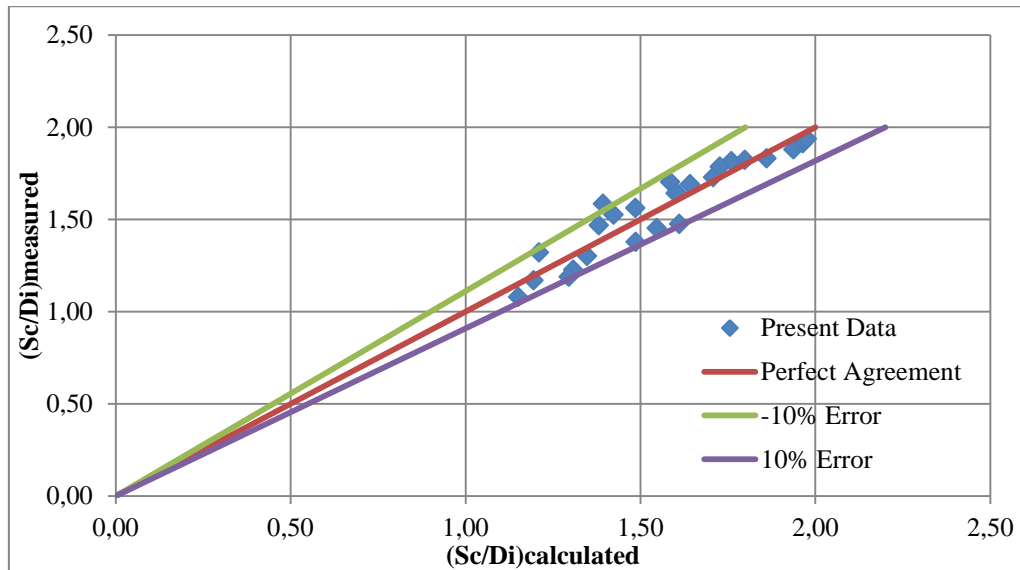


Figure 5.21 Comparison of $(S_c/D_i)_{calculated}$ data obtained from Equation 5.5, with $(S_c/D_i)_{measured}$ data for single water intake structure under asymmetrical approach flow conditions

5.2.2.3.2 Simplified Empirical Equations for S_c/D_i

To obtain simplified empirical equations for S_c/D_i , dimensionless parameters; ψ , We and Re , were omitted from the general expression of S_c/D_i one by one, Equation 3.7, and then applying the regression analysis to the available data Equations 5.6- 5.8 were derived. Variation of $(S_c/D_i)_{measured}$ data with $(S_c/D_i)_{calculated}$ data obtained from the above mentioned equations were shown in Figures 5.22- 5.24.

$$S_c/D_i = Fr^{-0.017} Re^{-0.417} We^{0.631} \quad \text{and } R^2 = 0.728 \quad 5.6$$

$$S_c/D_i = Fr^{0.799} Re^{0.028} \quad \text{and } R^2 = 0.728 \quad 5.7$$

$$S_c/D_i = 1.441 * Fr^{0.827} \quad \text{and } R^2 = 0.728 \quad 5.8$$

Although the correlation coefficients of the equations above do not change, the values of \pm error lines which cover the available data increases 15% while the corresponding values for Equation 5.5 are $\pm 10\%$.

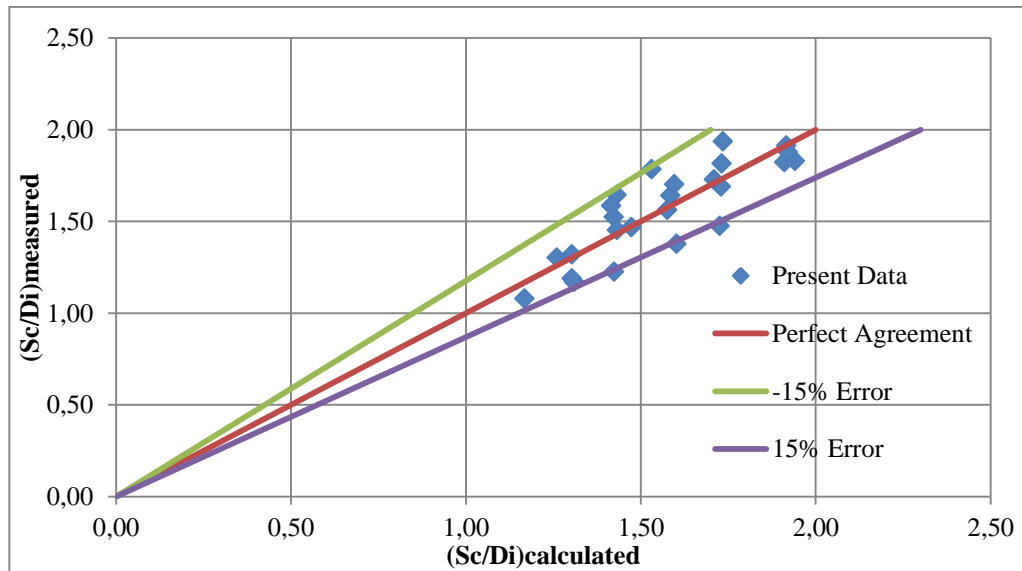


Figure 5.22 Comparison of $(S_c/D_i)_{calculated}$ data obtained from Equation 5.6, with $(S_c/D_i)_{measured}$ data for single water intake structure under asymmetrical approach flow conditions

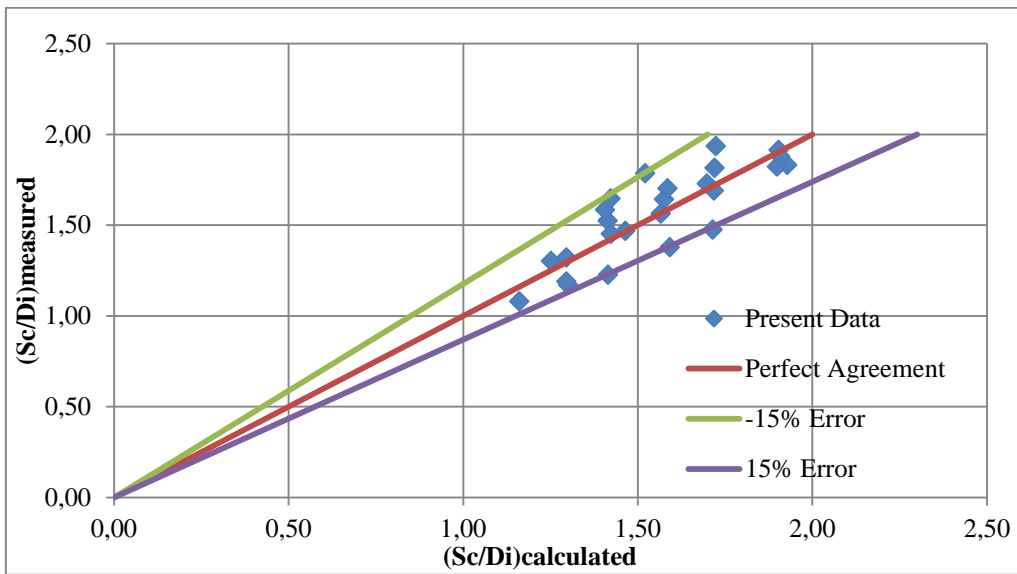


Figure 5.23 Comparison of $(S_c/D_i)_{\text{calculated}}$ data obtained from Equation 5.7, with $(S_c/D_i)_{\text{measured}}$ data for single water intake structure under asymmetrical approach flow conditions

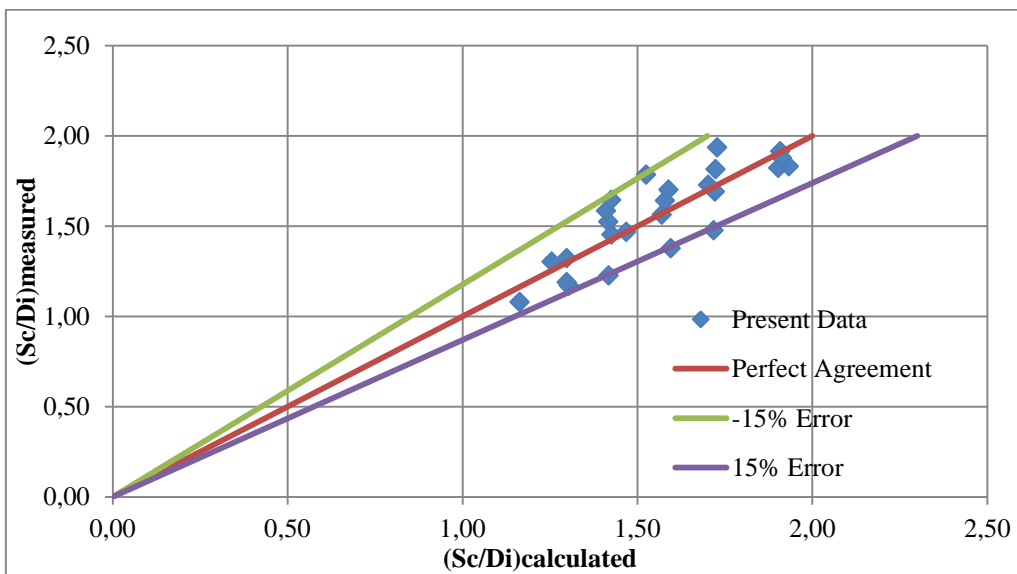


Figure 5.24 Comparison of $(S_c/D_i)_{\text{calculated}}$ data obtained from Equation 5.8, with $(S_c/D_i)_{\text{measured}}$ data for single water intake structure under asymmetrical approach flow conditions

5.2.2.4 Comparison of the Results of Present Study with the Empirical Equations Proposed by Göğüş et al. (2015)

Göğüş et al. (2015) based on their experimental data obtained a general empirical equation (Equation 2.19) and simplified empirical equations (Equations 2.20- 2.22) for S_c/D_i for horizontal intake structures under asymmetrical approach flow conditions. To see how match up present study with the equations of Göğüş et al. (2015), the data of present study were applied to these equations and calculated S_c/D_i data, $(S_c/D_i)_{\text{calculated}}$, were presented with $(S_c/D_i)_{\text{measured}}$ data of the present study in Figures 5.25- 5.28 with upper and lower error lines. From these figures it can be stated that the empirical equations for S_c/D_i stated above, Equations 2.19- 2.22 can represent S_c/D_i data of the present study within the $\pm 25\%$ error lines. These limit values of the error lines become $\pm 30\%$ in Figures 5.26- 5.28 when the independent dimensionless parameters; ψ , We and Re are eliminated one by one from the original expression of S_c/D_i . Finally it can be concluded that Equation 2.19 and 2.20 can be used to estimate the value of S_c/D_i for a model similar to the one used in the present study within the error lines stated above.

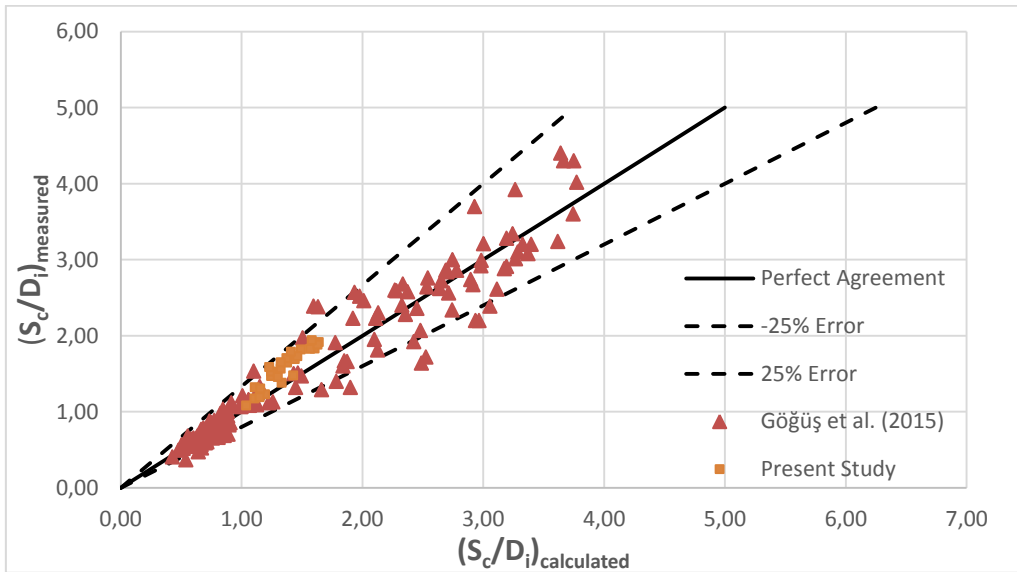


Figure 5.25 Comparison of $(S_c/D_i)_{measured}$ of the present study with $(S_c/D_i)_{calculated}$ from Equation 2.19 proposed by Göğüş et al. (2015) for symmetrical approach flow conditions

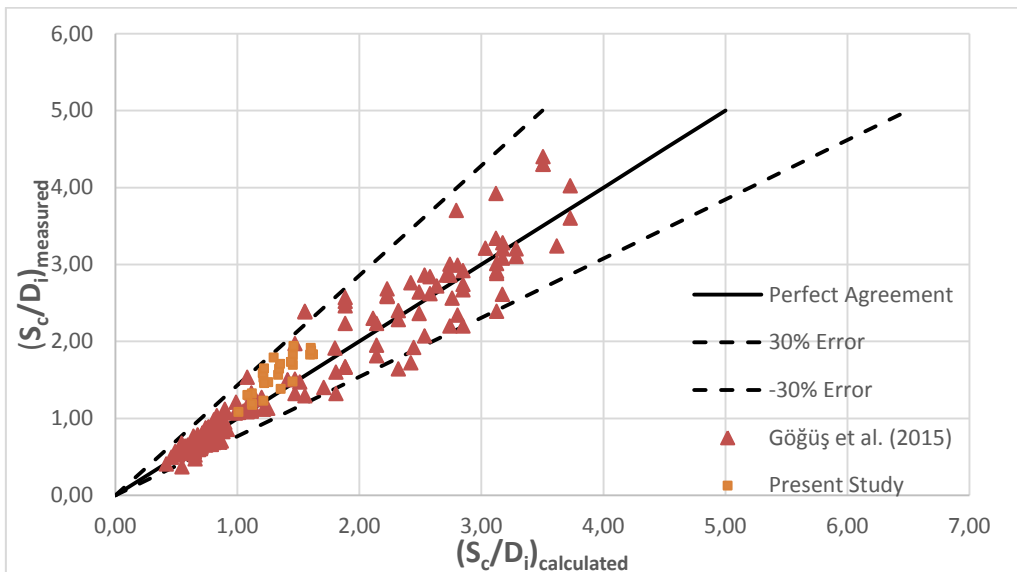


Figure 5.26 Comparison of $(S_c/D_i)_{measured}$ of the present study with $(S_c/D_i)_{calculated}$ from Equation 2.20 proposed by Göğüş et al. (2015) for symmetrical approach flow conditions

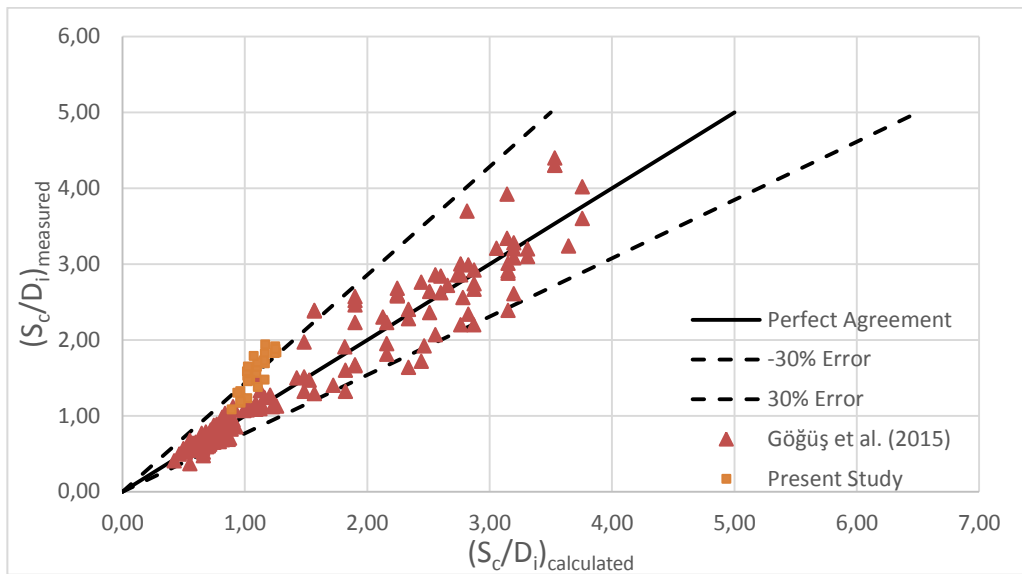


Figure 5.27 Comparison of $(S_c/D_i)_{\text{measured}}$ of the present study with $(S_c/D_i)_{\text{calculated}}$ from Equation 2.21 proposed by Göğüş et al. (2015) for symmetrical approach flow conditions

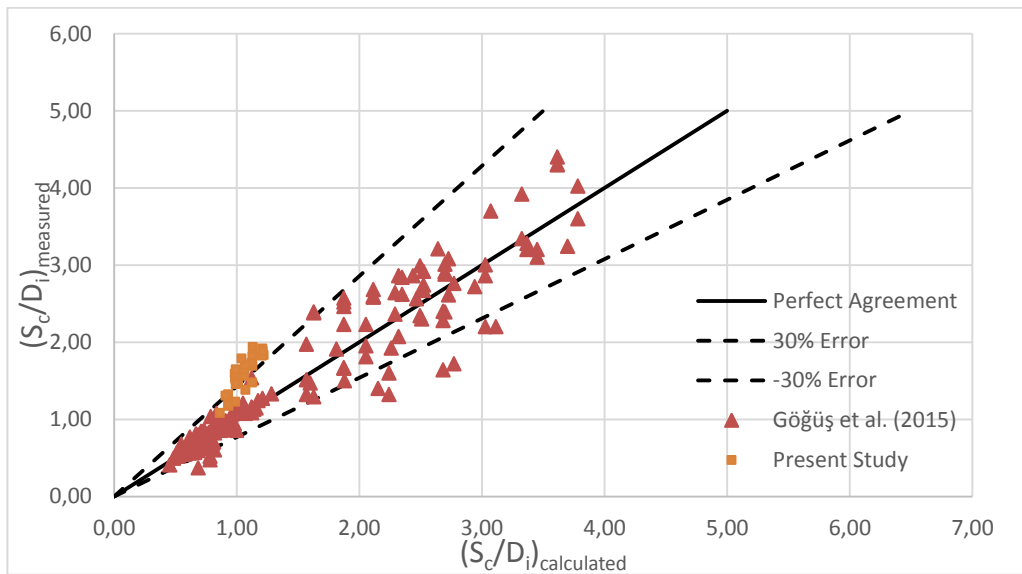


Figure 5.28 Comparison of $(S_c/D_i)_{\text{measured}}$ of the present study with $(S_c/D_i)_{\text{calculated}}$ from Equation 2.22 proposed by Göğüş et al. (2015) for symmetrical approach flow conditions

5.3 Double Water Intake Structure

5.3.1 Symmetrical Approach Flow Conditions

Important hydraulic and geometrical parameters used in the experiments and calculations are given in Table 5.3.

Table 5.3 The ranges of important hydraulic and geometrical parameters used and calculated in the experiments of symmetrical approach flow conditions

D_i (cm)	Ranges of Parameters						Number of Observations
	Q_i (lt/s)	S_c/D_i	Fr	Re	We	2b/D_i	
26.5	124.58	1.82	1.40	598583	18539	9.06	28
	~ 63.58	~ 1.42	~ 0.72	~ 305497	~ 4829	~ 5.28	

5.3.1.1 Variation of S_c/D_i with Dimensionless Flow Parameters under Symmetrical Approach Flow Conditions

Variation of S_c/D_i values with the related hydraulic parameters; Fr, Re and We as a function of 2b/D_i are shown in Figures 5.29- 5.31. From these figures the following conclusions can be made: for a given 2b/D_i, S_c/D_i increases with increasing Fr, Re and We numbers. Tested 2b/D_i values can be generalized that for a given Fr, Re and We numbers, when 2b/D_i increases, S_c/D_i also increases. Since the curves of different 2b/D_i intersect each other, it can not be stated that for a given Fr, Re and We numbers, S_c/D_i value increases or decreases with increasing 2b/D_i. Thus, an empirical relationship should be derived for S_c/D_i as a function of related parameters.

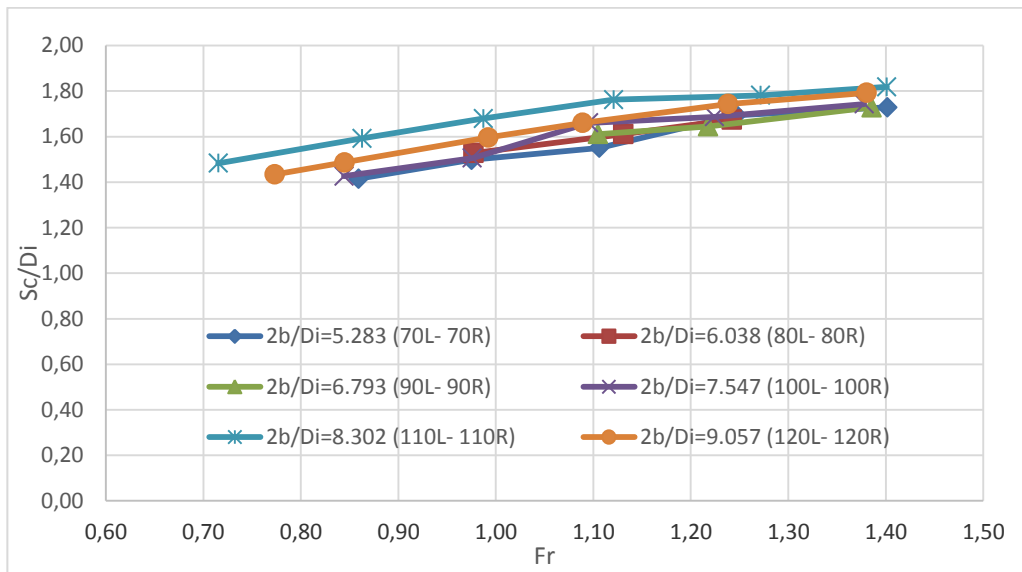


Figure 5.29 Variation of S_c/D_i with Fr for symmetrical approach flow conditions at double water intake structure

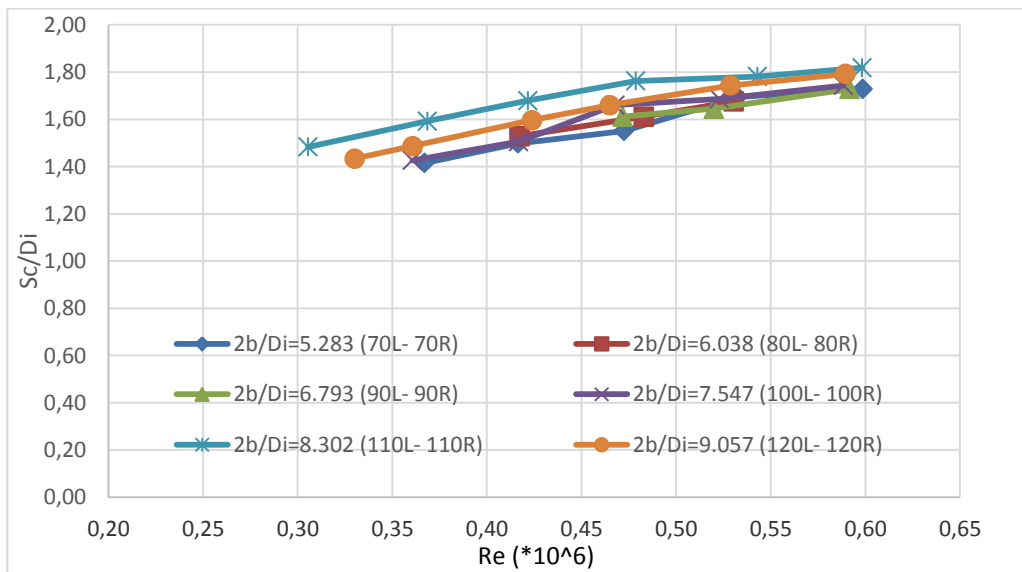


Figure 5.30 Variation of S_c/D_i with Re for symmetrical approach flow conditions at double water intake structure

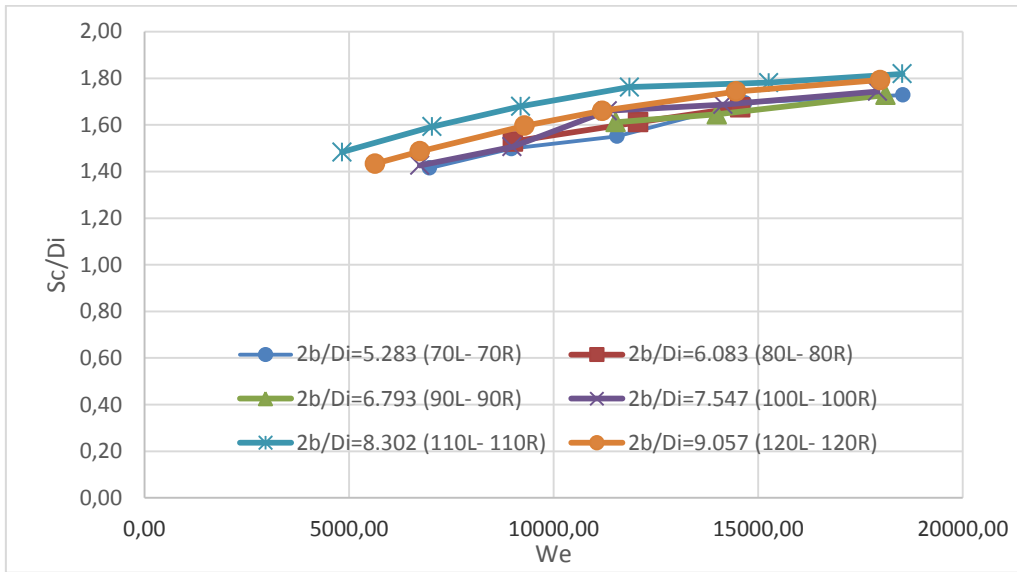


Figure 5.31 Variation of S_c/D_i with We for symmetrical approach flow conditions at double water intake structure

5.3.1.2 Derivation of Empirical Equations for Dimensionless Critical Submergence

5.3.1.2.1 The General Case

Variation of S_c/D_i with the related parameters for symmetrical approach flow conditions was given in Equation 3.6. By considering this equation, regression analysis were applied to the data of present study and Equation 5.9 was obtained with $R^2=0.875$.

$$S_c/D_i = Fr^{-2.860} Re^{-1.733} We^{2.477} (2b/D_i)^{0.127} \quad 5.9$$

Figure 5.32 shows that S_c/D_i values of the present study can be calculated from Equation 5.9 with an error range of $\pm 10\%$. Equation 5.9 is valid for the ranges of dimensionless parameters presented in Table 5.3.

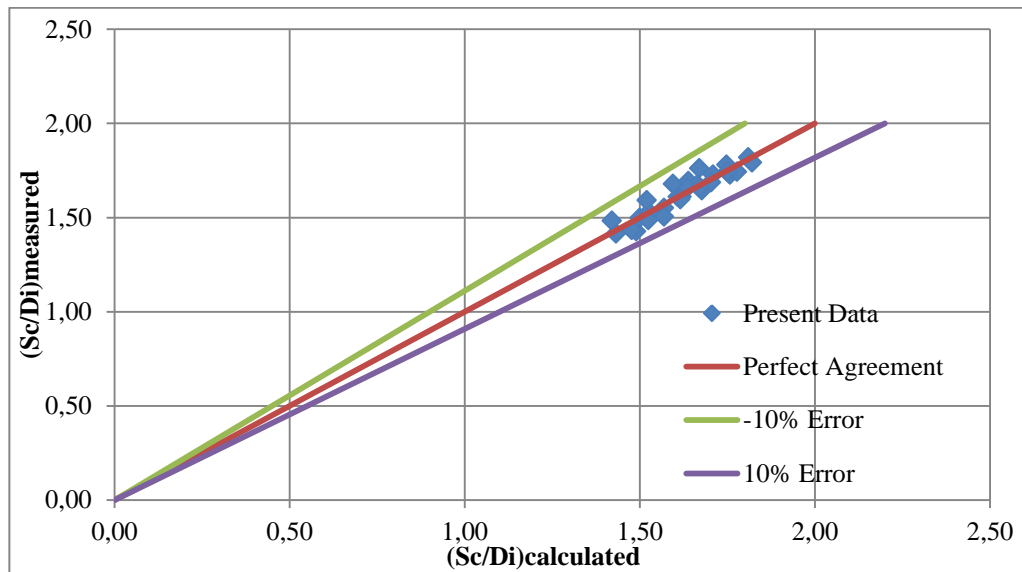


Figure 5.32 Comparison of $(S_c/D_i)_{\text{calculated}}$ data obtained from Equation 5.9, with $(S_c/D_i)_{\text{measured}}$ data for double water intake structure under symmetrical approach flow conditions

5.3.1.2.2 Simplified Empirical Equations for S_c/D_i

To obtain simplified empirical equations for S_c/D_i , the dimensionless parameters; $2b/D_i$, Reynolds and Weber numbers, were omitted one by one from the original equation of S_c/D_i , Equation 3.6, as described before, and then the Equations 5.10- 5.12 were obtained by using regression analysis. Variation of $(S_c/D_i)_{\text{measured}}$ data with $(S_c/D_i)_{\text{calculated}}$ data were shown in Figures 5.33- 5.35 for three different cases presented above.

$$S_c/D_i = Fr^{3.441} Re^{1.747} We^{-2.424} \quad \text{and } R^2 = 0.767 \quad 5.10$$

$$S_c/D_i = Fr^{0.304} Re^{0.035} \quad \text{and } R^2 = 0.767 \quad 5.11$$

$$S_c/D_i = 1,579 * Fr^{0.339} \quad \text{and } R^2 = 0.767 \quad 5.12$$

Reduction of $2b/D_i$ from the general expression of S_c/D_i reduces the value of R^2 from 0.875 to 0.767 in Equation 5.10 while R^2 values of the other equations,

Equations 5.10- 5.12, are not changing. On the other hand, upper and lower error line values of all these equations are the same and equal to $\pm 10\%$. From these discussions it may be stated that $2b/D_i$ is the most important dimensionless parameter on which S_c/D_i depends compared to the other parameters.

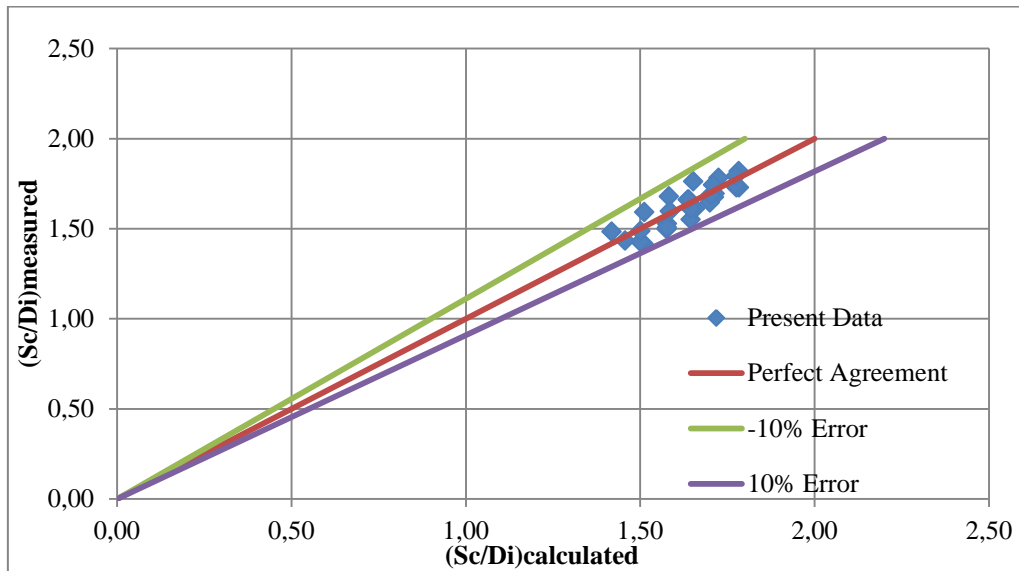


Figure 5.33 Comparison of $(S_c/D_i)_{\text{calculated}}$ data obtained from Equation 5.10, with $(S_c/D_i)_{\text{measured}}$ data for double water intake structure under symmetrical approach flow conditions

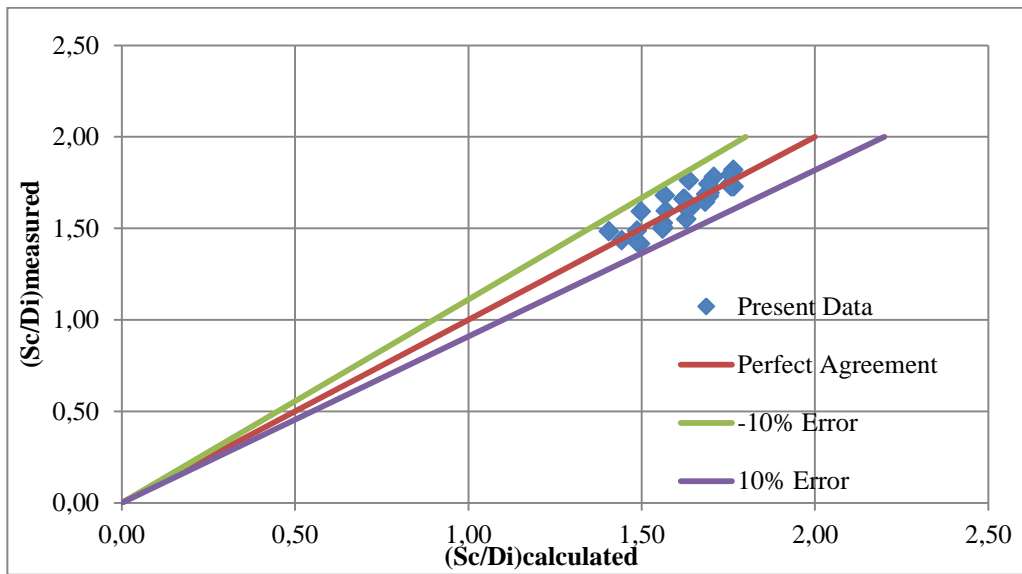


Figure 5.34 Comparison of $(S_c/D_i)_{\text{calculated}}$ data obtained from Equation 5.11, with $(S_c/D_i)_{\text{measured}}$ data for double water intake structure under symmetrical approach flow conditions

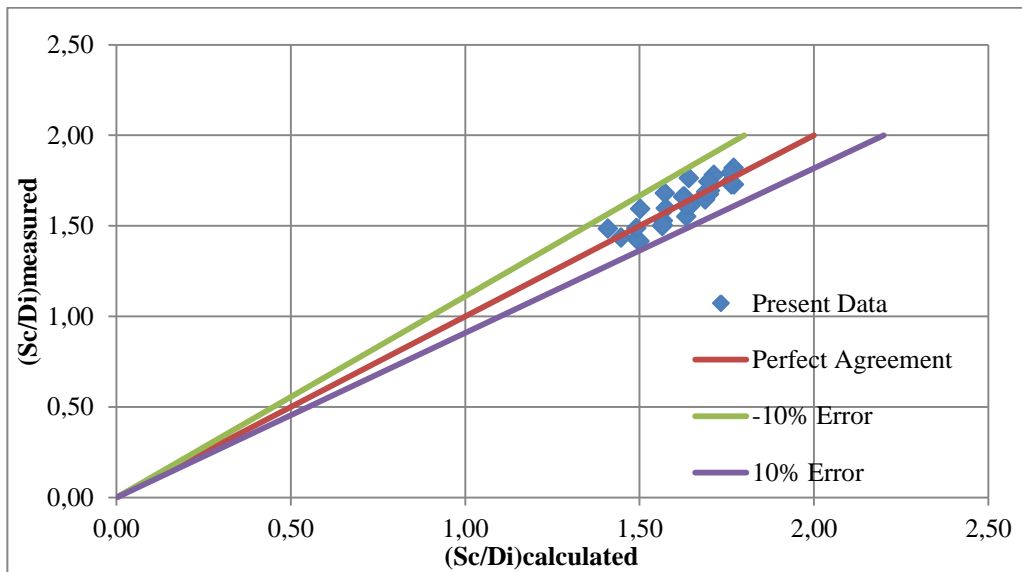


Figure 5.35 Comparison of $(S_c/D_i)_{\text{calculated}}$ data obtained from Equation 5.12, with $(S_c/D_i)_{\text{measured}}$ data for double water intake structure under symmetrical approach flow conditions

5.3.2 Asymmetrical Approach Flow Conditions

Important hydraulic and geometrical parameters used in the experiments and calculations are given in Table 5.4.

Table 5.4 The ranges of important hydraulic and geometrical parameters used and calculated in the experiments of asymmetrical approach flow conditions

D_i (cm)	Ranges of Parameters						Number of Observations
	Q_i (lt/s)	S_c/D_i	Fr	Re	We	ψ	
26.5	125	1.91	1.41	600585	18663	7.96	77
	~ 60.19	~ 1.13	~ 0.68	~ 289215	~ 4328	~ 4.18	

5.3.2.1 Variation of S_c/D_i with Dimensionless Flow Parameters under Asymmetrical Approach Flow Conditions

Variation of S_c/D_i values with the related hydraulic parameters Fr, Re and We as a function of ψ are shown in Figures 5.36- 5.38. These figures reveal that for a given ψ value, S_c/D_i increases with increasing Fr, Re and We numbers. Since curves of different ψ data intersect each other, it is not possible to make a general comment about the effect of ψ on the value of S_c/D_i for a given Fr, Re and We. Thus, empirical relations were developed for S_c/D_i as a function of the related parameters.

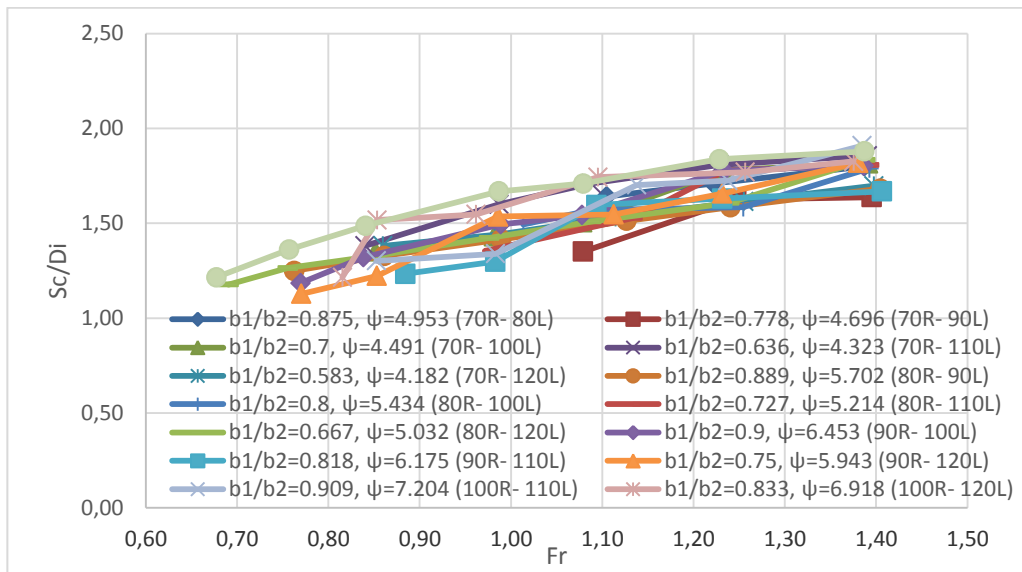


Figure 5.36 Variation of S_c/D_i with Fr for asymmetrical approach flow conditions at double water intake structure

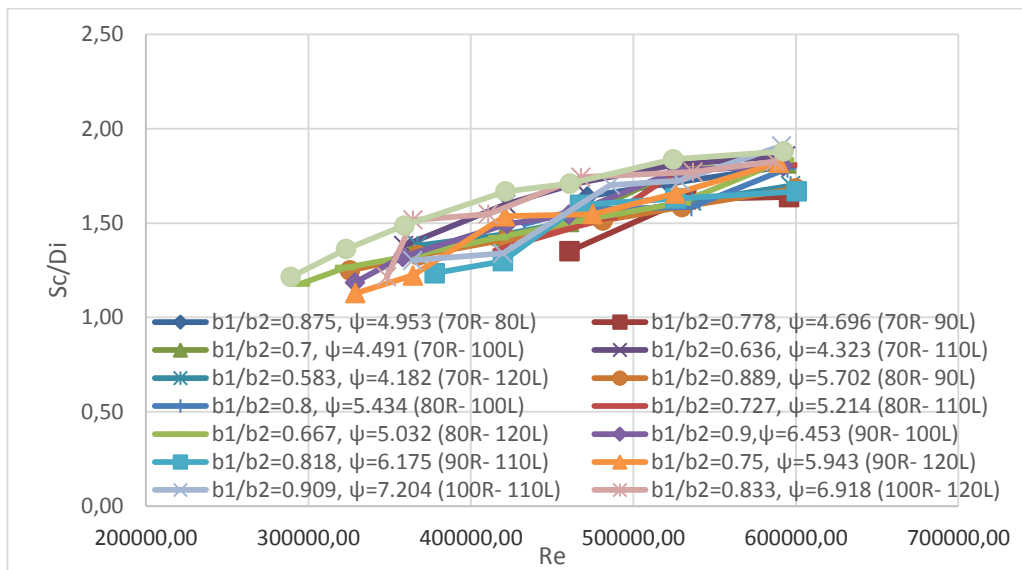


Figure 5.37 Variation of S_c/D_i with Re for asymmetrical approach flow conditions at double water intake structure

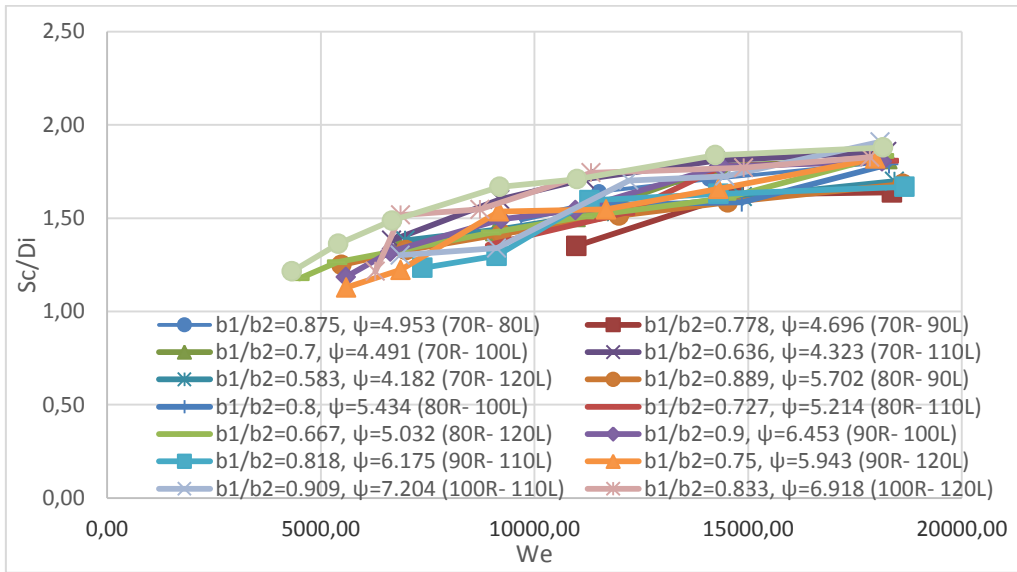


Figure 5.38 Variation of S_c/D_i with We for asymmetrical approach flow conditions at double water intake structure

5.3.2.2 Derivation of Empirical Equations for Dimensionless Critical Submergence

5.3.2.2.1 The General Case

Variation of S_c/D_i with the related parameters for asymmetrical approach flow conditions was given in Equation 3.7. By considering this equation, regression analysis was applied to the data of present study and Equation 5.13 was obtained with $R^2=0.812$.

$$S_c/D_i = Fr^{3.768} Re^{1.749} We^{-2.451} \psi^{0.085} \quad 5.13$$

Figure 5.39 compares the measured S_c/D_i data with those calculated from Equation 5.13 which is valid for the ranges of dimensionless parameters presented in Table 5.4. The values of upper and lower error lines of the calculated data are $\pm 15\%$.

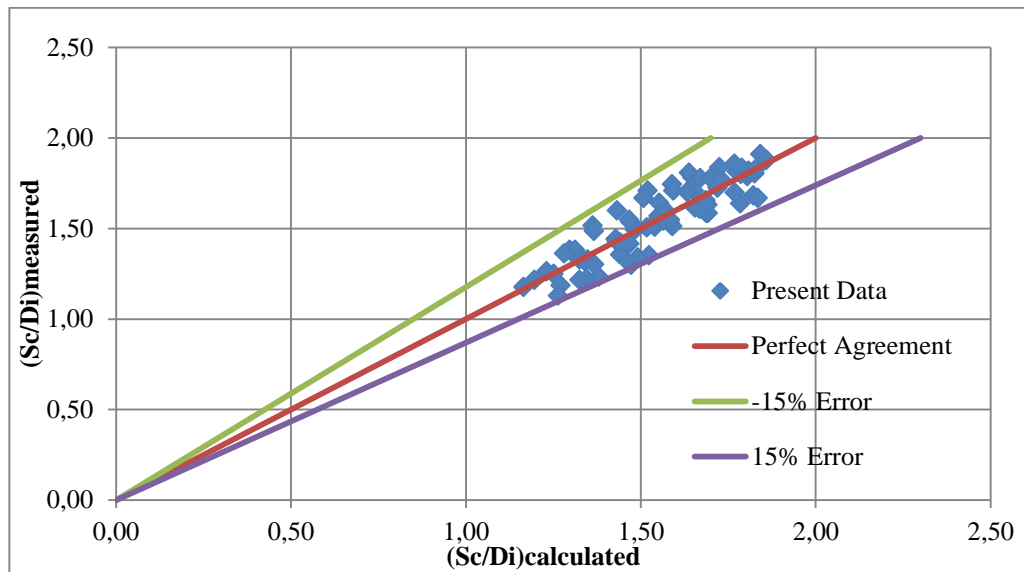


Figure 5.39 Comparison of $(S_c/D_i)_{\text{calculated}}$ data obtained from Equation 5.13, with $(S_c/D_i)_{\text{measured}}$ data for double water intake structure under asymmetrical approach flow conditions

5.3.2.2.2 Simplified Empirical Equations for S_c/D_i

By reducing the numbers of independent dimensionless terms; ψ , Re and We , one by one from the general equation of S_c/D_i the simplified empirical equations, Equations 5.14- 5.16, were derived by applying regression analysis to the related data. Variation of $(S_c/D_i)_{\text{measured}}$ data with $(S_c/D_i)_{\text{calculated}}$ data obtained from the above mentioned equations were shown in Figures 5.40- 5.42.

$$S_c/D_i = Fr^{2.130} Re^{0.880} We^{-1.204} \quad \text{and } R^2 = 0.798 \quad 5.14$$

$$S_c/D_i = Fr^{0.572} Re^{0.03} \quad \text{and } R^2 = 0.798 \quad 5.15$$

$$S_c/D_i = 1.479 * Fr^{0.602} \quad \text{and } R^2 = 0.798 \quad 5.16$$

The correlation coefficient of Equation 5.13 which covers all the independent dimensionless terms is not much different from those of Equations 5.14- 5.16.

At the same time, the ranges of the error lines are the same for Equations 5.13 and 5.14, which is $\pm 15\%$, while those of the last two equations, Equations 5.15 and 5.16, are $\pm 20\%$. From all these evaluations it can be concluded that, Equation 5.16 may be used to estimate the values of S_c/D_i due to the most simplified form.

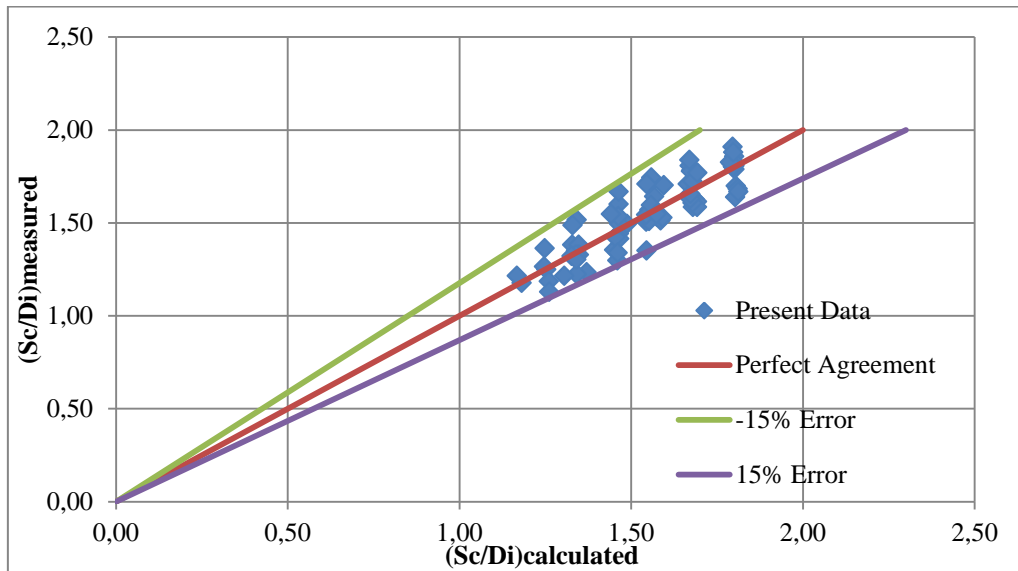


Figure 5.40 Comparison of $(S_c/D_i)_{\text{calculated}}$ data obtained from Equation 5.14, with $(S_c/D_i)_{\text{measured}}$ data for double water intake structure under asymmetrical approach flow conditions

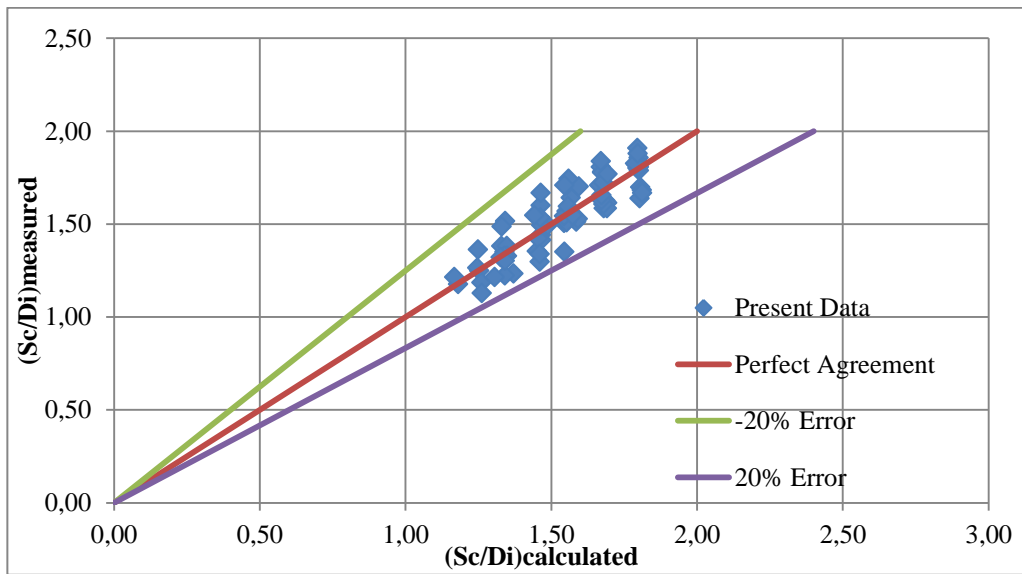


Figure 5.41 Comparison of $(S_c/D_i)_{\text{calculated}}$ data obtained from Equation 5.15, with $(S_c/D_i)_{\text{measured}}$ data for double water intake structure under asymmetrical approach flow conditions

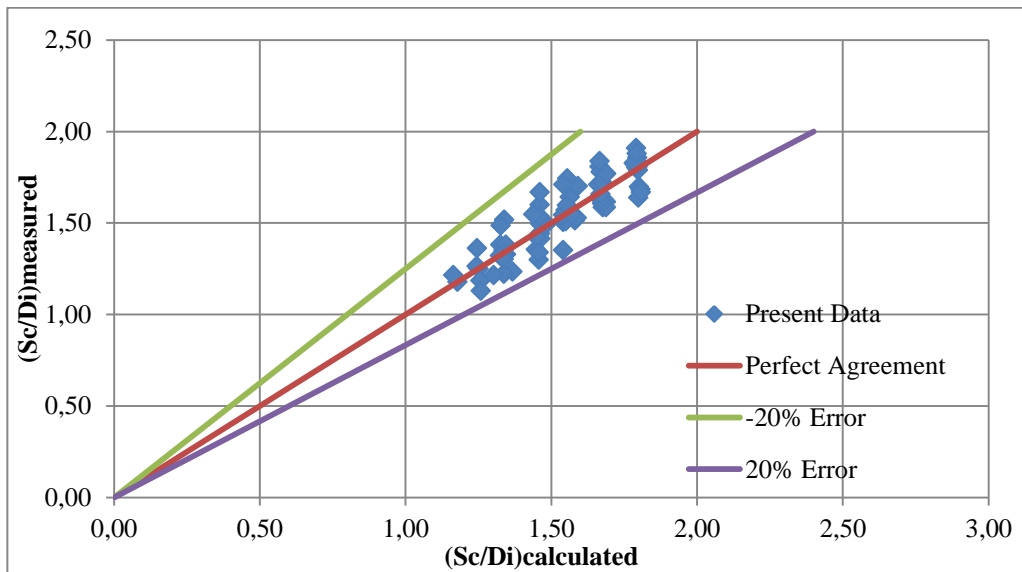


Figure 5.42 Comparison of $(S_c/D_i)_{\text{calculated}}$ data obtained from Equation 5.16, with $(S_c/D_i)_{\text{measured}}$ data for double water intake structure under asymmetrical approach flow conditions

5.4 Triple Water Intake Structure

5.4.1 Symmetrical Approach Flow Conditions

Important hydraulic and geometrical parameters used in the experiments and calculations, are given in Table 5.5.

Table 5.5 The ranges of important hydraulic and geometrical parameters used and calculated in the experiments of symmetrical approach flow conditions

D_i (cm)	Ranges of Parameters						Number of Observations
	Q_i (lt/s)	S_c/D_i	Fr	Re	We	$2b/D_i$	
26.5	98.78	1.88	1.11	474595	11654	10.57	9
	~ 59.35	~ 1.30	~ 0.67	~ 285167	~ 4208	~ 9.06	

5.4.1.1 Variation of S_c/D_i with Dimensionless Flow Parameters under Symmetrical Approach Flow Conditions

Due to the limited dimensions of the available model used in this study, only four different $2b/D_i$ values experiments were conducted. Variation of S_c/D_i values with the related hydraulic parameters; Fr, Re and We as a function of $2b/D_i$ are shown in Figures 5.43- 5.45. From these figures it can be stated that for a given $2b/D_i$ value, S_c/D_i increases with increasing Fr, Re and We numbers. Since, there are limited data; it is not possible to make any comments about effect of $2b/D_i$ parameter on S_c/D_i . So, empirical equations were developed to determine S_c/D_i value by using regression analysis as described in earlier sections.

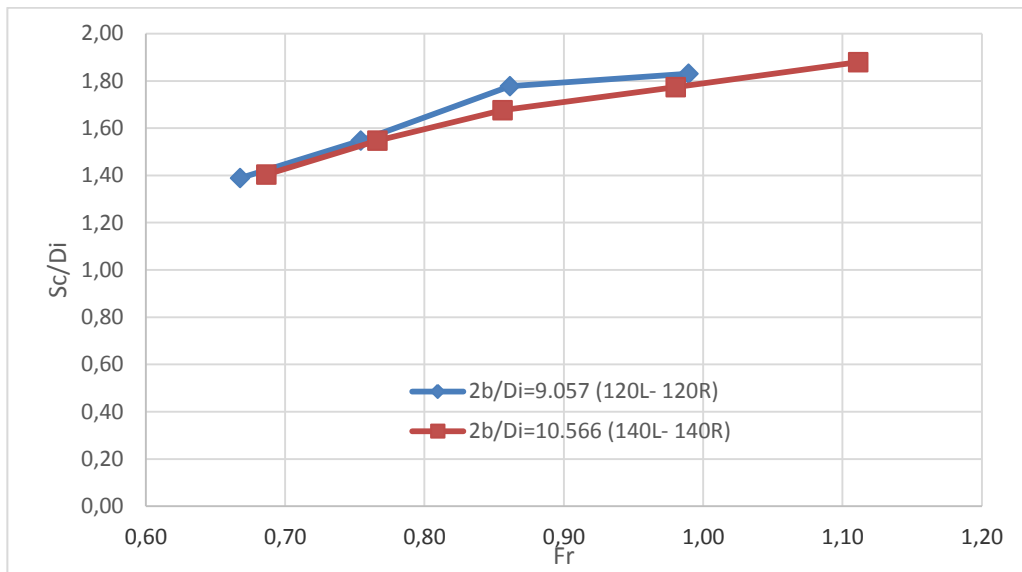


Figure 5.43 Variation of S_c/D_i with Fr for symmetrical approach flow conditions at triple water intake structure

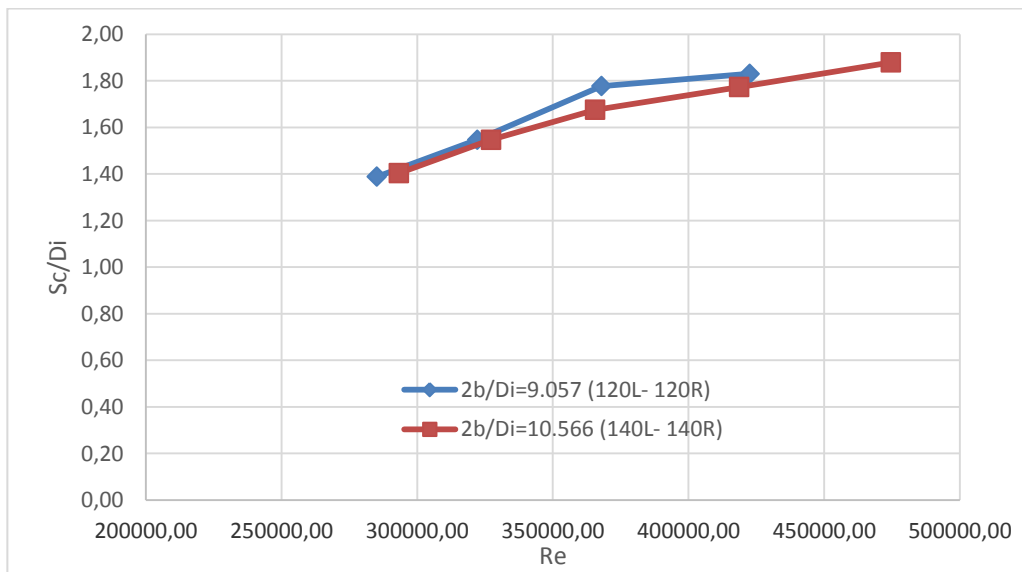


Figure 5.44 Variation of S_c/D_i with Re for symmetrical approach flow conditions at triple water intake structure

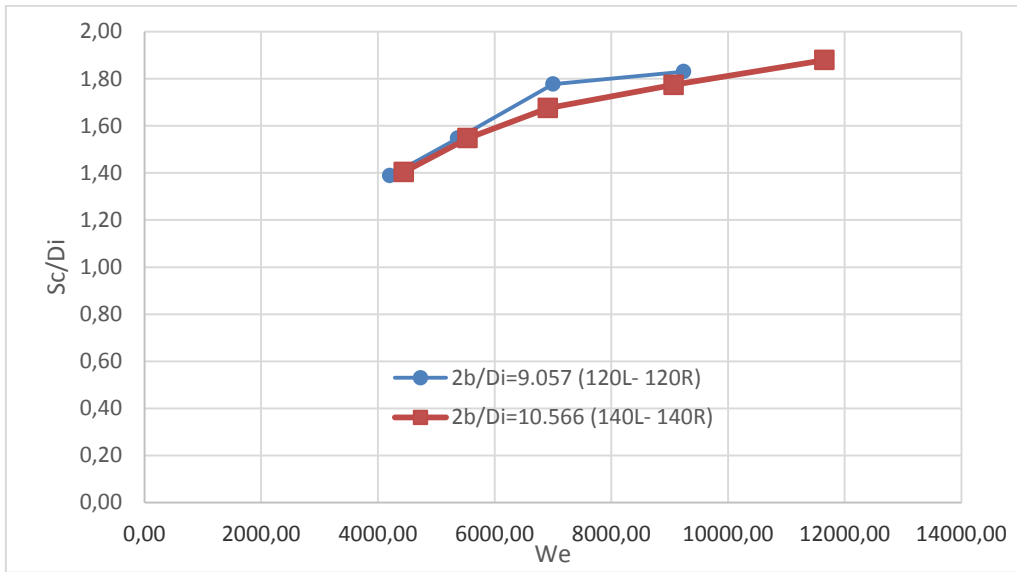


Figure 5.45 Variation of S_c/D_i with We for symmetrical approach flow conditions at triple water intake structure

5.4.1.2 Derivation of Empirical Equations for Dimensionless Critical Submergence

5.4.1.2.1 The General Case

Variation of S_c/D_i with the related parameters for symmetrical approach flow conditions was given in Equation 3.6. By considering this equation, regression analysis were applied to the data of present study and Equation 5.17 was obtained with $R^2=0.946$.

$$S_c/D_i = Fr^{1.299} Re^{0.485} We^{-0.570} (2b/D_i)^{-0.203} \quad 5.17$$

Figure 5.46 shows that S_c/D_i data which was calculated from Equation 5.17, are located between $\pm 5\%$ error lines.

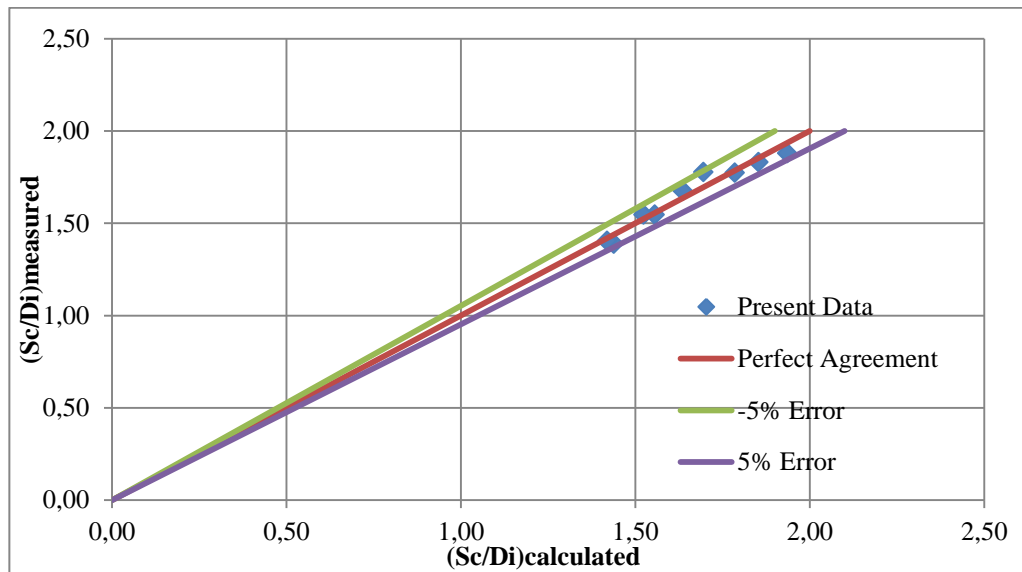


Figure 5.46 Comparison of $(S_c/D_i)_{\text{calculated}}$ data obtained from Equation 5.17, with $(S_c/D_i)_{\text{measured}}$ data for triple water intake structure under symmetrical approach flow conditions

5.4.1.2.2 Simplified Empirical Equations for S_c/D_i

As described in previous sections the simplified empirical equations for S_c/D_i , Equations 5.18- 5.20, were determined by regression analysis. Variation of $(S_c/D_i)_{\text{measured}}$ data with $(S_c/D_i)_{\text{calculated}}$ data were shown together with upper and lower error lines in Figures 5.47- 5.49 for three simplified equations of S_c/D_i mentioned above.

$$S_c/D_i = Fr^{-1.658} Re^{-1.173} We^{1.728} \quad \text{and} \quad R^2 = 0.926 \quad 5.18$$

$$S_c/D_i = Fr^{0.577} Re^{0.046} \quad \text{and} \quad R^2 = 0.926 \quad 5.19$$

$$S_c/D_i = 1.824 * Fr^{0.624} \quad \text{and} \quad R^2 = 0.926 \quad 5.20$$

Elimination of $2b/D_i$ parameter from Equation 5.17 results in a small decrease in the value of R^2 from to 0.946 to 0.926. On the other hand, the values of R^2 for Equations 5.18- 5.20 are the same and equal to 0.926 which is slightly less

than 0.946, and also the values of the upper and lower error lines are the same, $\pm 10\%$, for all the equations presented. Therefore, within the ranges of parameters used in this study to estimate the value of S_c/D_i Equation 5.20 may be used due to its simplified form.

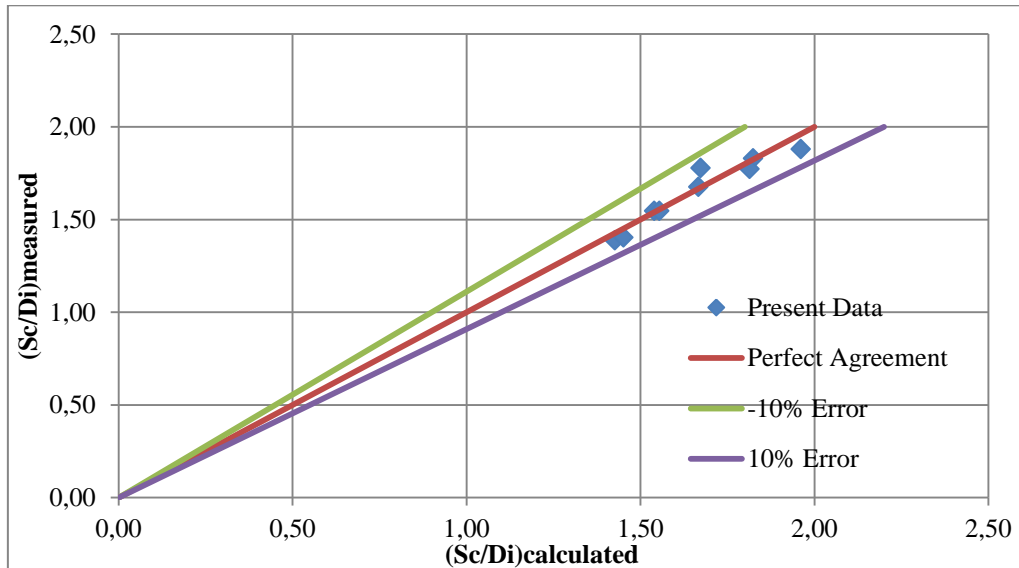


Figure 5.47 Comparison of $(S_c/D_i)_{\text{calculated}}$ data obtained from Equation 5.18, with $(S_c/D_i)_{\text{measured}}$ data for triple water intake structure under symmetrical approach flow conditions

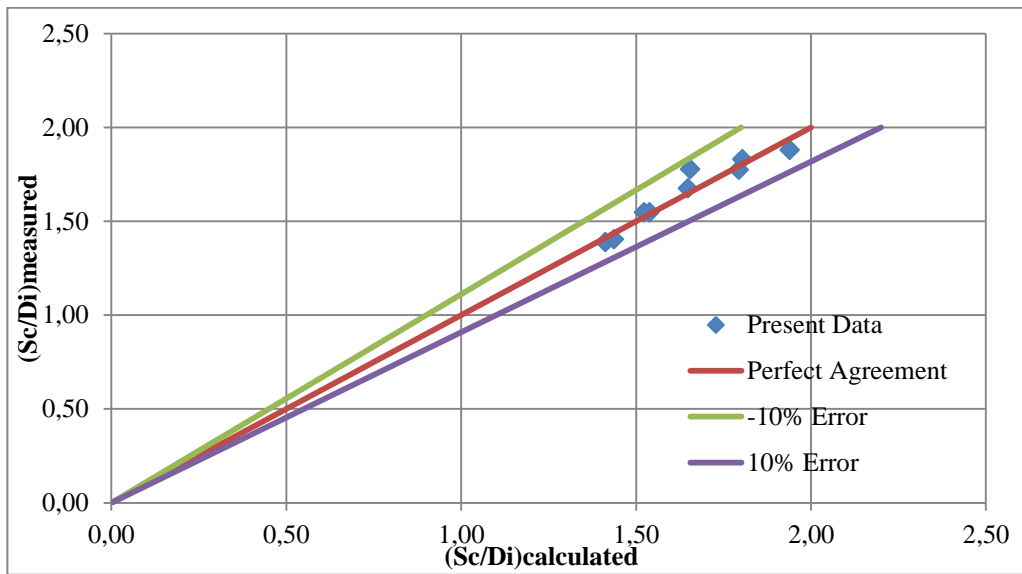


Figure 5.48 Comparison of $(S_c/D_i)_{\text{calculated}}$ data obtained from Equation 5.19, with $(S_c/D_i)_{\text{measured}}$ data for triple water intake structure under symmetrical approach flow conditions

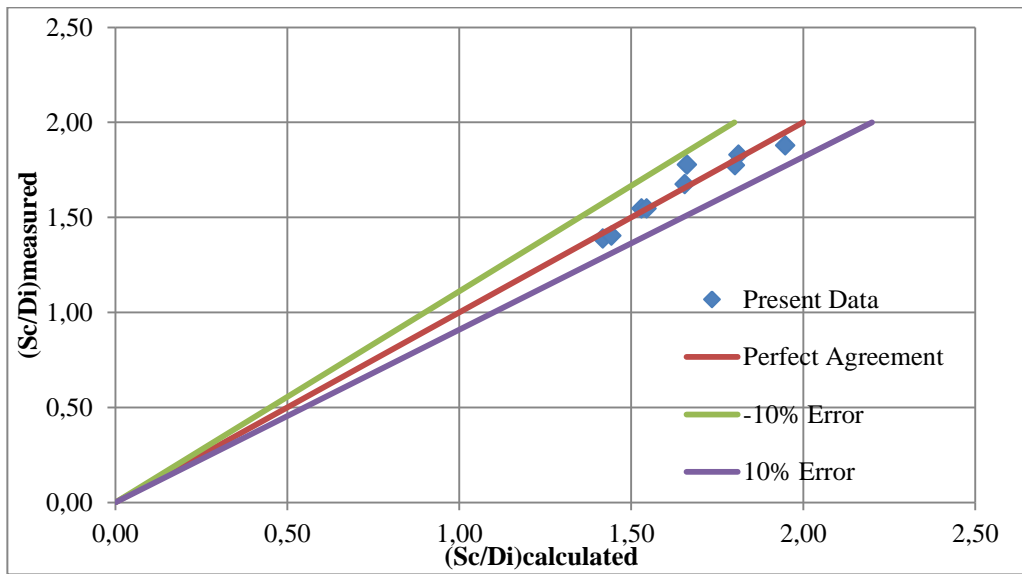


Figure 5.49 Comparison of $(S_c/D_i)_{\text{calculated}}$ data obtained from Equation 5.20, with $(S_c/D_i)_{\text{measured}}$ data for triple water intake structure under symmetrical approach flow conditions

5.4.2 Asymmetrical Approach Flow Conditions

Important hydraulic and geometrical parameters used in the experiments and calculations, are given in Table 5.6.

Table 5.6 The ranges of important hydraulic and geometrical parameters used and calculated in the experiments of asymmetrical approach flow conditions

D_i (cm)	Ranges of Parameters						Number of Observations
	Q_i (lt/s)	S_c/D_i	Fr	Re	We	ψ	
26.5	100.56	1.94	1.13	483137	12078	10	24
	~	~	~	~	~	~	
	48.89	1.26	0.55	234895	2855	8.41	

5.4.2.1 Variation of S_c/D_i with Dimensionless Flow Parameters under Asymmetrical Approach Flow Conditions

Variation of S_c/D_i values with the related hydraulic parameters; Fr, Re and We as a function of ψ are shown in Figures 5.50- 5.52. Totally 5 different ψ values were tested and they vary between 7.92 and 10.003. The trend lines of each ψ given in the related figures are very close to each other and intersect each other at various points. Therefore, within the ranges of ψ tested it can not be stated that how S_c/D_i varies with varying ψ. However, it can be concluded that for a given ψ, S_c/D_i increases with increasing related hydraulic parameters. Empirical equations were developed to show the effect of ψ and related hydraulic parameters on S_c/D_i.

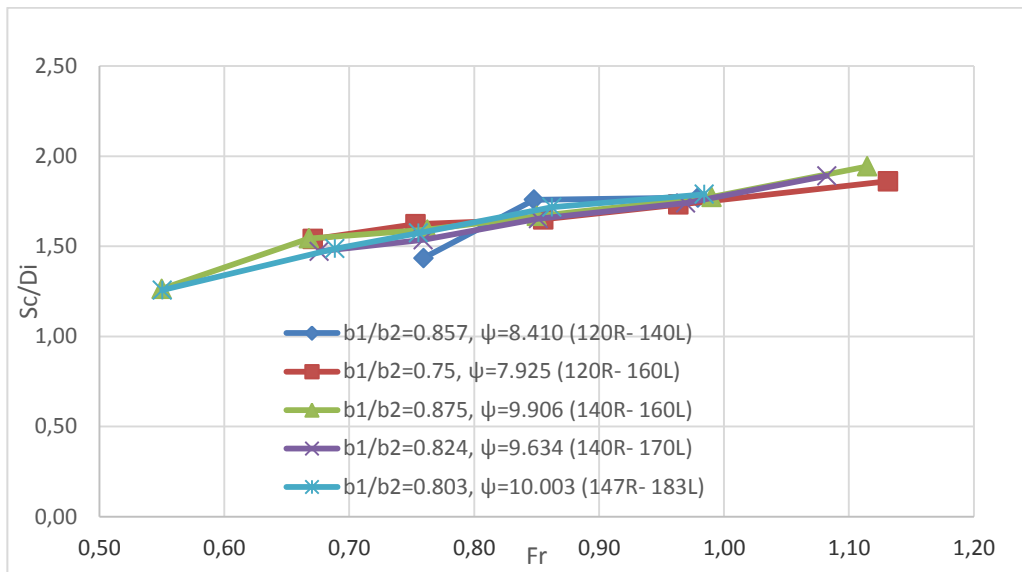


Figure 5.50 Variation of S_c/D_i with Fr for asymmetrical approach flow conditions at triple water intake structure

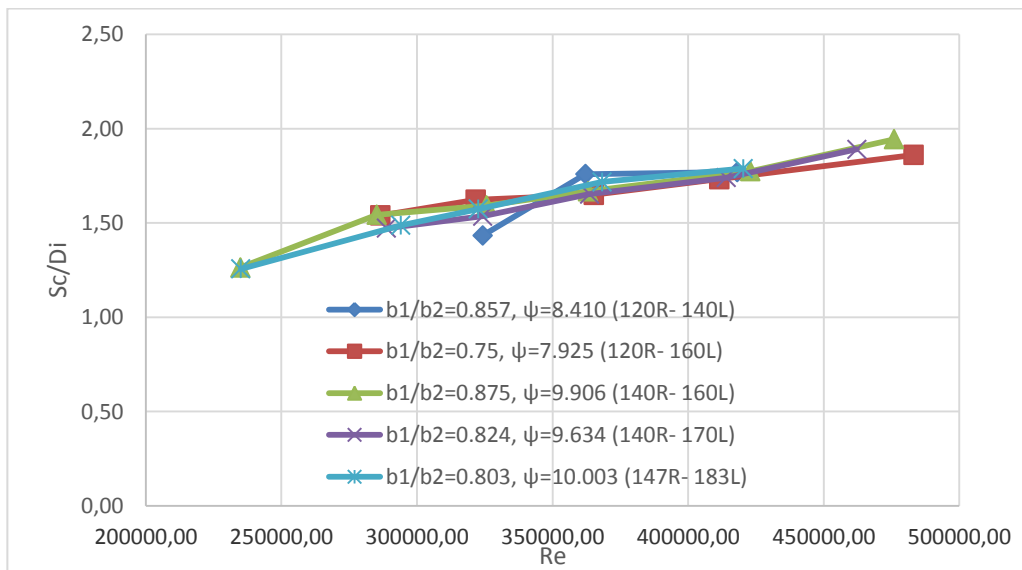


Figure 5.51 Variation of S_c/D_i with Re for asymmetrical approach flow conditions at triple water intake structure

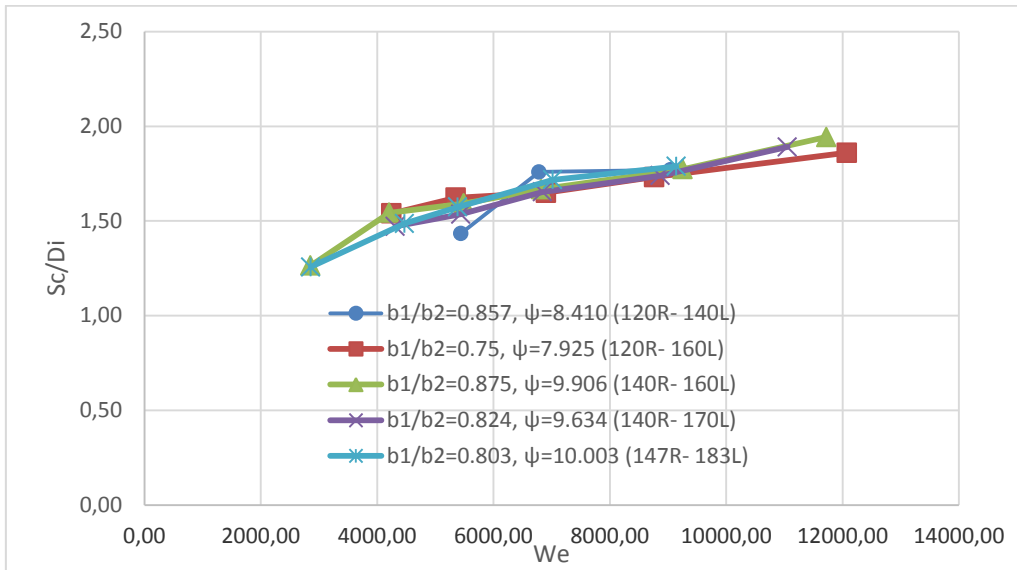


Figure 5.52 Variation of S_c/D_i with We for asymmetrical approach flow conditions at triple water intake structure

5.4.2.2 Derivation of Empirical Equations for Dimensionless Critical Submergence

5.4.2.2.1 The General Case

Variation of S_c/D_i with the related parameters for asymmetrical approach flow conditions was given in Equation 3.7. By considering this equation, regression analysis were applied to the data of present study and Equation 5.21 was obtained with $R^2=0.908$.

$$S_c/D_i = Fr^{-0.364} Re^{-0.416} We^{0.654} (\psi)^{0.001} \quad 5.21$$

Figure 5.53 shows the variation of S_c/D_i data calculated from Equation 5.21 with those of measured within the upper and lower error lines of $\pm 10\%$.

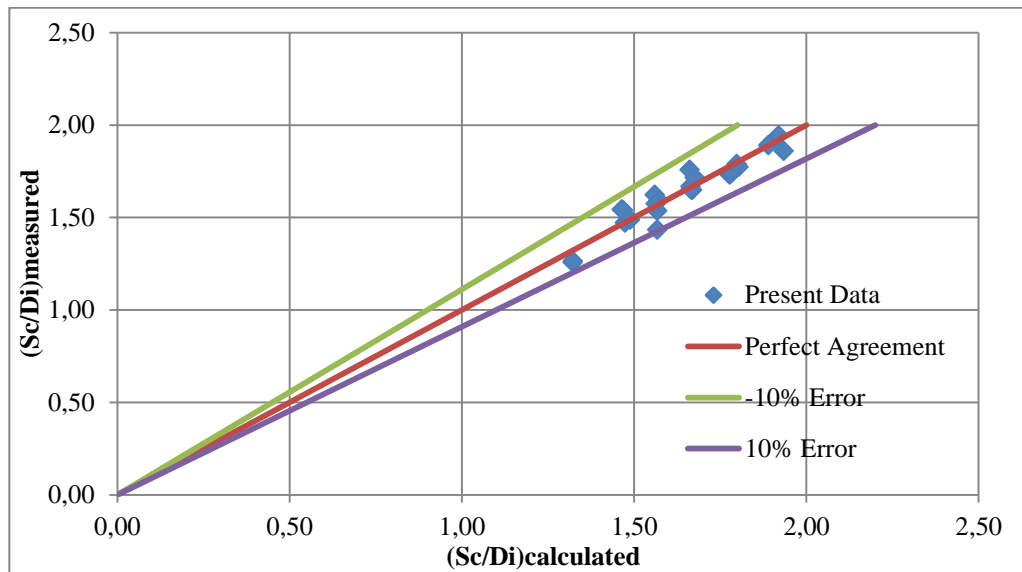


Figure 5.53 Comparison of $(S_c/D_i)_{\text{calculated}}$ data obtained from Equation 5.21, with $(S_c/D_i)_{\text{measured}}$ data for triple water intake structure under asymmetrical approach flow conditions

5.4.2.2.2 Simplified Empirical Equations for S_c/D_i

Simplified empirical equations for S_c/D_i , Equations 5.22- 5.24, were derived as discussed in previous sections by applying regression analysis. Variation of $(S_c/D_i)_{\text{measured}}$ data with $(S_c/D_i)_{\text{calculated}}$ data were shown together with error ranges in Figures 5.54- 5.56 for three different cases presented above.

$$S_c/D_i = Fr^{-0.355} Re^{-0.412} We^{0.648} \quad \text{and } R^2 = 0.908 \quad 5.22$$

$$S_c/D_i = Fr^{0.484} Re^{0.046} \quad \text{and } R^2 = 0.908 \quad 5.23$$

$$S_c/D_i = 1.806 * Fr^{0.529} \quad \text{and } R^2 = 0.908 \quad 5.24$$

For 4 equations of S_c/D_i given above, the correlation coefficients and error ranges as seen in the related figures are the same. For this reason, it can be stated that there is no almost difference between the general empirical equation and the most simplified equation of S_c/D_i . Finally it can be concluded that

Equation 5.24 can be used to calculate S_c/D_i values within the ranges of parameters tested in this study and presented in Table 5.6.

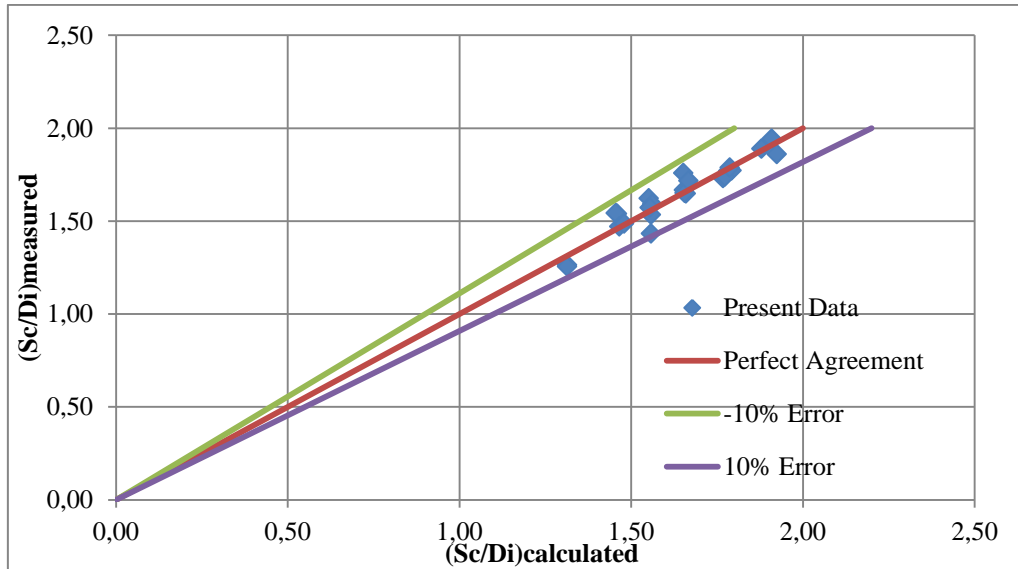


Figure 5.54 Comparison of $(S_c/D_i)_{\text{calculated}}$ data obtained from Equation 5.22, with $(S_c/D_i)_{\text{measured}}$ data for triple water intake structure under asymmetrical approach flow conditions

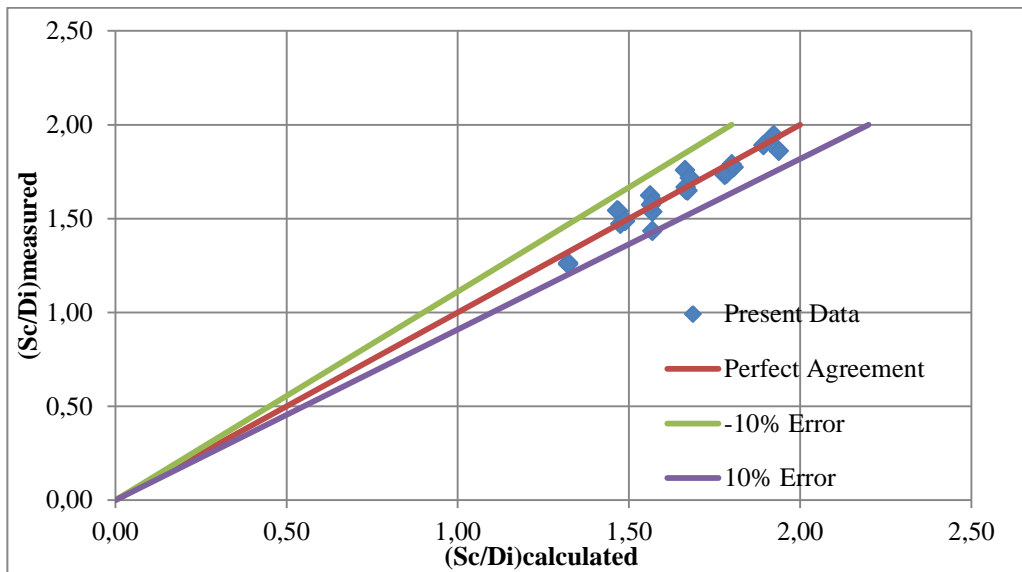


Figure 5.55 Comparison of $(S_c/D_i)_{\text{calculated}}$ data obtained from Equation 5.23, with $(S_c/D_i)_{\text{measured}}$ data for triple water intake structure under asymmetrical approach flow conditions

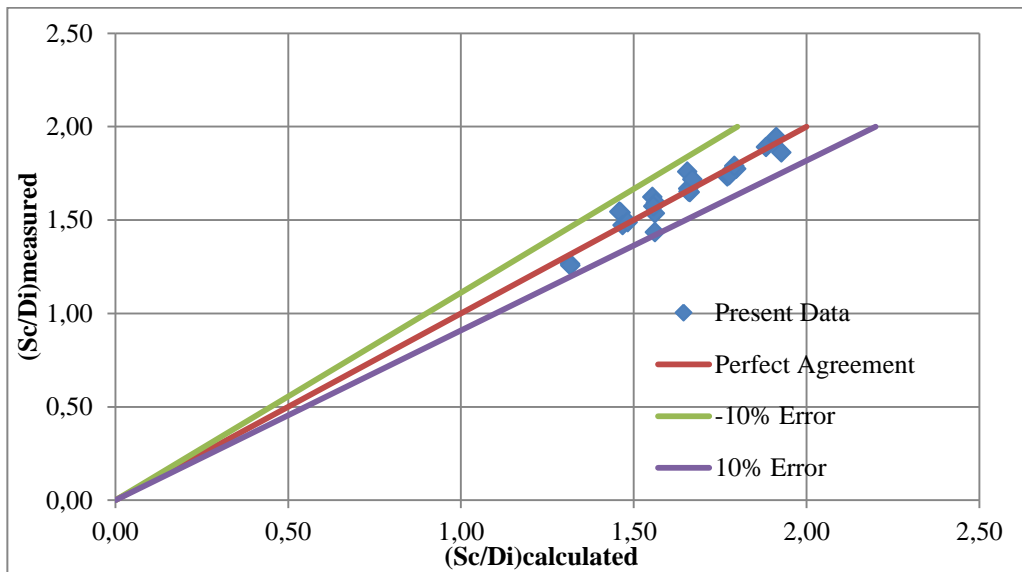


Figure 5.56 Comparison of $(S_c/D_i)_{\text{calculated}}$ data obtained from Equation 5.24, with $(S_c/D_i)_{\text{measured}}$ data for triple water intake structure under asymmetrical approach flow conditions

5.5 Comparison of Simplified Empirical S_c/D_i Equations for Single, Double and Triple Water Intake Structures at Symmetrical and Asymmetrical Approach Flow Conditions

5.5.1 Comparison of S_c/D_i Equations Derived for Symmetrical Approach Flow Conditions

At single, double and triple water intake structures, Equations 5.4, 5.12 and 5.20 are the most simplified equations for S_c/D_i . These equations were expressed as a function of Froude number only. In practical cases, most of the empirical equations used to calculate S_c/D_i is only depended on Froude number. Effect of the other parameters is accepted negligible (Gordon, 1970; Reddy and Pickford, 1972). To make a comparison, all these equations which were expressed above, and Equation 2.5 proposed by Göğüş et al. (2015) were drawn together and presented in Figure 5.57.

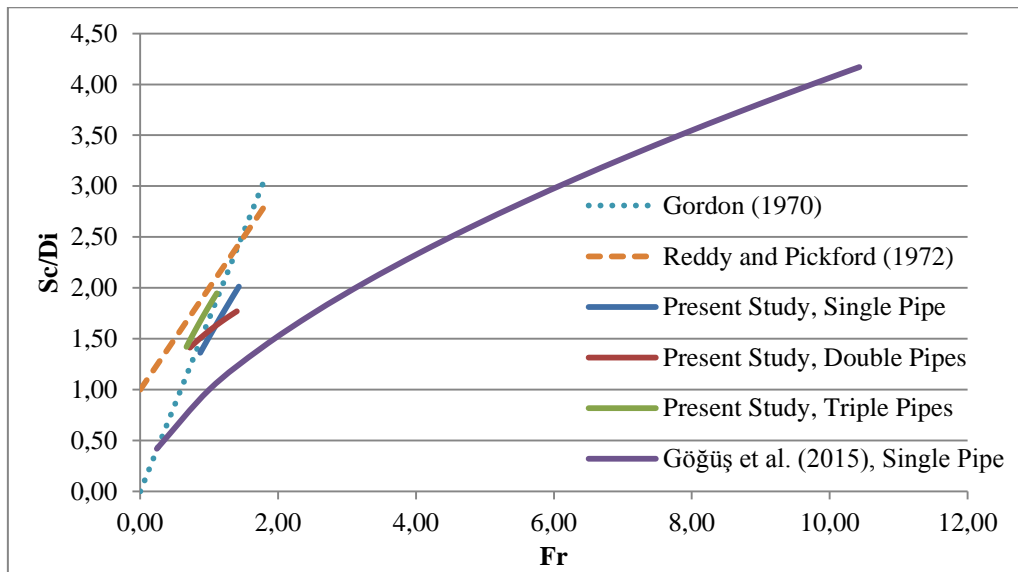


Figure 5.57 Comparison of S_c/D_i equations obtained from the present study and Göğüş et al.'s (2015) study which are only dependent on Froude Number for symmetrical approach flow conditions

S_c/D_i equations derived from this study are only valid for water intake structures having small pipe diameters. Since complete similarity is not provided between model and prototype for all the dimensionless parameters involved in the phenomenon, except Froude number, at small scaled models the results of the experiments can not be converted directly into prototype values due to the scale effect (Göğüş et al. 2015). Thus, the equations obtained from the model studies and drawn in Figure 5.57, are not suitable for practical use. To use the equations of model studies for estimation of S_c/D_i values in prototypes, the model values must be multiplied by a “scale effect correction coefficient” which is function of the length scale of the model. Since the equations of Gordon (1970) and Reddy and Picford (1972) were developed from the measured prototype data of S_c/D_i for single intake structures, for a given Fr these equations yield larger S_c/D_i values than those of Göğüş et al. (2015) and the present study.

If one compares the curves of single water intake structures given in Figure 5.57 for the present study and the one proposed by Göğüş et al. (2015), it can be stated that the curve of the present study belongs to the data of a single pipe diameter, $D_i=26.5$ cm. Whereas the other one is obtained by using the data of six different pipe diameters and includes lots of data. Therefore, these two curves are not proper curves to be compared with each other. However, the curves of S_c/D_i versus Fr for a single pipe, double pipes and triple pipes of the present study can be compared with each other to see the effect of number of intake structures in operation on the values of S_c/D_i . The two curves of single and double pipes intersects each other at the value of about $Fr=1.20$. For $Fr \leq 1.20$, the curve of single pipe yields larger S_c/D_i values than that of double pipe. If $Fr > 1.20$, the reverse situation occurs. This means that as Fr gets larger values than 1.20, double intake structure yields larger S_c/D_i values than those of a single intake structure for a given Fr. As Fr increases, the discharge of the intake structure increases, and therefore, the flow structure in front of the

intake structure becomes more complicated and it results in disturbed water surfaces, formation of eddies and finally air- entraining vortices.

As for the S_c/D_i versus Fr curve of the triple intake structure, it appears well above the other curves of single and double intake structures. In this case all of the three intake structures are in operation and withdrawing the same discharge. The flows entering each intake structure strongly influence each other. This situation is observed on the free surface and results in formation of eddies and rotating flows on the free surface in front of the intake structures. Therefore, air- entraining vortices occur at larger S_c/D_i values for a given Fr compared to those of single and double intake structures. As a final conclusion it can be stated that when the number of intake structures in operation increases, at higher reservoir water levels air- entraining vortices occur. Therefore, in the case of estimation of S_c/D_i values for water intake structures more than one, one should not use the S_c/D_i equations derived for only one intake structure.

5.5.2 Comparison of S_c/D_i Equations Derived for Asymmetrical Approach Flow Conditions

At single, double and triple water intake structures, Equations 5.8, 5.16 and 5.24 are the most simplified equations for S_c/D_i and are functions of Fr only. To make a comparison, these equations were drawn together with Equation 2.8 proposed by Göğüş et al. (2015) and Gordon's (1970) equation and presented in Figure 5.58.

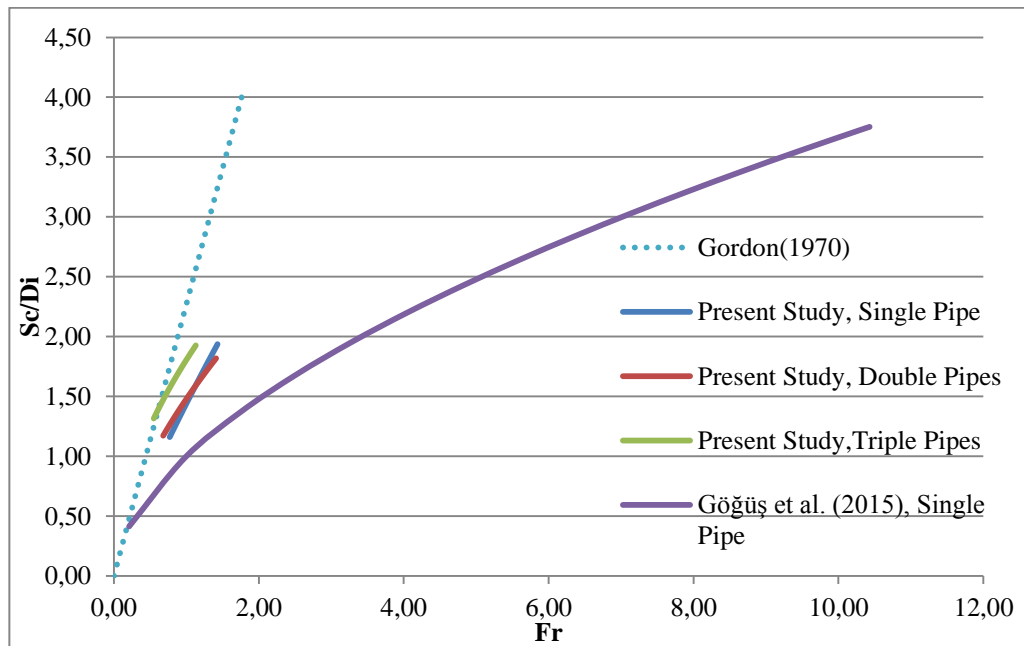


Figure 5.58 Comparison of S_c/D_i equations obtained from the present study and Göğüş et al.'s (2015) study which are only dependent on Froude Number for asymmetrical approach flow conditions

For asymmetrical approach flow conditions, the relationships between S_c/D_i and Fr for all types of intake structures tested; single pipe, double pipe and triple pipes, are almost the same as those of symmetrical approach flow conditions. Present study's single water intake curve falls above Göğüş et al.'s (2015) curve same as the symmetrical approach flow conditions. Moreover, single and double water intake structures' curves of present study intersect each other at about Fr= 1.20 and the curve of triple water intake structure appears above the other curves and yields larger S_c/D_i values same as the symmetrical approach flow conditions. Gordon's (1970) curve given for asymmetrical approach flow conditions is well above all the other curves presented and therefore gives the largest S_c/D_i values for a given Froude number. If scale effect were involved in the calculations of present study,

larger S_c/D_i values having consistence with Gordon's (1970) equation would be obtained. Since higher Froude numbers are generally obtained from models having small pipe diameters, the scale effect correction coefficients which have to be applied to the model values increases. If S_c/D_i obtained from the model for the case of large Froude number are multiplied with the scale effect correction coefficient, much larger S_c/D_i values are to be obtained for the prototype which will be compatible with the Gordon's (1970) S_c/D_i values. On the other hand, for small Froude numbers, the similar argument can be made. At these Froude numbers the S_c/D_i curves derived from model studies give small S_c/D_i values. When these values are converted into prototype values, they are multiplied by small scale effect correction coefficients and finally the corresponding prototype values of S_c/D_i becomes around or above the S_c/D_i values to be determined from Gordon's (1970) equations.

5.5.3 Comparison of S_c/D_i versus Fr Curves of Symmetrical and Asymmetrical Approach Flows

Figure 5.58 shows the most simplified relations between S_c/D_i and Fr derived under symmetrical and asymmetrical approach flow conditions for single, double and triple intake structures all together along with those proposed by Göğüş et al. (2015) and Gordon (1970) to compare them with each other. S_c/D_i versus Fr curves of each intake structure group for symmetrical and asymmetrical approach flow conditions almost coincide with each other. In other words, for a given Fr, the deviation between the S_c/D_i versus Fr curves of symmetrical and asymmetrical approach flow conditions is not so significant. This means that the wall clearance- induced asymmetry created in the approach channel of the intake structure does not disturb the flow pattern in front of the intake structure significantly to cause the formation of air- entraining vortices.

However, the situation is different when the number of intake structures in operation is considered. For Froude numbers up to about 1.20, S_c/D_i versus Fr

curve of the double intake structure yields larger S_c/D_i for a given Fr than that of the single intake structure, which is about 20% at most for the minimum value of Fr tested. As Fr increases toward the value of 1.20, that difference gradually decreases and gets the value of zero at $Fr=1.20$. For Froude numbers larger than 1.20, the curves of the single intake structure gives larger S_c/D_i values than that of the double intake structure starting with almost zero difference at $Fr=1.20$ but then as Fr increases, this difference gradually increases.

Triple intake structures attain the critical submergence much earlier than single and double intake structures for a given Froude number. This is due to the significantly disturbed flow patterns prevailing in front of the intake structures. When triple intake structure starts withdrawing water from the reservoir, rotating flows and eddy formations are observed on the surface of the reservoir and also the flow depths in front of the intake structures.

As a final conclusion it can be stated that the dimensionless critical submergence, S_c/D_i , of a multiple intake structure should not be determined by using the available S_c/D_i versus Fr relations derived for single intake structures.

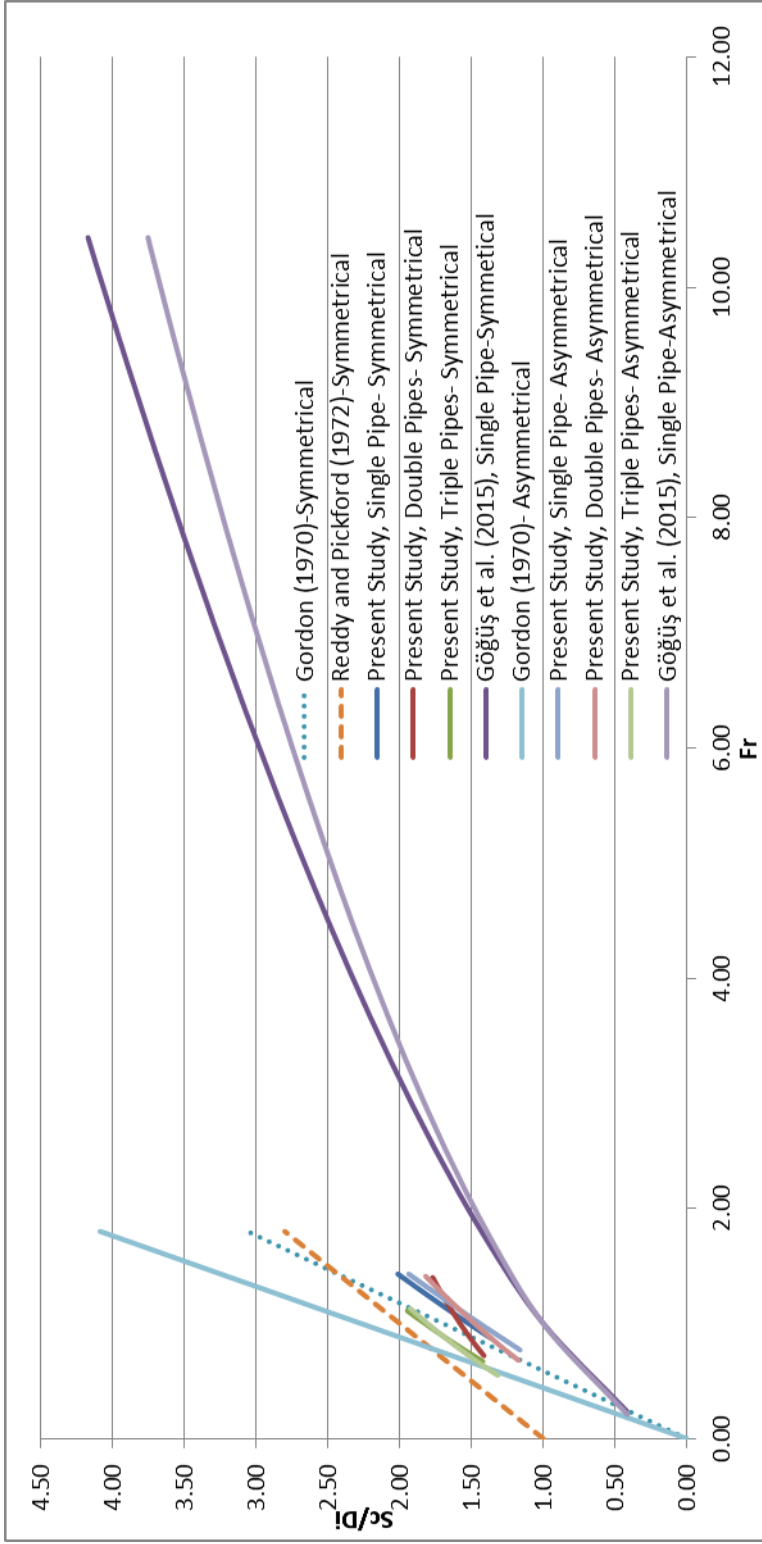


Figure 5.59 Comparison of S_c/D_1 equations obtained from the present study and Gögüş et al.'s (2015) Study which are only dependent on Froude Number for both symmetrical and asymmetrical approach flow conditions

5.6 Prevention of Air- Entraining Vortices for Symmetrical and Asymmetrical Approach Flow Conditions

In Göğüş et al.'s (2015) study, detailed research was done for vortex prevention and it was proposed that the most efficient way to prevent occurrence of vortices is using “floating horizontal rafts”. For single intake structures, the most ideal dimensionless raft sizes were specified as $L_{\text{Raft}}/D_i=2$ and as $W_{\text{Raft}}/D_i=2$ where L_{Raft} and W_{Raft} are the length and width of the raft, respectively. From this point of view, to stay on the safe side and to keep one of the raft dimensions constant, the lengths of the rafts were taken the same as the length of the side wall clearances to be used in the experiments. Since there were no space between the rafts and the approach- channel side walls, vortices would not occur on the sides of the rafts. Moreover, the width of the rafts were taken as 10 cm or 20 cm according to the approach flow conditions to prevent vortex formation.

5.6.1 Prevention of Air- Entraining Vortices for Symmetrical Approach Flow Conditions

At single, double and triple water intakes, vortex experiments were done for specified side wall clearance and waited until air- entraining vortices occur and critical submergence values were determined. After that, floating rafts which are 10 or 20 cm in width and having lengths equal to the side wall clearances were tested to prevent vortex formation for each water intake structure. The results of the experimental studies about this topic were presented in Table 5.7. This table includes; side wall clearances (b_1 and b_2), D_i , $2b/D_i$, L_{Raft} , W_{Raft} , L_{Raft}/D_i , W_{Raft}/D_i data which were used at single, double and triple water intake structures and finally the “results” to show the effect of floating rafts on the occurrence of air- entraining vortices. For single and double water intake structures, 10 cm width; for triple water intake structure, 20 cm width were successful for vortex prevention. In these models, diameter of water intakes is

constant and 26.5 cm and W_{Rafts}/D_i values which gave successful results are 0.38 for single and double intake structures, 0.75 for triple water intake structure. In Göğüş et al.'s (2015) study, W_{Raft}/D_i values were 0.50 for $D_i=25$ cm. From all these values, to be in safe side it may be proposed that the rafts of $W_{Raft}/D_i=0.75$ can protect the formation of air- entraining vortices for a single, double and triple intake structures.

Table 5.7 Summary of performances of floating rafts for symmetrical approach flow conditions

Number of Water Intake Structures	Side Wall Clearances		Di (cm)	2b/Di	Size of Raft		Lraft/Di	Wraft/Di	Location of vortex before using raft	Location of vortex after using raft	Result
	b1 (cm)	b2 (cm)			Lraft (cm)	Wraft (cm)					
1	60	60	26.5	4.53	120	10	4.53	0.38	Middle Zone	-	Successful
	80	80	26.5	6.04	160	10	6.04	0.38	Middle Zone	-	Successful
	120	120	26.5	9.06	240	10	9.06	0.38	Middle Zone	-	Successful
	140	140	26.5	10.57	280	10	10.57	0.38	Middle Zone	-	Successful
2	70	70	26.5	5.28	140	10	5.28	0.38	Right Zone	-	Successful
	80	80	26.5	6.04	160	10	6.04	0.38	Right Zone	-	Successful
	90	90	26.5	6.79	180	10	6.79	0.38	Right Zone	-	Successful
	100	100	26.5	7.55	200	10	7.55	0.38	Right & Left Zone	-	Successful
	110	110	26.5	8.30	220	10	8.30	0.38	Left Zone	-	Successful
	120	120	26.5	9.06	240	10	9.06	0.38	Left Zone	-	Successful
3	120	120	26.5	9.06	240	20	9.06	0.75	Middle Zone	-	Successful
	140	140	26.5	10.57	280	20	10.57	0.75	Middle Zone	-	Successful

5.6.2 Prevention of Air- Entraining Vortices for Asymmetrical Approach Flow Conditions

Vortex prevention experiments were conducted for asymmetrical approach flow conditions exactly applying the same procedure as described in the previous section and the results were tabulated in Table 5.8. In this part, more experiments were conducted for asymmetrical approach flow conditions than those of symmetrical approach flow conditions and similar results were obtained. For single and double water intake structures, 10 cm width; for triple water intake structure, 20 cm width were found to be successful for vortex prevention. The rafts of $W_{Rafts}/D_i=0.75$ gave successful results in preventing air- entraining vortices for each water intake structure investigated.

Table 5.8 Summary of performances of floating rafts for asymmetrical approach flow conditions

Number of Water Intake Structures	Side Wall Clearances		Di (cm)	ψ	Size of Raft		Lraft/Di	Wraft/Di	Location of vortex before using raft	Location of vortex after using raft	Result
	b1 (cm)	b2 (cm)			Lraft (cm)	Wraft (cm)					
1	40	80	26.5	2.26	120	10	4.53	0.38	Left Middle Zone	-	Successful
	40	120	26.5	2.01	160	10	6.04	0.38	Left Middle Zone	-	Successful
	60	100	26.5	3.62	160	10	6.04	0.38	Left Middle Zone	-	Successful
	60	140	26.5	3.23	200	10	7.55	0.38	Left Middle Zone	-	Successful
	100	160	26.5	6.13	260	10	9.81	0.38	Left Middle Zone	-	Successful
	120	160	26.5	7.92	280	10	10.57	0.38	Left Middle Zone	-	Successful
	70	80	26.5	4.95	150	10	5.66	0.38	Left Zone	-	Successful
	70	90	26.5	4.70	160	10	6.04	0.38	Right Zone	-	Successful
	70	100	26.5	4.49	170	10	6.42	0.38	Left Zone	-	Successful
	70	110	26.5	4.32	180	10	6.79	0.38	Right Zone	-	Successful
	70	120	26.5	4.18	190	10	7.17	0.38	Right Zone	-	Successful
	80	90	26.5	5.70	170	10	6.42	0.38	Right Zone	-	Successful
2	80	100	26.5	5.43	180	10	6.79	0.38	Left Zone	-	Successful
	80	110	26.5	5.21	190	10	7.17	0.38	Right Zone	-	Successful
	80	120	26.5	5.03	200	10	7.55	0.38	Right Zone	-	Successful
	90	100	26.5	6.45	190	10	7.17	0.38	Right Zone	-	Successful
	90	110	26.5	6.17	200	10	7.55	0.38	Right Zone	-	Successful
	90	120	26.5	5.94	210	10	7.92	0.38	Right Zone	-	Successful
	100	110	26.5	7.20	210	10	7.92	0.38	Left Zone	-	Successful
	100	120	26.5	6.92	220	10	8.30	0.38	Left & Right Zone	-	Successful
	110	120	26.5	7.96	230	10	8.68	0.38	Left & Right Zone	-	Successful
	120	140	26.5	8.41	260	20	9.81	0.75	Middle Zone	-	Successful
	120	160	26.5	7.92	280	20	10.57	0.75	Middle Zone	-	Successful
	140	160	26.5	9.91	300	20	11.32	0.75	Middle Zone	-	Successful
3	140	170	26.5	9.63	310	20	11.70	0.75	Middle Zone	-	Successful
	147	183	26.5	10.00	330	20	12.45	0.75	Right Zone	-	Successful

CHAPTER 6

CONCLUSIONS AND RECOMMENDATIONS

In this study, a series of experiments were conducted to investigate the formation of air- entraining vortices in a physical model available at the laboratory under symmetrical and asymmetrical approach flow conditions when single, double and triple water intake structures were in operation, respectively. Empirical formulas which were composed of related hydraulic and geometrical parameters were developed for each water intake structure to estimate the critical submergence. Simplified equations of these empirical formulas were also presented and compared with similar equations used in practical cases. Moreover, floating rafts were used as anti-vortex device and performance of them were investigated. Obtained results from this study are summarized below:

1. Variation of single, double and triple water intake structures' S_c/D_i values with related hydraulic parameters; Fr , Re and We have the same features with Göğüş et al.'s (2015) data. Variation of S_c/D_i with $2b/D_i$ in symmetrical approach flow conditions and variation of S_c/D_i with ψ in asymmetrical approach flow conditions show complexity.
2. Elimination of dimensionless geometrical parameters $2b/D_i$ or ψ , Re , and We from the general expression of S_c/D_i one by one result in reductions in the values of correlation coefficients of the equations of

S_c/D_i at various magnitudes. In some cases the changes in the values of correlation coefficients are not significant at all.

3. The most simplified equations of S_c/D_i derived in this study and the one proposed by Göğüş et al. (2015) for single intake structure do not match each other well especially at large Froude numbers for both symmetrical and asymmetrical approach flow conditions.
4. The variation of S_c/D_i with Fr for single, double and triple intake structures show very similar trends for both symmetrical and asymmetrical approach flow conditions.
5. As the number of the intake structures in operation increases, the flow pattern in front of the intake structures becomes more complicated and, in general, air- entraining vortices occur at large values of S_c/D_i .
6. Critical submergence equations derived from the data of single intake structures by Göğüş et al. (2015) underestimate S_c/D_i values of multiple water intake structures for a given Froude number.
7. S_c/D_i versus Fr relations given in the literature are mainly valid for prototype structures, Gordon (1970) and Reddy and Pickford (1972), estimate S_c/D_i values for a given Fr larger than those given in this study, due to the “scale effect” of the models used.
8. Floating rafts which are used as anti- vortex device, are very successful to prevent occurrence of air- entraining vortices for both symmetrical and asymmetrical approach flow conditions.

For further studies, additional research should be done in the future studies which are presented below:

1. Multiple intake structures having lateral distances from each other and different diameters than $D_i=26.5$ cm used in this study can be tested to get a wide range of S_c/D_i data set.

2. Prototype data of S_v/D_i corresponding to the model studies conducted should be provided to get a clear idea about “scale effect”.

REFERENCES

- Anwar, H.O. (1967), "Vortices at Low Head Intakes", *Water Power* 1967(11), 455-457.
- Anwar, H.O. (1968), "Prevention of Vortices at Intakes", *Water Power* 1968(10), 393-401.
- Anwar, H.O., Weller, J.A. and Amphlett, M.B. (1978), "Similarity of Free-Vortex at Horizontal Intake", *J. Hydraulic Res.* 1978(2), 95-105.
- Baykara, A., (2013), "Effect of Hydraulic Parameters on the Formation of Vortices at Intake Structures", M.S. Thesis, Civil Engineering Dept., METU.
- Daggett, L.L. and Keulegan, G.H. (1974), "Similitude in Free-Surface Vortex Formations", *J. Hydraulic Div., ASCE*, HY11, 1565-1581.
- Durgin, W.W. and Hecker, G.E. (1978), *The Modeling of Vortices in Intake Structures. Proc IAHR-ASME-ASCE Joint Symposium on Design and Operation of Fluid Machinery, CSU Fort Collins, June 1978 vols I and III.*
- Gordon, J.L. (1970), "Vortices at Intakes", *Water Power* 1970(4), 137-138.
- Göğüş, M., Köken, M., Gökmener, S. and Haspolat, E. (2015), "Su Alma Yapılarında Girdap Oluşumu ve Önlenmesi için Gerekli Düzeneklerin Belirlenmesi", *Sonuç Raporu, TÜBİTAK, Proje No: 1001- 110M676, Ankara.*
- Rindels, A.J. and Gulliver, J.S. (1983), "An Experimental Study of Critical Submergence to Avoid Free-surface Vortices at Vertical Intakes", *Project*

Report No: 224, University of Minnesota, St. Anthony Falls Hydraulic Laboratory.

Gürbüzdal, F., (2009), “Scale effects on the formation of vortices at intake structures”, M.S. Thesis, Civil Engineering Dept., METU.

Hecker, G.E. (1981) “Model- Prototype Comparison of Free Surface Vortices”, J. Hydraulic Div., ASCE, HY10, 1243-1259.

Jain, A.K., Kittur, G.R.R., and Ramanchandra, J.G. (1978), “Vortex Formation at Vertical Pipe Intakes”, J. Hydraulic Div., ASCE, HY10, 1429-1448.

Jiming, M., Yuanbo, L. and Jitang, H. (2000), “Minimum Submergence before Double- Entrance Pressure Intakes”, J. Hydraulic Div., ASCE, HY10, 628-631

Johnson, P.L (1972), “Hydraulic Model Studies of the Forebay Reservoir Inlet-Outlet Structure for Mt. Elbert Pumped-Storage Powerplant, Friyingpan-Arkansas Project, Colorado” Engineering and Research Center, U.S. Bureau of Reclamation, Denver, Colorado

Knauss, J. (1987), “Swirling Flow Problems at Intakes”, A.A. Balkema, Rotterdam.

Padmanabhan, M. and Hecker, G.E. (1984), “Scale Effects in Pump Sump Models”, J. Hydraulic Engineering, ASCE, 110, HY11, 1540-1556.

Reddy, Y.R. and Pickford, J.A. (1972), “Vortices at Intakes in Conventional Sumps”, Water Power 1972(3), 108-109.

Taştan, K. and Yıldırım, N. (2010), “Effects of Dimensionless Parameters on Air-entraining Vortices”, J. Hydraulic Research, 48:1, 57-64.

Taştan, K. and Yıldırım, N. (2014), “Effects of Froude, Reynolds, and Weber numbers on an air- entraining vortex”, J. Hydraulic Research, 52:3, 421-425.

Volkart, P. and Rutschmann, P. (1986), “Aerators on Spillway Chutes: Fundamentals and Application”, Proceedings of the ASCE Specialty Conference on Advancements in Aerodynamics, Fluid Mechanics, and Hydraulics, Minneapolis, MN.

Yıldırım, N. and Kocabaş, F. (1995), “Critical Submergence for Intakes in Open Channel Flow”, J. Hydraulic Engng., ASCE, 121, HY12, 900-905.

Yıldırım, N., Kocabaş, F. and Gülcan, S.C (2000), “Flow-Boundary Effects on Critical Submergence of Intake Pipe”, J. Hydraulic Engng., ASCE, 126, HY4, 288-297.

Yıldırım, N., Taştan, K. and Arslan, M.M. (2009) “Critical Submergence for Dual Pipe Intakes”, J. Hydraulic Research, 47:2, 242-249.

Zeigler, E.R. (1976), “Hydraulic Model Vortex Study Grand Coulee Third Powerplant”, Engineering and Research Center, U.S Bureau of Reclamation, Denver, Colorado.

APPENDIX A

EXPERIMENTAL RESULTS OF SYMMETRICAL APPROACH FLOW

In this part, experimental results of symmetrical approach flow conditions are given in tables which involve critical submergence and related important flow properties. In calculation of flow parameters such as Froude, Reynolds and Weber numbers, gravity and physical properties of water are taken as;

$$g= 9.81 \text{ (m/s}^2\text{)} \quad \nu= 1.004\text{E-}6 \text{ (m}^2\text{/s)}$$

$$\sigma=7.28\text{E-}2 \text{ (N/m)} \quad \rho= 998 \text{ (kg/m}^3\text{)}$$

Table A.1 Experimental results of critical submergence and related important flow parameters for $b= 60$ cm at single water intake structure

Obs.	Q(lt/s)	V(m/s)	Fr	Re	We	Sc (cm)	Sc/Di
1	122.89	2.23	1.38	590441.5	18038.2	49.1	1.85
2	110.08	2	1.24	528914.9	14474.8	47.7	1.8
3	96.97	1.76	1.09	465920.3	11232.2	39.7	1.5
4	86.56	1.57	0.97	415871.5	8948.67	37.6	1.42
5	77.53	1.41	0.87	372496	7179.32	36.2	1.37

Table A.2 Experimental results of critical submergence and related important flow parameters for b= 80 cm at single water intake structure

Obs.	Q(lt/s)	V(m/s)	Fr	Re	We	Sc (cm)	Sc/Di
1	126.83	2.30	1.43	609393.27	19214.79	51.40	1.94
2	110.08	2.00	1.24	528914.92	14474.78	49.00	1.85
3	101.14	1.83	1.14	485939.75	12218.14	47.20	1.78
4	87.61	1.59	0.99	420943.14	9168.27	40.20	1.52

Table A.3 Experimental results of critical submergence and related important flow parameters for b= 120 cm at single water intake structure

Obs.	Q(lt/s)	V(m/s)	Fr	Re	We	Sc (cm)	Sc/Di
1	123.61	2.24	1.39	593911.53	18250.88	52.20	1.97
2	110.14	2.00	1.24	529181.84	14489.39	50.80	1.92

Table A.4 Experimental results of critical submergence and related important flow parameters for b= 140 cm at single water intake structure

Obs.	Q(lt/s)	V(m/s)	Fr	Re	We	Sc (cm)	Sc/Di
1	126.00	2.28	1.42	605389.37	18963.12	52.10	1.97
2	110.00	1.99	1.24	528514.53	14452.87	50.90	1.92
3	97.53	1.77	1.10	468589.52	11361.23	43.80	1.65

Table A.5 Experimental results of critical submergence and related important flow parameters for b= 70 cm at double water intake structure

Obs.	Q(lt/s)	V(m/s)	Fr	Re	We	Sc (cm)	Sc/Di
1	124.58	2.26	1.40	598582.74	18539.10	45.80	1.73
2	110.83	2.01	1.25	532518.43	14672.68	44.90	1.69
3	98.33	1.78	1.11	472459.96	11549.69	41.10	1.55
4	86.67	1.57	0.97	416405.39	8971.66	39.70	1.50
5	76.39	1.38	0.86	367023.98	6969.94	37.50	1.42

Table A.6 Experimental results of critical submergence and related important flow parameters for b= 80 cm at double water intake structure

Obs.	Q(lt/s)	V(m/s)	Fr	Re	We	Sc (cm)	Sc/Di
1	110.42	2.00	1.24	530516.48	14562.57	44.40	1.68
2	100.51	1.82	1.13	482936.82	12067.60	42.70	1.61
3	86.85	1.57	0.98	417272.90	9009.08	40.50	1.53

Table A.7 Experimental results of critical submergence and related important flow parameters for b= 90 cm at double water intake structure

Obs.	Q(lt/s)	V(m/s)	Fr	Re	We	Sc (cm)	Sc/Di
1	123.17	2.23	1.39	591776.12	18119.87	45.80	1.73
2	108.24	1.96	1.22	520039.61	13993.07	43.60	1.65
3	98.19	1.78	1.10	471792.64	11517.09	42.70	1.61

Table A.8 Experimental results of critical submergence and related important flow parameters for b= 100 cm at double water intake structure

Obs.	Q(lt/s)	V(m/s)	Fr	Re	We	Sc (cm)	Sc/Di
1	122.49	2.22	1.38	588506.27	17920.19	46.20	1.74
2	108.82	1.97	1.22	522842.34	14144.31	44.70	1.69
3	97.35	1.76	1.10	467722.01	11319.21	44.00	1.66
4	86.75	1.57	0.98	416805.78	8988.93	39.90	1.51
5	75.06	1.36	0.84	360617.74	6728.75	37.80	1.43

Table A.9 Experimental results of critical submergence and related important flow parameters for b= 110 cm at double water intake structure

Obs.	Q(lt/s)	V(m/s)	Fr	Re	We	Sc (cm)	Sc/Di
1	124.54	2.26	1.40	598382.55	18526.70	48.20	1.82
2	113.03	2.05	1.27	543062.02	15259.46	47.20	1.78
3	99.63	1.81	1.12	478666.00	11855.11	46.70	1.76
4	87.75	1.59	0.99	421610.45	9197.36	44.50	1.68
5	76.71	1.39	0.86	368558.81	7028.36	42.20	1.59
6	63.58	1.15	0.72	305497.41	4828.98	39.30	1.48

Table A.10 Experimental results of critical submergence and related important flow parameters for b= 120 cm at double water intake structure

Obs.	Q(lt/s)	V(m/s)	Fr	Re	We	Sc (cm)	Sc/Di
1	122.69	2.22	1.38	589507.24	17981.20	47.50	1.79
2	110.04	2.00	1.24	528714.72	14463.82	46.20	1.74
3	96.79	1.75	1.09	465052.75	11190.38	44.00	1.66
4	88.21	1.60	0.99	423812.60	9293.69	42.30	1.60
5	75.08	1.36	0.84	360751.20	6733.73	39.40	1.49
6	68.72	1.25	0.77	330188.12	5641.09	38.00	1.43

Table A.11 Experimental results of critical submergence and related important flow parameters for b= 120 cm at triple water intake structure

Obs.	Q(lt/s)	V(m/s)	Fr	Re	We	Sc (cm)	Sc/Di
1	87.96	1.59	0.99	422633.67	9242.05	48.50	1.83
2	76.57	1.39	0.86	367913.73	7003.78	47.10	1.78
3	67.06	1.22	0.75	322180.32	5370.79	41.00	1.55
4	59.35	1.08	0.67	285166.51	4207.63	36.80	1.39

Table A.12 Experimental results of critical submergence and related important flow parameters for $b= 140$ cm at triple water intake structure

Obs.	Q(lt/s)	V(m/s)	Fr	Re	We	Sc (cm)	Sc/Di
1	98.78	1.79	1.11	474595.37	11654.33	49.80	1.88
2	87.14	1.58	0.98	418674.26	9069.70	47.00	1.77
3	76.09	1.38	0.86	365600.37	6915.98	44.40	1.68
4	68.11	1.23	0.77	327251.92	5541.21	41.00	1.55
5	61.03	1.11	0.69	293218.79	4448.61	37.20	1.40

APPENDIX B

EXPERIMENTAL RESULTS OF ASYMMETRICAL APPROACH FLOW

In this part, experimental results of asymmetrical approach flow conditions are given in tables which involve critical submergence and related important flow properties. In calculation of flow parameters such as Froude, Reynolds and Weber numbers, gravity and physical properties of water are taken as;

$$g= 9.81 \text{ (m/s}^2\text{)} \quad v= 1.004\text{E-}6 \text{ (m}^2\text{/s)}$$

$$\sigma=7.28\text{E-}2 \text{ (N/m)} \quad \rho= 998 \text{ (kg/m}^3\text{)}$$

Table B.1 Experimental results of critical submergence and related important flow parameters for $b_1= 40 \text{ cm}$. $b_2= 80 \text{ cm}$ at single water intake structure

Obs.	Q(lt/s)	V(m/s)	Fr	Re	We	Sc (cm)	Sc/Di
1	126.81	2.30	1.43	609259.80	19206.37	48.50	1.83
2	110.28	2.00	1.24	529849.16	14525.96	44.80	1.69
3	98.58	1.79	1.11	473661.13	11608.49	41.40	1.56
4	90.92	1.65	1.02	436825.27	9873.15	38.90	1.47
5	78.39	1.42	0.88	376633.33	7339.69	35.00	1.32

Table B.2 Experimental results of critical submergence and related important flow parameters for $b_1= 40$ cm. $b_2= 120$ cm cm at single water intake structure

Obs.	Q(lt/s)	V(m/s)	Fr	Re	We	Sc (cm)	Sc/Di
1	124.44	2.26	1.40	597915.43	18497.79	48.30	1.82
2	110.00	1.99	1.24	528514.53	14452.87	39.10	1.48
3	100.56	1.82	1.13	483137.02	12077.61	36.50	1.38
4	87.19	1.58	0.98	418941.19	9081.27	32.50	1.23
5	78.81	1.43	0.89	378635.28	7417.93	31.00	1.17

Table B.3 Experimental results of critical submergence and related important flow parameters for $b_1= 60$ cm. $b_2= 100$ cm cm at single water intake structure

Obs.	Q(lt/s)	V(m/s)	Fr	Re	We	Sc (cm)	Sc/Di
1	124.86	2.26	1.40	599917.37	18621.87	50.70	1.91
2	110.42	2.00	1.24	530516.48	14562.57	48.10	1.82
3	99.31	1.80	1.12	477131.17	11779.20	43.50	1.64
4	87.14	1.58	0.98	418674.26	9069.70	40.40	1.52
5	78.39	1.42	0.88	376633.33	7339.69	31.50	1.19
6	68.67	1.24	0.77	329921.19	5631.98	28.60	1.08

Table B.4 Experimental results of critical submergence and related important flow parameters for $b_1= 60$ cm. $b_2= 140$ cm cm at single water intake structure

Obs.	Q(lt/s)	V(m/s)	Fr	Re	We	Sc (cm)	Sc/Di
1	125.22	2.27	1.41	601652.40	18729.73	49.80	1.88
2	108.75	1.97	1.22	522508.68	14126.26	45.80	1.73
3	100.08	1.81	1.13	480868.14	11964.44	45.10	1.70
4	86.61	1.57	0.97	416138.46	8960.17	42.00	1.58

Table B.5 Experimental results of critical submergence and related important flow parameters for $b_1= 100$ cm. $b_2= 160$ cm cm at single water intake structure

Obs.	Q(lt/s)	V(m/s)	Fr	Re	We	Sc (cm)	Sc/Di
1	87.81	1.59	0.99	421877.38	9209.01	38.50	1.45
2	75.22	1.36	0.85	361418.52	6758.67	34.50	1.30

Table B.6 Experimental results of critical submergence and related important flow parameters for $b_1= 120$ cm. $b_2= 160$ cm cm at single water intake structure

Obs.	Q(lt/s)	V(m/s)	Fr	Re	We	Sc (cm)	Sc/Di
1	110.72	2.01	1.25	531984.57	14643.28	51.30	1.94
2	95.22	1.73	1.07	457512.07	10830.42	47.30	1.78
3	87.75	1.59	0.99	421610.45	9197.36	43.60	1.65

Table B.7 Experimental results of critical submergence and related important flow parameters for $b_1= 70$ cm. $b_2= 80$ cm cm at double water intake structure

Obs.	Q(lt/s)	V(m/s)	Fr	Re	We	Sc (cm)	Sc/Di
1	123.29	2.24	1.39	592376.70	18156.67	47.70	1.80
2	108.61	1.97	1.22	521841.36	14090.21	45.30	1.71
3	98.19	1.78	1.10	471792.64	11517.09	43.50	1.64

Table B.8 Experimental results of critical submergence and related important flow parameters for $b_1= 70$ cm. $b_2= 90$ cm cm at double water intake structure

Obs.	Q(lt/s)	V(m/s)	Fr	Re	We	Sc (cm)	Sc/Di
1	124.01	2.25	1.40	595846.75	18370.01	43.40	1.64
2	110.83	2.01	1.25	532518.43	14672.68	43.10	1.63
3	95.90	1.74	1.08	460781.92	10985.79	35.80	1.35

Table B.9 Experimental results of critical submergence and related important flow parameters for $b_1= 70$ cm. $b_2= 100$ cm cm at double water intake structure

Obs.	Q(lt/s)	V(m/s)	Fr	Re	We	Sc (cm)	Sc/Di
1	123.67	2.24	1.39	594178.45	18267.29	48.10	1.82
2	109.68	1.99	1.23	526979.70	14369.05	47.20	1.78
3	95.83	1.74	1.08	460448.26	10969.88	39.90	1.51
4	87.22	1.58	0.98	419074.65	9087.05	37.90	1.43
5	75.69	1.37	0.85	363687.40	6843.79	35.80	1.35

Table B.10 Experimental results of critical submergence and related important flow parameters for $b_1= 70$ cm. $b_2= 110$ cm cm at double water intake structure

Obs.	Q(lt/s)	V(m/s)	Fr	Re	We	Sc (cm)	Sc/Di
1	123.60	2.24	1.39	593844.80	18246.78	49.20	1.86
2	109.19	1.98	1.23	524644.09	14241.96	47.90	1.81
3	96.69	1.75	1.09	464585.62	11167.91	45.30	1.71
4	87.72	1.59	0.99	421476.99	9191.54	42.40	1.60
5	74.67	1.35	0.84	358749.26	6659.20	36.60	1.38

Table B.11 Experimental results of critical submergence and related important flow parameters for $b_1= 70$ cm. $b_2= 120$ cm cm at double water intake structure

Obs.	Q(lt/s)	V(m/s)	Fr	Re	We	Sc (cm)	Sc/Di
1	124.22	2.25	1.40	596847.72	18431.78	45.00	1.70
2	111.57	2.02	1.26	536055.20	14868.23	42.80	1.62
3	99.07	1.80	1.11	475996.73	11723.26	40.60	1.53
4	87.79	1.59	0.99	421810.65	9206.09	38.20	1.44
5	76.43	1.39	0.86	367224.17	6977.55	36.60	1.38

Table B.12 Experimental results of critical submergence and related important flow parameters for $b_1= 80$ cm. $b_2= 90$ cm cm at double water intake structure

Obs.	Q(lt/s)	V(m/s)	Fr	Re	We	Sc (cm)	Sc/Di
1	124.86	2.26	1.40	599917.37	18621.87	44.60	1.68
2	110.28	2.00	1.24	529849.16	14525.96	42.00	1.58
3	100.14	1.82	1.13	481135.07	11977.73	40.10	1.51
4	87.92	1.59	0.99	422411.23	9232.33	37.50	1.42
5	76.53	1.39	0.86	367691.29	6995.31	35.20	1.33
6	67.78	1.23	0.76	325650.37	5487.11	33.10	1.25

Table B.13 Experimental results of critical submergence and related important flow parameters for $b_1= 80$ cm. $b_2= 100$ cm cm at double water intake structure

Obs.	Q(lt/s)	V(m/s)	Fr	Re	We	Sc (cm)	Sc/Di
1	123.79	2.24	1.39	594779.04	18304.24	47.40	1.79
2	111.51	2.02	1.25	535788.28	14853.43	42.00	1.58
3	96.76	1.75	1.09	464919.28	11183.96	41.60	1.57
4	90.10	1.63	1.01	432888.10	9695.98	39.60	1.49

Table B.14 Experimental results of critical submergence and related important flow parameters for $b_1= 80$ cm. $b_2= 110$ cm cm at double water intake structure

Obs.	Q(lt/s)	V(m/s)	Fr	Re	We	Sc (cm)	Sc/Di
1	123.76	2.24	1.39	594645.58	18296.02	47.90	1.81
2	109.79	1.99	1.24	527513.55	14398.18	47.10	1.78
3	100.74	1.83	1.13	484004.53	12121.02	40.50	1.53
4	86.35	1.57	0.97	414870.56	8905.65	35.90	1.35

Table B.15 Experimental results of critical submergence and related important flow parameters for $b_1= 80$ cm. $b_2= 120$ cm cm at double water intake structure

Obs.	Q(lt/s)	V(m/s)	Fr	Re	We	Sc (cm)	Sc/Di
1	123.38	2.24	1.39	592777.09	18181.22	48.60	1.83
2	110.14	2.00	1.24	529181.84	14489.39	42.60	1.61
3	96.71	1.75	1.09	464652.36	11171.12	40.00	1.51
4	86.78	1.57	0.98	416939.24	8994.68	37.70	1.42
5	75.68	1.37	0.85	363620.66	6841.28	35.20	1.33
6	67.15	1.22	0.76	322647.44	5386.38	33.50	1.26
7	61.39	1.11	0.69	294953.81	4501.41	31.20	1.18

Table B.16 Experimental results of critical submergence and related important flow parameters for $b_1= 90$ cm. $b_2= 100$ cm cm at double water intake structure

Obs.	Q(lt/s)	V(m/s)	Fr	Re	We	Sc (cm)	Sc/Di
1	123.22	2.23	1.39	592043.04	18136.22	47.80	1.80
2	109.65	1.99	1.23	526846.24	14361.77	47.10	1.78
3	95.81	1.74	1.08	460314.80	10963.52	40.90	1.54
4	87.89	1.59	0.99	422277.77	9226.49	39.60	1.49
5	74.51	1.35	0.84	358015.21	6631.98	35.00	1.32
6	68.40	1.24	0.77	328653.29	5588.77	31.40	1.18

Table B.17 Experimental results of critical submergence and related important flow parameters for $b_1= 90$ cm. $b_2= 110$ cm cm at double water intake structure

Obs.	Q(lt/s)	V(m/s)	Fr	Re	We	Sc (cm)	Sc/Di
1	125.00	2.27	1.41	600584.69	18663.32	44.20	1.67
2	109.44	1.98	1.23	525845.26	14307.25	43.20	1.63
3	97.22	1.76	1.09	467121.43	11290.15	42.30	1.60
4	87.36	1.58	0.98	419741.97	9116.02	34.40	1.30
5	78.61	1.43	0.88	377701.04	7381.36	32.70	1.23

Table B.18 Experimental results of critical submergence and related important flow parameters for $b_1= 90$ cm. $b_2= 120$ cm cm at double water intake structure

Obs.	Q(lt/s)	V(m/s)	Fr	Re	We	Sc (cm)	Sc/Di
1	122.69	2.22	1.38	589507.24	17981.20	48.20	1.82
2	109.44	1.98	1.23	525845.26	14307.25	43.90	1.66
3	98.89	1.79	1.11	475129.22	11680.56	41.00	1.55
4	87.63	1.59	0.99	421009.87	9171.17	40.70	1.54
5	75.83	1.37	0.85	364354.71	6868.93	32.40	1.22
6	68.47	1.24	0.77	328986.95	5600.12	29.90	1.13

Table B.19 Experimental results of critical submergence and related important flow parameters for $b_1= 100$ cm. $b_2= 110$ cm cm at double water intake structure

Obs.	Q(lt/s)	V(m/s)	Fr	Re	We	Sc (cm)	Sc/Di
1	123.08	2.23	1.38	591375.73	18095.36	50.60	1.91
2	110.03	1.99	1.24	528647.99	14460.17	45.70	1.72
3	101.13	1.83	1.14	485873.01	12214.79	45.10	1.70
4	87.38	1.58	0.98	419808.70	9118.92	35.50	1.34
5	75.79	1.37	0.85	364154.52	6861.38	34.50	1.30

Table B.20 Experimental results of critical submergence and related important flow parameters for $b_1= 100$ cm. $b_2= 120$ cm cm at double water intake structure

Obs.	Q(lt/s)	V(m/s)	Fr	Re	We	Sc (cm)	Sc/Di
1	122.26	2.22	1.38	587438.56	17855.22	48.40	1.83
2	111.71	2.03	1.26	536722.52	14905.27	46.90	1.77
3	97.38	1.77	1.10	467855.47	11325.67	46.20	1.74
4	85.49	1.55	0.96	410733.20	8728.91	41.00	1.55
5	75.86	1.38	0.85	364488.18	6873.96	40.20	1.52
6	72.49	1.31	0.82	348272.39	6275.93	32.20	1.22

Table B.21 Experimental results of critical submergence and related important flow parameters for $b_1= 110$ cm. $b_2= 120$ cm cm at double water intake structure

Obs.	Q(lt/s)	V(m/s)	Fr	Re	We	Sc (cm)	Sc/Di
1	123.31	2.24	1.39	592443.43	18160.76	49.80	1.88
2	109.17	1.98	1.23	524510.63	14234.72	48.70	1.84
3	95.94	1.74	1.08	460982.12	10995.34	45.30	1.71
4	87.69	1.59	0.99	421343.53	9185.71	44.20	1.67
5	74.72	1.35	0.84	359016.18	6669.12	39.40	1.49
6	67.29	1.22	0.76	323314.76	5408.68	36.10	1.36
7	60.19	1.09	0.68	289214.89	4327.94	32.20	1.22

Table B.22 Experimental results of critical submergence and related important flow parameters for $b_1= 120$ cm. $b_2= 140$ cm cm at triple water intake structure

Obs.	Q(lt/s)	V(m/s)	Fr	Re	We	Sc (cm)	Sc/Di
1	87.03	1.58	0.98	418140.41	9046.58	46.90	1.77
2	75.37	1.37	0.85	362130.32	6785.32	46.60	1.76
3	67.50	1.22	0.76	324315.73	5442.22	38.00	1.43

Table B.23 Experimental results of critical submergence and related important flow parameters for $b_1= 120$ cm. $b_2= 160$ cm cm at triple water intake structure

Obs.	Q(lt/s)	V(m/s)	Fr	Re	We	Sc (cm)	Sc/Di
1	100.56	1.82	1.13	483137.02	12077.61	49.30	1.86
2	85.65	1.55	0.96	411511.73	8762.03	45.90	1.73
3	76.02	1.38	0.86	365244.47	6902.52	43.70	1.65
4	66.94	1.21	0.75	321646.47	5353.01	43.00	1.62
5	59.63	1.08	0.67	286501.14	4247.11	40.80	1.54

Table B.24 Experimental results of critical submergence and related important flow parameters for $b_1= 140$ cm. $b_2= 160$ cm cm at triple water intake structure

Obs.	Q(lt/s)	V(m/s)	Fr	Re	We	Sc (cm)	Sc/Di
1	99.07	1.80	1.11	476018.98	11724.35	51.50	1.94
2	88.02	1.60	0.99	422900.60	9253.73	47.00	1.77
3	75.57	1.37	0.85	363109.06	6822.04	44.20	1.67
4	67.78	1.23	0.76	325650.37	5487.11	42.20	1.59
5	59.35	1.08	0.67	285166.51	4207.63	40.90	1.54
6	48.89	0.89	0.55	234895.35	2854.89	33.50	1.26

Table B.25 Experimental results of critical submergence and related important flow parameters for $b_1= 140$ cm. $b_2= 170$ cm cm at triple water intake structure

Obs.	Q(lt/s)	V(m/s)	Fr	Re	We	Sc (cm)	Sc/Di
1	96.20	1.74	1.08	462227.77	11054.84	50.10	1.89
2	86.18	1.56	0.97	414047.53	8870.35	46.10	1.74
3	75.69	1.37	0.85	363642.91	6842.12	43.80	1.65
4	67.49	1.22	0.76	324271.25	5440.73	40.70	1.54
5	60.08	1.09	0.68	288681.04	4311.98	39.00	1.47

Table B.26 Experimental results of critical submergence and related important flow parameters for $b_1= 147$ cm. $b_2= 183$ cm cm at triple water intake structure

Obs.	Q(lt/s)	V(m/s)	Fr	Re	We	Sc (cm)	Sc/Di
1	87.49	1.59	0.98	420364.80	9143.09	47.40	1.79
2	76.65	1.39	0.86	368269.63	7017.33	45.50	1.72
3	67.15	1.22	0.76	322625.20	5385.63	41.70	1.57
4	61.19	1.11	0.69	294019.57	4472.94	39.40	1.49
5	48.92	0.89	0.55	235028.81	2858.13	33.30	1.26